RD&E CENTER

Technical Report

No. 13475

PISTON AND RING ASSEMBLY FRICTION STUDIES IN CUMMINS 903 ENGINE

CONTRACT DAAE07-84-C-R134

JUNE 1989

DONALD J. PATTERSON
KEVIN M. MORRISON
GEORGE B. SCHWARTZ

DEPARTMENT OF MECHANICAL ENGINEERING AND APPLIED MECHANICS
THE UNIVERSITY OF MICHIGAN
ANN ARBOR, MICHIGAN 48109-2121

AND

U.S. ARMY TANK-AUTOMOTIVE COMMAND
WARREN, MICHIGAN 48397-5000

By _____

U.S. ARMY TANK-AUTOMOTIVE COMMAND
RESEARCH, DEVELOPMENT & ENGINEERING CENTER
Warren, Michigan 48397-5000

NOTICES

This report is not to be construed as an official Department of the Army position.

Mention of any trade names or manufacturers in this report shall not be construed as an official endorsement or approval of such products or companies by the U.S. Government.

Destroy this report when it is no longer needed. Do not return it to the originator.

Unclassified

SECURITY CLASSIFICATION OF THIS PAGE

REPORT DOCUMENTATION PAGE

Form Approved OMB No. 0704-0188

1a. REPORT SECURITY CLASSIFICATION: Unclassified	1b. RESTRICTIVE MARKINGS
2a. SECURITY CLASSIFICATION AUTHORITY	3. DISTRIBUTION/AVAILABILITY OF REPORT: Approved for public release; distribution is unlimited.
2b. DECLASSIFICATION/DOWNGRADING SCHEDULE	
4. PERFORMING ORGANIZATION REPORT NUMBER(S): 13475	5. MONITORING ORGANIZATION REPORT NUMBER(S)
6a. NAME OF PERFORMING ORGANIZATION: Dept. Mech. Engr. & Appl. Mech. University of Michigan; 6b. OFFICE SYMBOL (If applicable)	7a. NAME OF MONITORING ORGANIZATION: TACOM
6c. ADDRESS (City, State, and ZIP Code): 2250 G.G. Brown Laboratory, Ann Arbor, Michigan 48109-2125	7b. ADDRESS (City, State, and ZIP Code): Warren, Michigan 48397-5000
8a. NAME OF FUNDING/SPONSORING ORGANIZATION: U.S. Army TACOM; 8b. OFFICE SYMBOL (If applicable)	9. PROCUREMENT INSTRUMENT IDENTIFICATION NUMBER: DAAE07-84-C-R134
8c. ADDRESS (City, State, and ZIP Code): Warren, Michigan 48397-5000	10. SOURCE OF FUNDING NUMBERS: PROGRAM ELEMENT NO. / PROJECT NO. / TASK NO. / WORK UNIT ACCESSION NO.

11. TITLE (Include Security Classification): Piston and Ring Assembly Friction Studies in Cummins 903 Engine (u)

12. PERSONAL AUTHOR(S): Patterson, Donald J., Morrison, Kevin M., and Schwartz, George B.

13a. TYPE OF REPORT	13b. TIME COVERED	14. DATE OF REPORT (Year, Month, Day)	15. PAGE COUNT
FINAL	FROM Oct. 84 TO Oct. 88	June 89	155

16. SUPPLEMENTARY NOTATION

17. COSATI CODES			18. SUBJECT TERMS (Continue on reverse if necessary and identify by block number)
FIELD	GROUP	SUB-GROUP	Friction, Piston, Piston rings, Uncooled Diesel

19. ABSTRACT (Continue on reverse if necessary and identify by block number)

Piston and ring assembly friction has been measured in a single cylinder Cummins 903 diesel. The engine was motored and fired, cooled and uncooled. For uncooled operation, plasma sprayed chromium oxide ring and liner coatings were employed with a synthetic lubricant. The Instantaneous IMEP and Fixed Sleeve methods were used for the friction measurement on a crank angle by crank angle basis, with a cycle average of about 1.5 to 4 psi fmep. Considerable effort was expended in developing the measurement techniques, with a major effort on the Instantaneous IMEP method. In a parallel effort a bench type, heated, piston ring and liner wear simulator was developed. This permitted rapid screening of promising candidate materials for uncooled engine tests. The plasma sprayed chromium oxide coatings were found to be best.

20. DISTRIBUTION/AVAILABILITY OF ABSTRACT: ☐ UNCLASSIFIED/UNLIMITED ☐ SAME AS RPT. ☐ DTIC USERS	21. ABSTRACT SECURITY CLASSIFICATION: Unclassified
22a. NAME OF RESPONSIBLE INDIVIDUAL: E. Schwartz	22b. TELEPHONE (Include Area Code): (313)574-5656 / 22c. OFFICE SYMBOL: AMSTA-RGRD

DD Form 1473, JUN 86 *Previous editions are obsolete.*

PREFACE

The very important role of the Cummins Engine Company, especially Ralph Slone and Malcolm Naylor is gratefully acknowledged. They supplied virtually all of the engine hardware, some experimental equipment, and the basic piston and ring laboratory fixture.

Furthermore, the authors thank Professor Zu-Wei Cui of Zhejiang University, China, and Professor Kenneth Ludema of The University of Michigan, for their assistance with development of the piston and ring simulator and the analysis of the results. Also, we wish to acknowledge the contributions of Guy Babbitt, graduate student, for his work in designing, constructing, and evaluating the Fixed-Sleeve method for the Cummins 903 engine.

We also thank Jack Brigham and Fred Rowe for their expert assistance in design and construction of the test equipment. Most importantly, we thank the Army-Tank Automotive Command for their financial and technical support. Special note is made of the important contributions of Dr Walter Bryzik, and Ernest Schwarz. They put the program together and coordinated the Cummins and University of Michigan efforts.

TABLE OF CONTENTS

TABLE OF CONTENTS (Continued)

LIST OF ILLUSTRATIONS

LIST OF TABLES

1.0. INTRODUCTION

This research at the University of Michigan was aimed at supporting the advanced technology diesel program of the U.S. Army Tank Automotive Command, working with the Cummins Engine Company. Piston and ring assembly friction, scuffing, and wear are expected to be stumbling blocks to the development of commercial, and even laboratory advanced technology engines, versions of which are expected to be minimally cooled. In such engines, liners may reach temperatures in the range of 500-600 C. At these temperatures, liquid lubricants decompose rapidly. Wear, scuffing, excessive friction, and general destruction of piston and ring rubbing surfaces may be expected. Consequently, a measure of piston and ring assembly (PRA) friction, together with assessment of the wear and scuffing of rubbing surfaces, are needed engine-development tools.

The problem is that there are no well-established techniques that give the piston and ring assembly friction, as the engine runs under loaded conditions. Furthermore, conventional bench-type wear testers do not lend themselves to total screening of advanced technology engine ring and liner components because of geometrical and environmental differences between bench and engine tests. The chief problem is duplication of the top-ring reversal temperature, load and lubrication environment.

At the University of Michigan, a PRA friction measurement technique, termed the Instantaneous IMEP method, had been developed prior to this program and reported by Uras in References 1-6. In that earlier work, it had produced useful results in running gasoline engines. The initial thrust of the present program was to apply that technique to a minimally cooled, advanced-technology engine. The Cummins 903 engine was selected. A single-cylinder version was used.

Because of possible experimental limitations of the Instantaneous IMEP method and the absolute necessity of determining reliable PRA friction data, it was decided to pursue an alternate method as well. That method, a derivative of so-called moveable bore methods, is termed the Fixed-Sleeve method. Its development had started in an earlier program at Michigan using a gasoline engine. That earlier work was reported by Ku in References 7 and 8. In the present program, the Fixed-Sleeve method was applied to a second Cummins 903 single-cylinder engine, and some of that work was reported in Reference 9.

To support their work on low-heat rejection engines, Cummins

had begun development of a bench-test simulator to permit rapid screening of materials with respect to piston and ring friction and wear. Rapid screening is desirable, since engine test are relatively complicated, time consuming, and expensive. That work was transferred to Michigan to support the present research program. Further development of that fixture has occurred and is reported herein, as well in References 13 and 15.

A good deal of the material in this report was included in Progress Reports to the U.S. Army, References 10 - 12. These reports contain more detail on some topics.

In the sections that follow, the overall program discussion is organized into three segments. They are:

1. Instantaneous IMEP Method
2. Fixed-Sleeve Method
3. Ring and Liner Bench Test

Motoring and firing friction results are reported on the 903 engine with the Instantaneous IMEP method, including results with ceramic-coated rings and liner, synthetic lubrication, and uncooled engine block. Motoring results are reported with the Fixed-Sleeve Method. A variety of results from the bench-test fixture are reported, including various ceramic coatings and lubricants. A comparison with Cameron Plint wear data, as well as engine worn samples is made. Microscopic examinations of fresh and worn surfaces are included. The piston and ring assembly friction has been reported as the quotient of the friction work per 720 crank angle degree engine cycle divided by the cylinder displacement. This is termed the PR MEP and is reported in units of psi.

2.0. OBJECTIVE

The objective of this research was to quantify the piston and ring friction of advanced technology, low-heat rejection engines. This mission involved:

1. Development of measuring techniques.

2. Evaluation of advanced materials including ceramics.

3. Evaluation of lubricant effects including synthetics.

4. Development of experimental screening methods for friction and wear of piston and ring-rubbing surfaces.

3.0. CONCLUSIONS AND OBSERVATIONS

The measurement of instantaneous piston and ring friction in a turbocharged, firing engine is a difficult challenge. Only near the end of the program were successful friction measurements made in a firing engine with the Instantaneous IMEP method and in a motored engine with the Fixed-Sleeve method. On the other hand, the bench-test simulator proved relatively easy to operate, and much data was obtained on ceramic-coatings, synthetic lubrication and high-temperature service.

Below are conclusions and observations for the various experimental methods within this program.

3.1. Instantaneous IMEP Method

The Instantaneous IMEP method appeared to give reasonable values for PRA friction in the 903 engine with intake air boost. The technique is promising for revealing significant changes in friction, or the appearance of unusual friction forces, such as those associated with an engine failure. On the other hand, it may be difficult to quantify small frictional changes because of the lack of sensitivity of the method. A major advantage of the method is that no significant engine modifications are required. Thus the data obtained correctly reflects the engine design. No other technique has this advantage. Some specific observations were:

1. Firing and motoring PRA friction were similar under motoring and firing conditions. Friction was in the boundary or mixed regime near the dead centers and appeared relatively hydrodynamic midstrokes. With cool oil (high viscosity), the friction was higher, but more hydrodynamic. Warm engine PR MEP values ranged from about 1.5 to 4 psi.

2. The synthetic lubricant gave lower friction than the conventional SAE 40 oil in conventional, cooled-engine operation.

3. Friction with an uncooled block and synthetic lubricant was similar in character to that of the base engine with cooling and conventional motor oil, when motoring. Firing results looked similar, but the PR MEP values were unreliable.

3.2. Fixed-Sleeve Method

Some difficulties were experienced in adapting this method to the Cummins 903 engine. As a result, limited data were obtained. PR MEP was 2.34 psi at 1000 rpm, motoring under warmed-up engine conditions. Results looked similar to those obtained with the Instantaneous IMEP method.

Below are some observations and conclusions.

1. Repeatability and the ability to differentiate small friction differences appear excellent. On the other hand, a special liner is required; thus engine modifications are necessary which themselves may modify base engine friction characteristics. The method appears to be readily adapted to engines with liners, such as the Cummins 903 engine.

2. The Fixed-Sleeve method permits relatively rapid change of piston, ring, and liner variables, and calibration is relatively straight forward. Design variables can be investigated relatively quickly.

3. This method is projected to be very useful for evaluating bore roundness, straightness, and surface finish effects. It will also be useful for evaluating new piston or ring designs.

4. The location of the strain-gauges, away from the heat and cylinder stresses, suggests that this method might be more easily used to measure friction in uncooled engines than the Instantaneous IMEP method.

3.3. Ring and Liner Bench Test

Below are some conclusions and observations on the bench test simulator for piston and ring wear, and friction.

1. In unlubricated tests, the titanium carbide, chromium carbide pair was a poor combination, whereas the chromium oxide pair was exceptional. The simulator tests correlated directionally with the Cameron Plint results and were in qualitative agreement with engine results.

2. Lubricated tests demonstrated lower wear and friction, as expected. Careful control of lubricant feed rate, targeting, and spray pattern are required for good repeatability and minimization of side-to-side variations. Air atomization of the lubricant is very helpful.

3. Additional work is needed to establish correlation between bench-testers and running engines. Such work includes development of standard test procedures, parametric evaluations, and more sophisticated surface analysis of wear samples. A better knowledge of the quantity and quality of the lubricant at the wear interface of running engines would be helpful in achieving a more correct laboratory simulation.

4. Overall, it is concluded that the simulator is a promising bench-test device for evaluating ring, liner, and lubricant combinations for advanced technology engines. While it will never be possible to totally eliminate engine testing, this efficient bench simulation should make the job of screening new materials, new lubricants, and new designs more efficient and cost effective.

4.0. RECOMMENDATIONS

4.1. Instantaneous IMEP Method

This method of measuring piston and ring assembly friction worked reasonably well on the boosted Cummins 903 engine. Problems were encountered developing the instrumentation, especially solving the problem of magnetic noise. Finally, results looked reasonable. This method is projected to be very useful for evaluating friction and friction-related problems in uncooled engines.

4.2. Fixed-Sleeve Method

The progress of this method was slow, since the major effort was on the Instantaneous IMEP method. By program end, a first-generation design had been implemented on a motoring engine. Some problems with strain-gauge lead wiring were suspected. The signal to noise ratio was poor. It was concluded that a new design was needed which would:

1. Eliminate the threaded liner hold-down in favor of a clamped design.

2. Use a thinner section on which the strain-gauges were applied.

3. Route the strain-gauge wires to produce less of an antenna effect.

4. Demagnetize all the moving parts in the crankcase.

4.3. Ring and Liner Bench Test

The ring and liner bench-test fixture worked quite well as developed within this program. It should prove useful as a screening tool for rings, liners, materials and lubricants. The number of engine tests required should therefore, be diminished considerably. A number of organizations have expressed interest in obtaining the simulator.

5.0. DISCUSSION

5.1. Background

The Instantaneous IMEP technique had been developed at the University of Michigan prior to the start of the present program. It had produced useful results on running gasoline engines. The initial thrust of the present program was to apply that technique to the minimally cooled, advanced technology diesel engine.

The first step was to apply the technique to the production Cummins 903, and a one-cylinder engine was set-up and instrumented for this. Once a successful result was obtained, the approach was applied to the same engine with "low-heat rejection components" and run under "low-heat rejection operation." That effort is described in par. 5.2.1., 5.3.1, and 5.4.1.

Early in the program, it was found that the instrumentation signals needed for the Instantaneous IMEP method were quite noisy with the 903 engine. In addition, it was anticipated that the differencing of the large numbers derived from this turbo-charged engine would make precise friction quantification quite difficult. Prior to the start of this program, the Fixed-Sleeve method had been initiated on an automotive-type gasoline engine. That technique worked extremely well on the Cadillac 4.1-litre V-8 engine, which had a die cast aluminum block and iron liner. That work was reported in references 7 and 8.

The success on the gasoline engine, coupled with concerns for precision of the Instantaneous IMEP technique, led us to apply the Fixed-Sleeve method to a second Cummins 903 single-cylinder engine. The design implementation is described in this report, but the test results, obtained prior to the end of this program, were disappointing. No useful results were obtained, although the approach still appears attractive. A summary of the design and results of the earlier work on the gasoline engine, together with extension to the 903 engine are included in this report.

(See par. 5.2.2., 5.3.2, and 5.4.2.)

Parallel to the above-engine program, a laboratory bench test friction and wear simulator was developed to assess surface damage, wear, and friction between liner segments and reciprocating ring. This simulator allowed rapid screening of candidate materials. The basic reciprocator was designed by Cummins. It was extensively modified and computer controlled at Michigan. The progress on this portion of the program has been rapid, and considerable data has been taken with this rig. The simulator has become a useful screening device for selecting promising, high-temperature engine materials and lubricants. This portion of the program is summarized in par. 5.2.3., 5.3.3. and 5.4.3. The simulator is discussed in references 13 and 15.

5.2. Design

Discussed below is the design of the various experimental methods explored within this program. These are:

1. Instantaneous IMEP Method
2. Fixed-Sleeve Method
3. Ring and Liner Bench Test

5.2.1. Instantaneous IMEP Method. The Instantaneous IMEP method employs a force balance between the measured cylinder pressure force, the compressive force in the connecting rod, the inertia force and the friction force. Considering the components of these forces acting along the cylinder axis, the sum of the other three equal the friction force of the piston, rings and piston pin assembly. Figure 5-1 shows the single-cylinder version of the Cummins 903 V-8 engine modified for the Instantaneous IMEP method. The large pipe emanating from the cylinder-head region is a vent for the crankcase. This provides atmospheric pressure on the backside of the piston. A crankangle encoder is mounted on the front of the engine. Simultaneous measurements of cylinder pressure and rod compressive force are made at each crank angle over the entire cycle. Table 5-1 gives relevant engine information about the production Cummins 903 engine.

In applying this method, inertia forces are commonly calculated from the well-known theoretical equation, assuming a constant crank-speed. As discussed later, for this one-cylinder engine, and where inertia forces are quite large, crank-speed variation must be taken into account in the calculation of the inertia forces. In the determination of the inertia forces, it is necessary to consider the reciprocating mass of the piston, rings, the pin, and that portion of the connecting rod which reciprocates with the

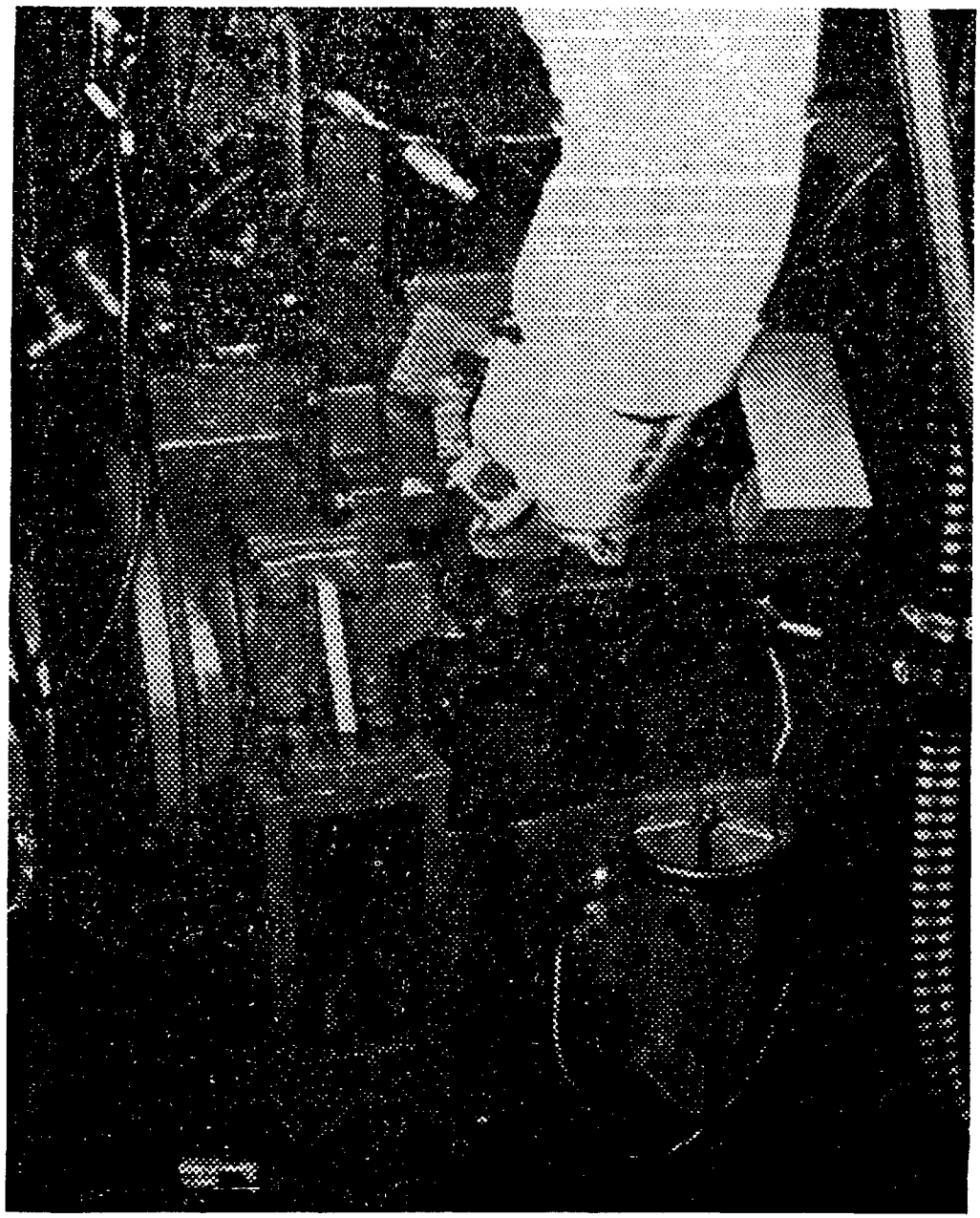

Figure 5-1. Single-Cylinder Cummins 903 Engine Equipped for Instantaneous IMEP Method

Table 5-1. Cummins V8-903 Engine Information

Bore	139 mm
Stroke	121 mm
Connecting Rod Length	208 mm
Displacement	903 cu in
Compression Ratio	15.5:1
Closed-Deck Iron Block	
Wet-Cast Iron Liner (Removable)	

piston. As reported in reference 1, a distributed model of the connecting rod inertia is necessary, since it was found that the error associated with the use of a lumped model was excessive.

Figure 5-2 shows the strain-gauged connecting rod used with the Instantaneous IMEP method. Pairs of 90 degree rosettes are installed on either side of a machined section located at approximately one-third of the connecting rod web length near the small end. Wires from the strain-gauges, power supply, and thermocouple, to measure the bridge temperature, are attached to the connecting rod. From the connecting rod, the wires are routed exterior to the engine by the use of a grasshopper linkage shown in Figure 5-3. More detail of the implementation of the Instantaneous IMEP technique is given in Section 5.3.1.

For purposes of illustration of the method, Figure 5-4 shows signals for Instantaneous IMEP method measurements made on a two-litre gasoline engine at 800 rpm motoring, part throttle. The top trace is the cylinder pressure, the center trace is the compressive force in the connecting rod, and the lower trace is the inertia force. Note that the strain-gauge signal includes abrupt jumps at the dead centers, indicated by the circles in the figure. These jumps arise from the change in static friction as the piston reverses direction. Differencing these forces to obtain piston ring assembly friction results in the top curve of Figure 5-5. This curve shows piston-ring assembly friction force as a function of crank angle. The static friction reversals at the dead centers are very apparent.

It is difficult to determine the factors that contribute to the shape of the friction force curve. This is because the curve reflects the skirt, the three piston rings, and the piston pin friction. Each component is operating in a somewhat different lubrication regime. Near the dead centers, the piston rings dominate the friction results. There, the rings operate in the mixed or boundary lubrication regime. In midstroke, probably all components are operating in the hydrodynamic regime.

The frictional work associated with these forces results from the product of friction force times piston velocity. The velocity is shown in the center portion of the figure. The power is shown at the bottom of Figure 5-5. The area under the curve of power versus crankangle is the total energy loss due to friction. The frictional work, divided by the displacement of the cylinder, has been termed the friction mean effective pressure (fmep) of the piston and ring assembly, (PR FMEP).

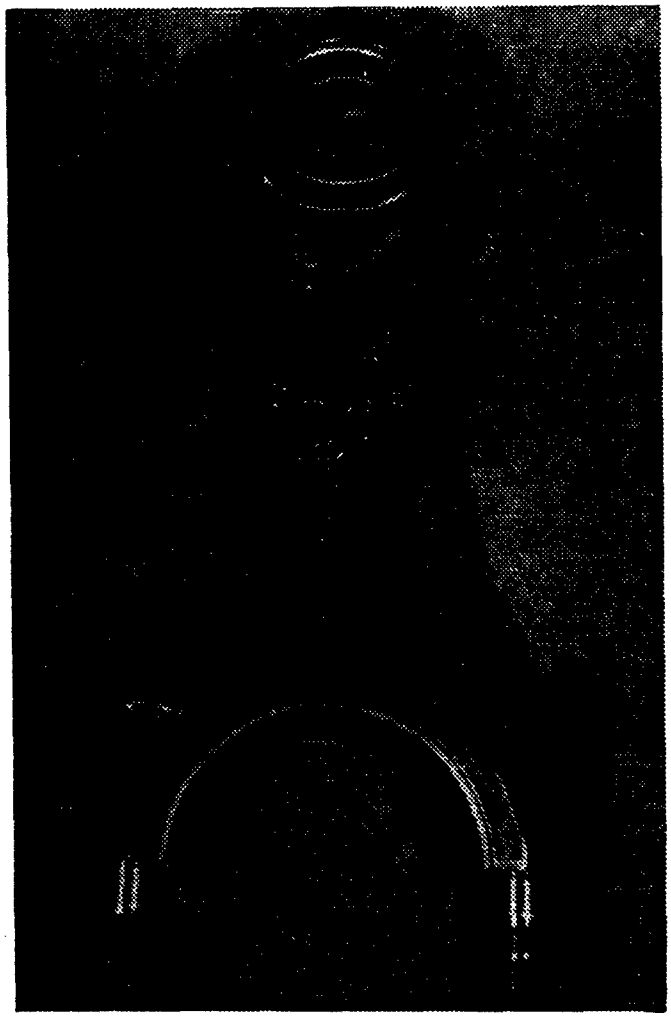

Figure 5-2. Stain-Gauged Connecting Rod

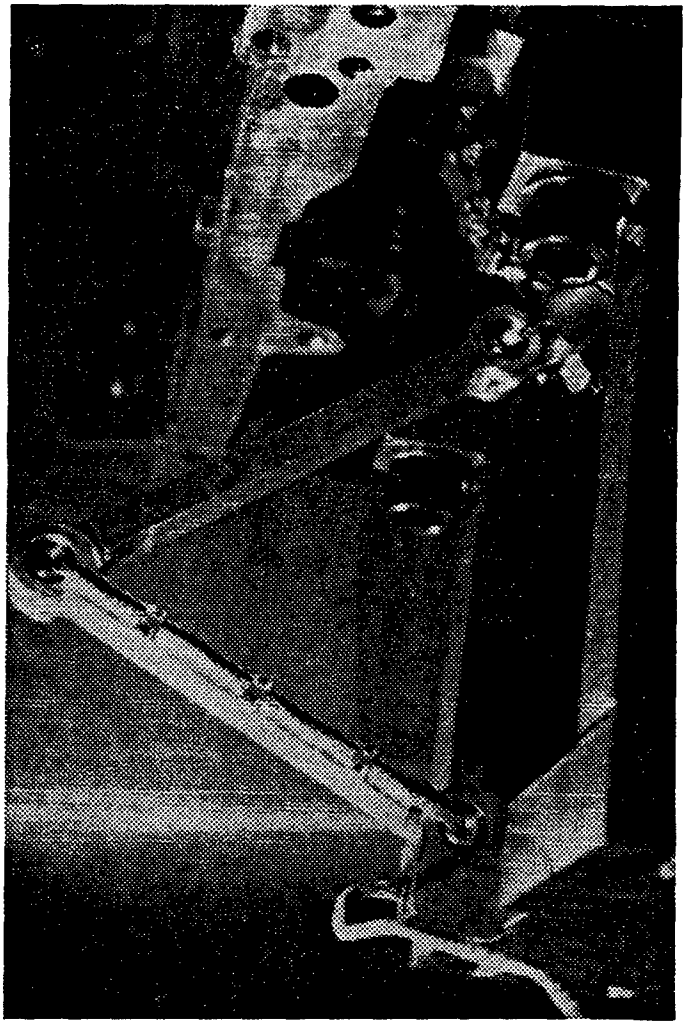

Figure 5-3. Grasshopper Linkage

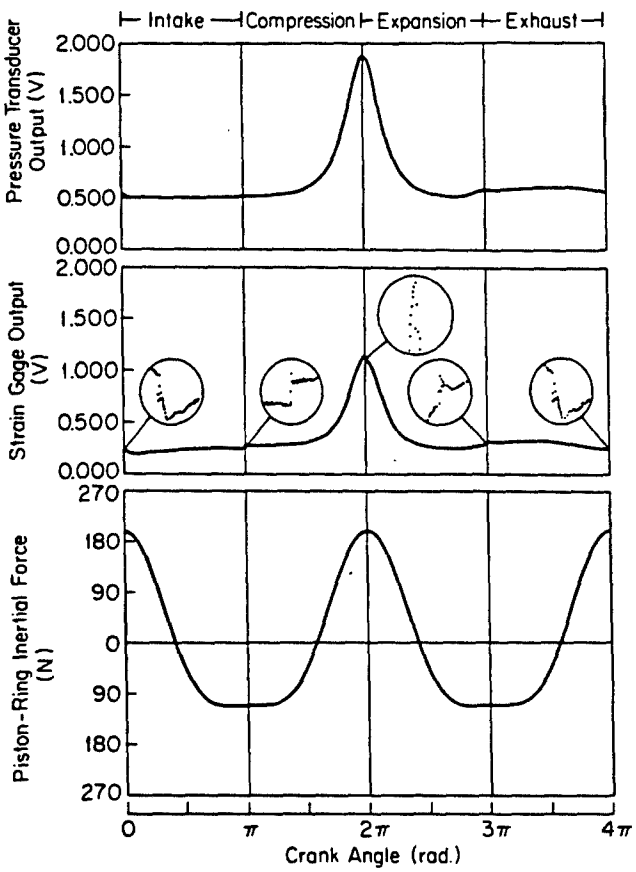

Figure 5-4. Typical Cylinder Pressure, Connecting Rod, and Inertia Forces

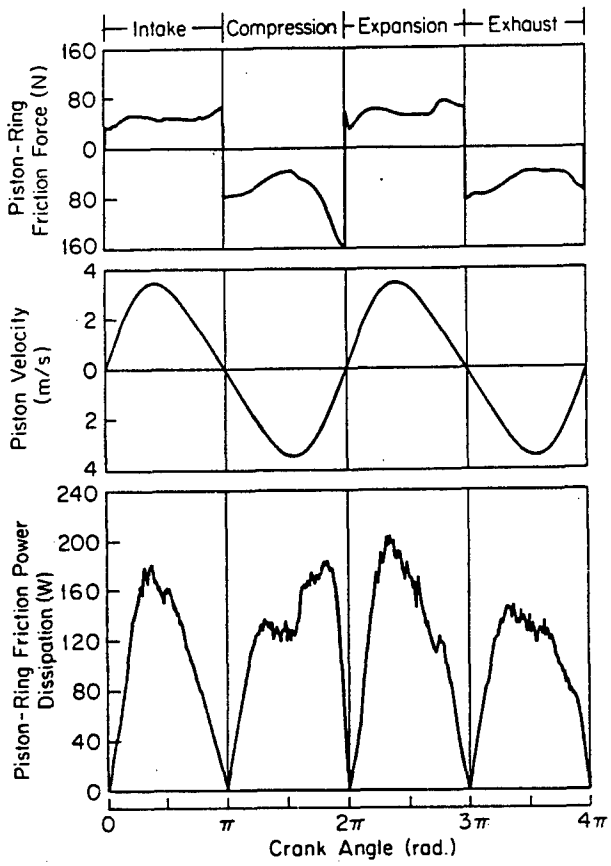

Figure 5-5. Piston and Ring Assembly Friction Force, Velocity and Power Dissipation

5.2.2. Fixed-Sleeve Method. The Fixed-Sleeve method is a derivative of a class of what is termed "movable bore" methods. It was implemented on a 4.1-litre gasoline engine (7), and considerable data were obtained. Table 5-2 gives relevant engine information for that engine. A brief comparison of the two methods, simultaneously implemented on the 4.1-litre engine, may be found on page 64 under "Comparison of the Fixed-Sleeve and Instantaneous IMEP methods on the 4.1-Litre engine."

Figure 5-6 shows a cross section of the Fixed-Sleeve design. The original 4.1-litre engine liner, which had an 88 mm bore is fitted with a smaller 80 mm sleeve which is attached to the outer liner by a pair of lock nuts located at the bottom of the assembly. Piano wire in tension is used near the top of the assembly to pilot the inner sleeve so that it does not touch the outer liner. O-rings are used to seal combustion gas, water and oil. Cooling water is permitted to circulate between the two sleeves. Strain-gauges are mounted on both inner and outer surfaces of the necked-down section near the bottom of the outer liner.

The outer liner, which is essentially identical to the production liner, is supported in the engine in the conventional way between the top of that liner and the support lip. Thus the inner liner is positioned like a standpipe, the top of which is shortened slightly so that it cannot contact the cylinder-head. Acting on the inner sleeve are the sum of the cylinder pressure force acting on the rim and the friction force. An example of these forces is shown in Figure 5-7. The upper figure shows cylinder pressure while motoring at 1000 rpm, wide open throttle. The center figure shows the strain-gauge signals, and the lower figure shows the friction force as a function of crankangle. This is found by differencing the two upper signals.

5.2.3. Ring and Liner Bench Test. The ring and liner bench test simulator provides a rapid means of screening candidate ring, liner, and lubricant combinations under simulated engine conditions. The rig simulates the most severe wear and friction conditions in the engine, namely directly after top dead-center, where piston speed is low, and loads and temperatures are high. The simulator incorporates a complete piston ring positioned in a disk- shaped holder. The ring ends are held together by pins and clamped to the nominal gap clearance. The holder with ring reciprocates with a stroke of 2.54 cm, and portions of the ring are loaded by two liner segments placed 180 degrees apart. Each stationary liner segment is about 3.8 cm long and 0.7 cm wide. It is cut from a finished liner. The ring holder is

Table 5-2. Cadillac V8-4.1-Litre Engine Information

Bore	88 mm
Stroke	84 mm
Connecting Rod Length	134 mm
Displacement	4100 cc
Compression Ratio	8.5:1
Closed-Deck Iron Block	
Wet-Cast Iron Liner (Removable)	

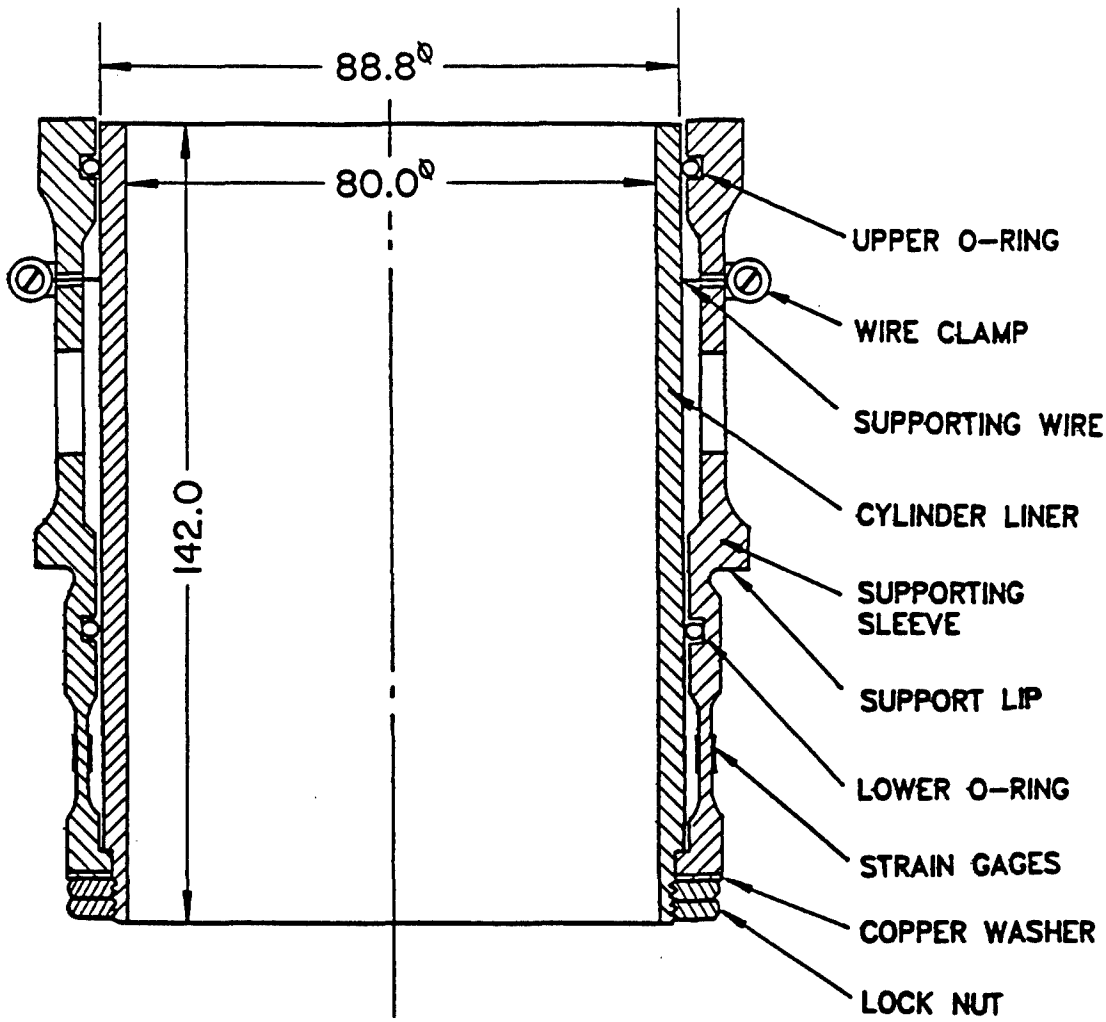

Figure 5-6. Fixed-Sleeve Design for the 4.1-Litre Gasoline Engine

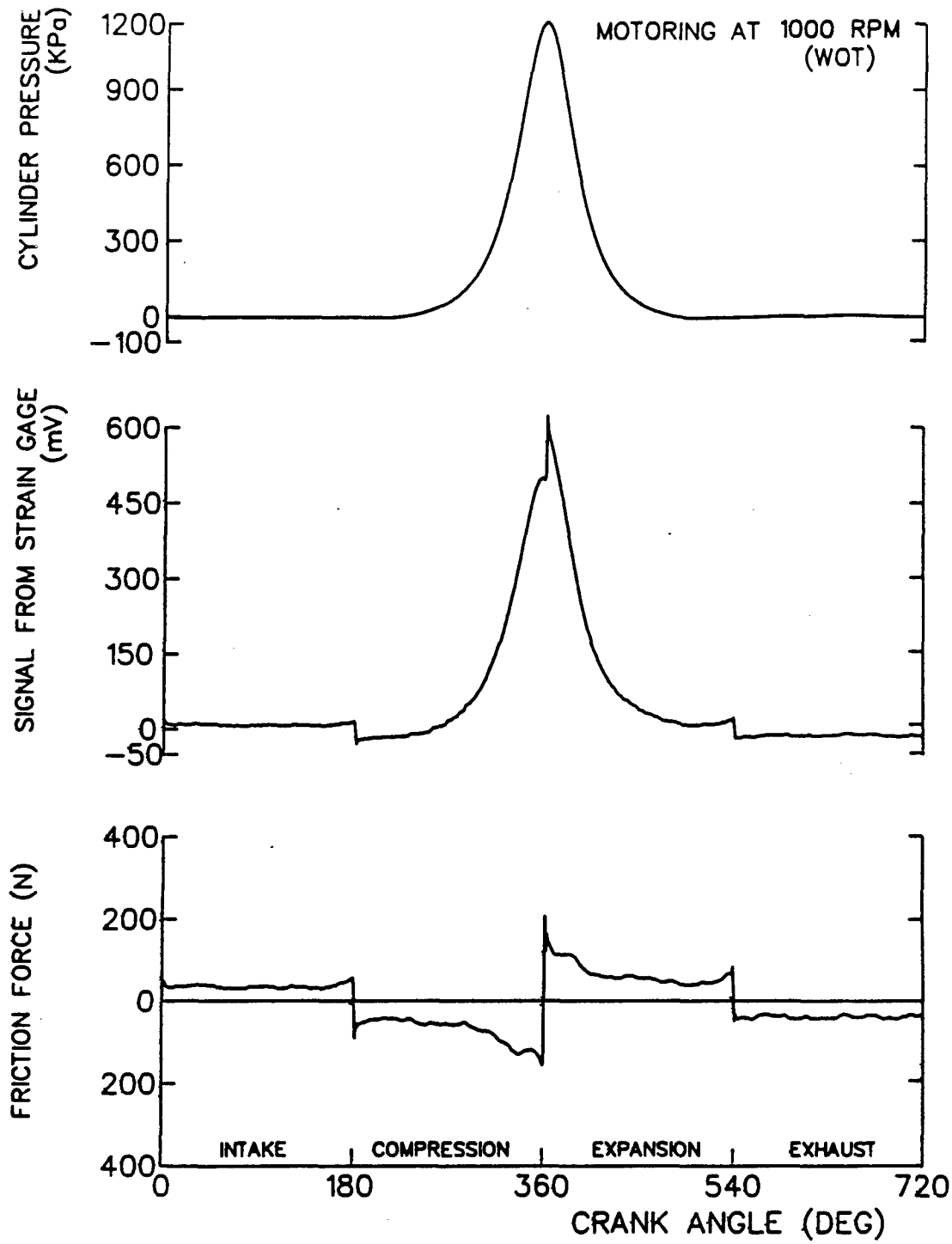

Figure 5-7. Cylinder Pressure (upper), Strain-Gauge Voltage (center), and Resulting Friction Force (lower), WOT, 1000 RPM, Motoring

powered by a 1.34 kw d.c. electric motor that is speed controlled by a SCR controller. Load is applied to the ring, liner interface by means of an air cylinder and lever arm arrangement. Provision is made for lubricant spray at the wear interface, and the entire unit may be heated to as high as 550 C, in order to simulate low-heat rejection engine top-ring reversal temperatures.

Data obtained from the simulator include friction force as a function of stroke and average friction coefficient as a function of time. As is often done after such tests, liner samples may be analyzed for wear volume, surface finish, and other meaningful wear parameters. Simulator results are available for both right and left wear interfaces.

Figure 5-8 shows a schematic of the simulator. By pressurizing the air cylinder, ring loads are applied which can simulate the high pressures experienced in highly turbocharged engines under peak pressure conditions. Maximum reciprocating speed is limited to 700 rpm by inertia forces. In effect the simulator attempts to duplicate the most severe ring and liner condition; namely low speed, high load at TDC firing. Most testing to date has been at speeds below 500 rpm. Very high speed operation, if desired would require addition of a reciprocating balance mechanism.

The friction force is transduced by strain-gauges mounted on both right and left arm pivots. This not only permits an independent friction measurement at both wear locations, but also eliminates unwanted bearing friction, inertia force, and noise from vibration which were characteristic of earlier designs.

As desired, lubrication is provided by means of water cooled stainless steel tubes through which a pressurized air and oil mixture pass. The oil is provided as a spray mist directed to the rubbing surfaces. A peristaltic pump, capable of precise, variable feed rate, is used to control oil quantity. A double wall, insulated, stainless steel oven surrounds the liner samples and ring. Electric heaters are used to produce high temperatures. Heater control is by means of the computer (IBM XT compatible), which cycles the heaters. Thermocouples are employed at several points within the oven to indicate temperature. An angle encoder with 250 pulses per revolution is used to tell the computer when to sample the strain-gauge force.

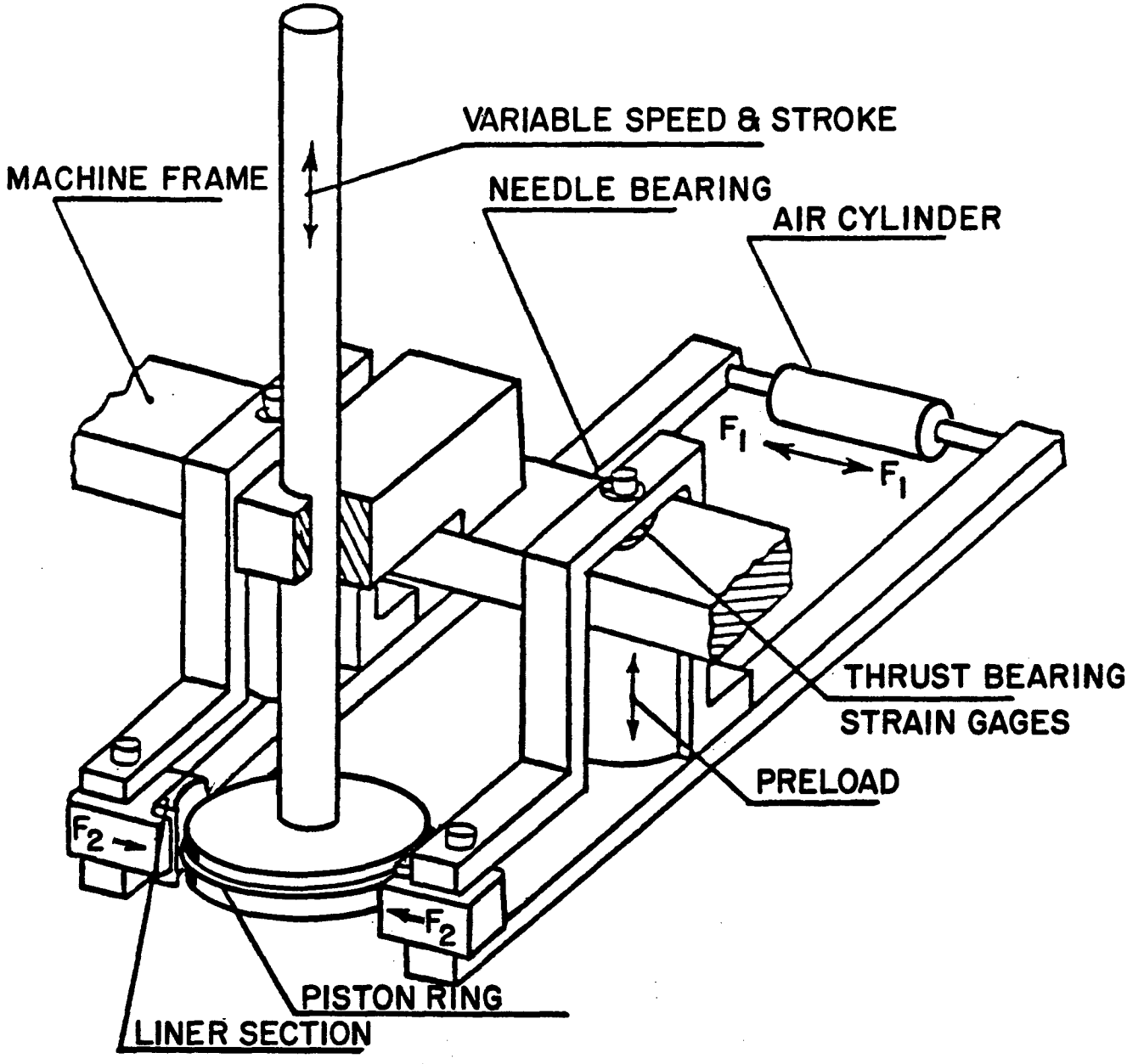

Figure 5-8. Schematic Showing Essential Features of Bench Test Simulator for Ring and Liner Wear and Friction

5.3. Implementation

Below is discussed the implementation of the various experimental methods conducted within this program. These are:

1. Instantaneous IMEP Method
2. Fixed-Sleeve Method
3. Ring and Liner Bench Test

5.3.1. Implementation of the Instantaneous IMEP Method.

5.3.1.1. Engine Installation. A single-cylinder Cummins 903 engine was obtained from Cummins Engine Company for this program. The engine was one of several made by Cummins for research purposes. It was constructed from a V-8 by cutting the block in such a manner as to leave two cylinders at the flywheel end of the engine. The crank, front end, cylinder-head, and fuel injection system were appropriately modified. Figure 1 showed the engine installed in Room 249 of the W. E. Lay Automotive Laboratory at the University of Michigan.

In this modified engine, only one cylinder was working. The other did not compress, due to a large hole placed in the piston crown. Additional weight was placed on the piston pin to preserve engine balance. By this means, a fairly smooth running single-cylinder engine is obtained.

The engine was installed and coupled to a 600 HP G.E. Electric Dynamometer. The dynamometer was improved with the addition of a 500 lbm maximum capacity load cell and a Daytronics Model 3270 strain-gauge conditioner/indicator to replace an existing "LINK" pneumatic system. One of the strain-gauge conditioner filter selections was modified to have a cut off frequency of about 0.2 Hz so that the dynamometer output torque was averaged over a longer period of time. This reduced low-frequency torque fluctuations which had made it difficult to get steady torque readings. The dynamometer speed controls were tuned thoroughly by G.E. personnel.

A system to convert the existing test cell engine coolant system from a total loss tap water type system to a closed 50/50 antifreeze system was designed and installed. This system used a 2 HP coolant pump which was provided by Cummins. A BCF 5-030-03-024-004, 24", 2-pass heat exchanger was purchased and installed to separate the coolant solution from the tap water coolant. An identical unit was installed for the oil system. Pneumatic temperature controllers were used for control of the coolant, oil, and inlet air temperatures. These were available in the laboratory.

Control valve bodies, with the proper flow coefficients, were installed. The smallest capacity units (Cv=0.5) gave best temperature control.

Oil-pressure supply to the engine was provided by a 2 HP pump. An adjustable pressure regulator was added in a by-pass configuration, to allow accurate control of oil pressure. It was found that the piping from the pump outlet to the heat exchanger, and on to the engine, had to be as large as possible (1" was used); otherwise, the pressure loss though the system dropped oil pressure below an acceptable level at the highest flow rate with the highest oil temperature. A dry sump oil reservoir was needed to avoid dragging the grasshopper linkage through the oil.

An intercooler unit modified from a multicylinder engine was used to preheat the pressurized intake air. This was done in order to simulate air temperatures encountered in the turbocharged/intercooled multicylinder engine (240oF). Heat was provided by steam at a pressure of about 30 psig. This steam was provided by a 40 kW electric mini-boiler in the equipment room above the test cell. The steam outlet temperature was monitored by the pneumatic controller temperature sensor in the intake pipe, and the controller regulated the flow of steam through the control valve. Both oil and coolant system heat exchangers were equipped with steam lines and traps, so that heat could be added when running motoring tests, and prior to starting.

Pressure in the intake manifold of up to 50 inches of mercury gauge pressure was provided by two screw-type air compressors. One was 40 hp. This was the regular building supply (110 psig). The second was an auxiliary unit of 30 hp placed above the test cell and was used only when the engine was run with boosted intake pressure. Air flow to the engine was measured by a critical flow orifice system consisting of five orifices in parallel. The air-flow orifices were calibrated with a 10 cu. ft. air bell. A large Heise gauge was installed upstream to monitor pressure there. A 35 psi relief valve was installed in the line to the intake manifold for safety reasons. Two-inch compressed air lines ducted the air from the compressors. Two low-resistance rayon air filters were installed to filter the air.

A variable speed fuel pump system was provided by Cummins. The pump was equipped with a small needle valve bypassing the pump output for fine pressure adjustment. Coarse adjustment was provided by controlling the speed. A Cox Instrument Model 402 weigh scale was used to measure flow.

Exhaust back pressure was controlled by a manually operated valve. An 80 in. Hg. well type manometer was installed to monitor the back pressure.

5.3.1.2. Grasshopper Linkage Design. The purpose of this two-bar linkage is to fully support a wiring harness containing a number of wires from their point of attachment on the connecting rod to a stationary point on the engine. From there, the wires are connected to external circuitry. Below are design criteria:

1. Minimize swing angles a1, a2, a3 for minimum wire twist.

2. Minimize link lengths for better clearance.

3. Minimize acceleration of the joints to minimize stresses.

4. Optimize geometry that will allow motion through all angles without interference with block and minimize modifications of the oil-pan.

The specific design was made with the assistance of a full-scale layout board, Figure 5-9 This was constructed of cardboard upon a full-scale drawing of the block. Pins and guides permitted rotary and reciprocating motion. Link lengths and attachment points were selected to avoid interferences and to minimize the swing angles. The top swing angle a1, is usually the largest, with some occasional wire breakage experienced with angles as large as 90 degrees. Angles less than 70 degrees are much preferred. Computer analysis of these linkages showed that the maximum acceleration is at the pivot point a2, which is the "elbow." This occurs just before the piston reaches bottom center. Figure 5-10 shows the completed linkage.

Figures 5-11 and 5-12 show the bracket design for holding the bottom (fixed) end of the grasshopper linkage in the modified oil-pan. The modified oil-pan is shown in Figures 5-13 and 5-14. A photograph of the bracket holding the fixed pivot of the grasshopper linkage is shown in Figure 5-15, upper. Figure 5-15, lower, shows a photograph of the modified oil-pan. Figure 5-16 shows the bracket attaching the grasshopper linkage to the big end of the connecting rod.

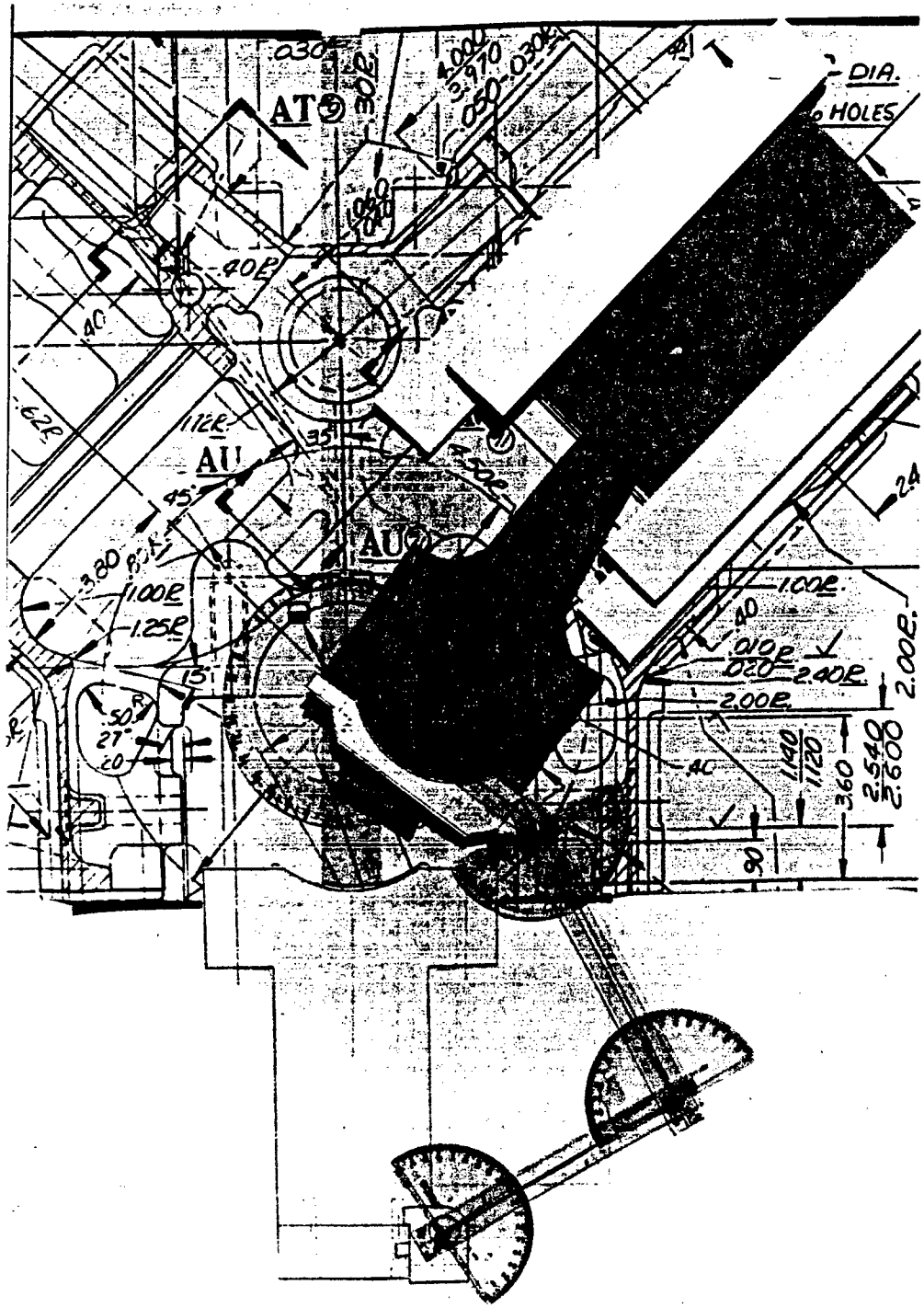

Figure 5-9. Photograph of Layout Board for Designing Grasshopper Linkage

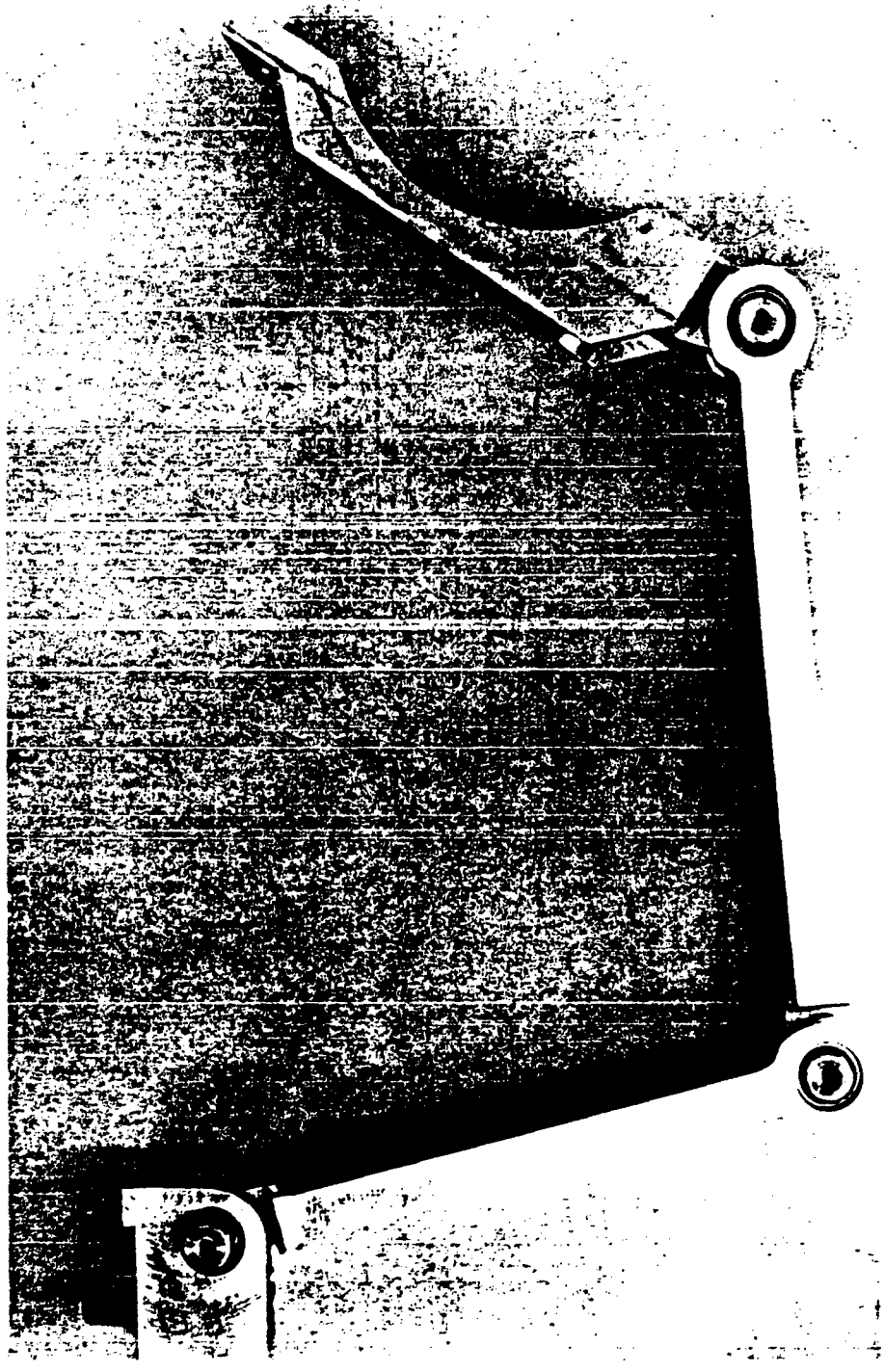

Figure 5-10. Photograph of Completed Grasshopper Linkage

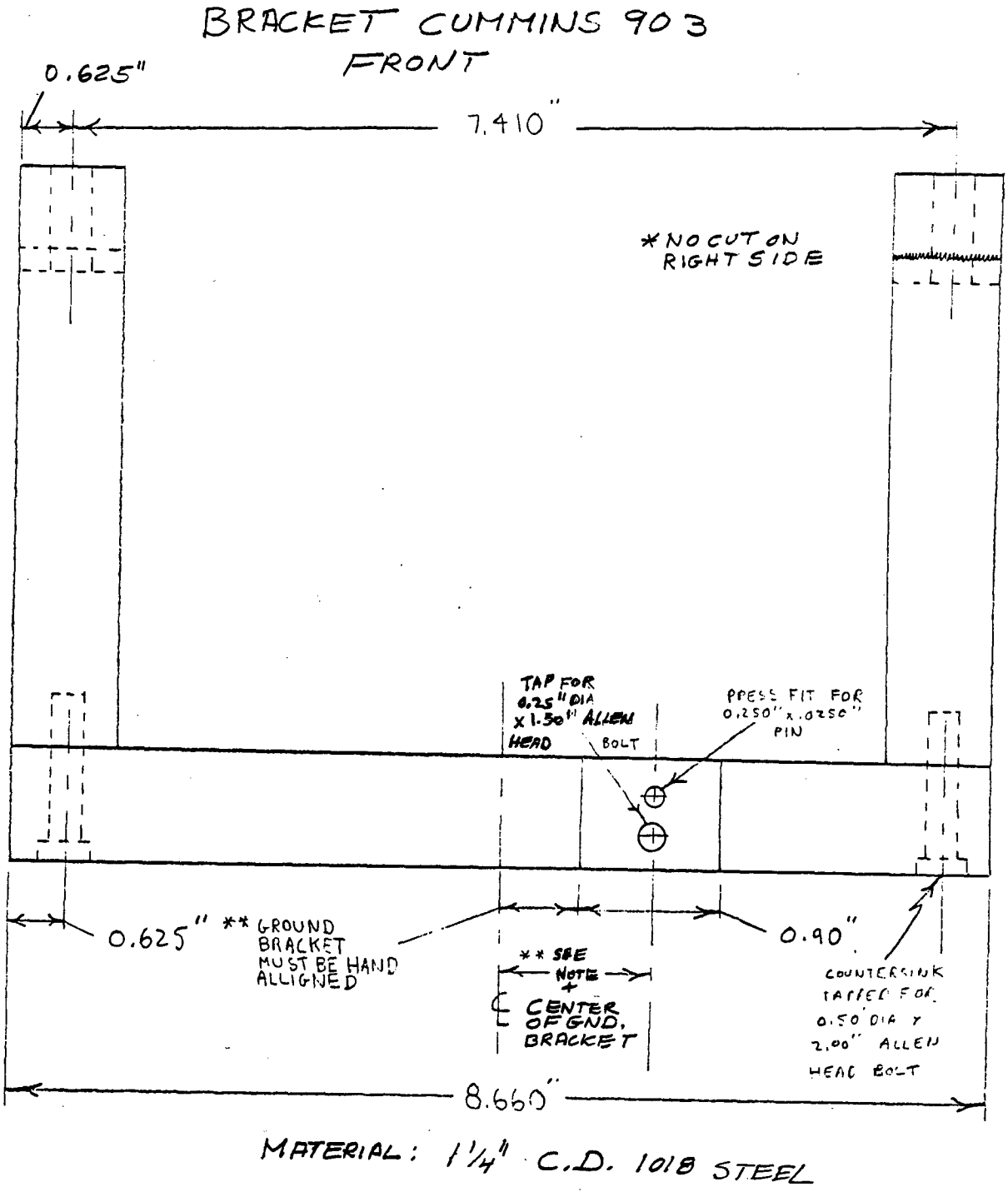

Figure 5-11. Lower-End Bracket, Side View

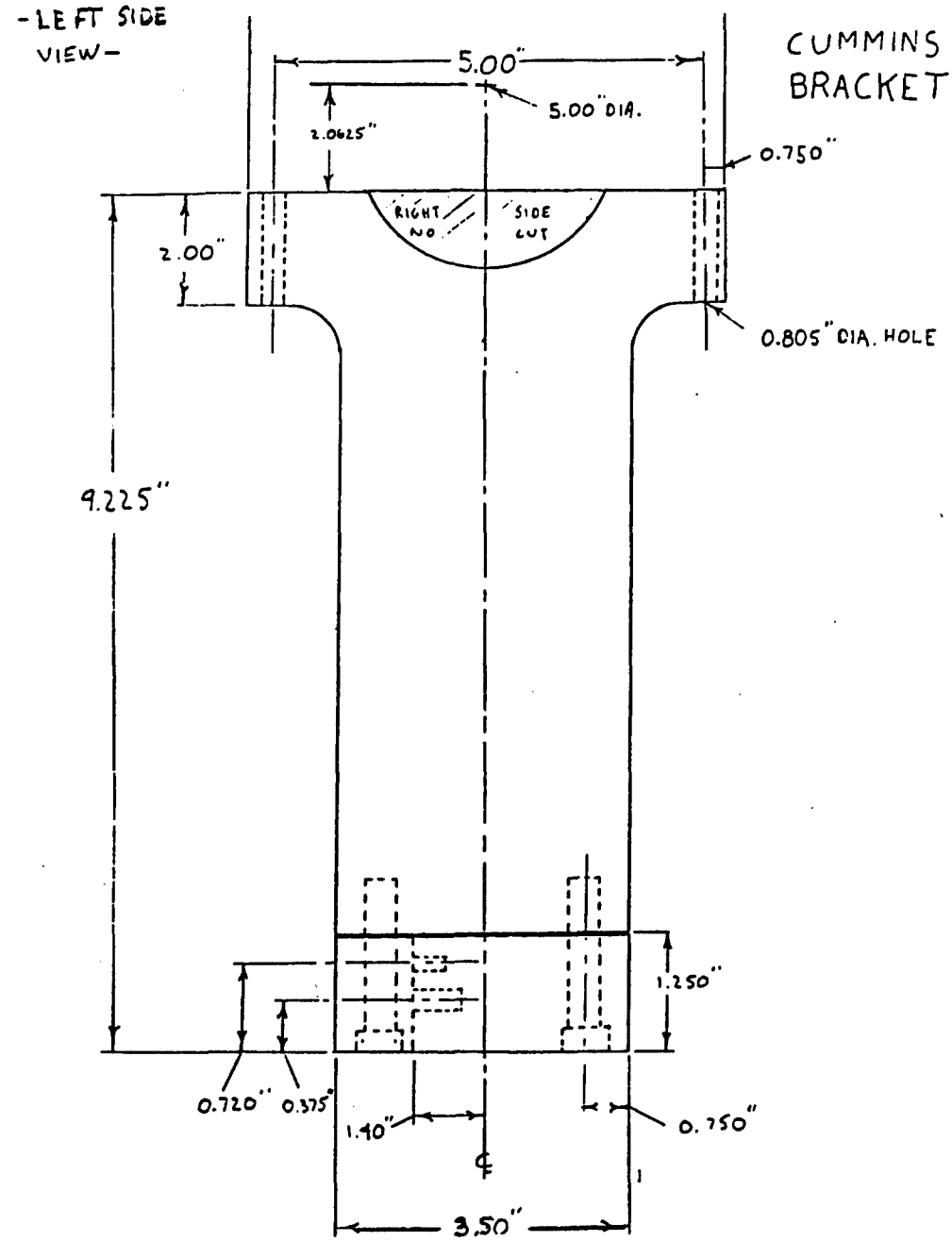

Figure 5-12. Lower-End Bracket, End View

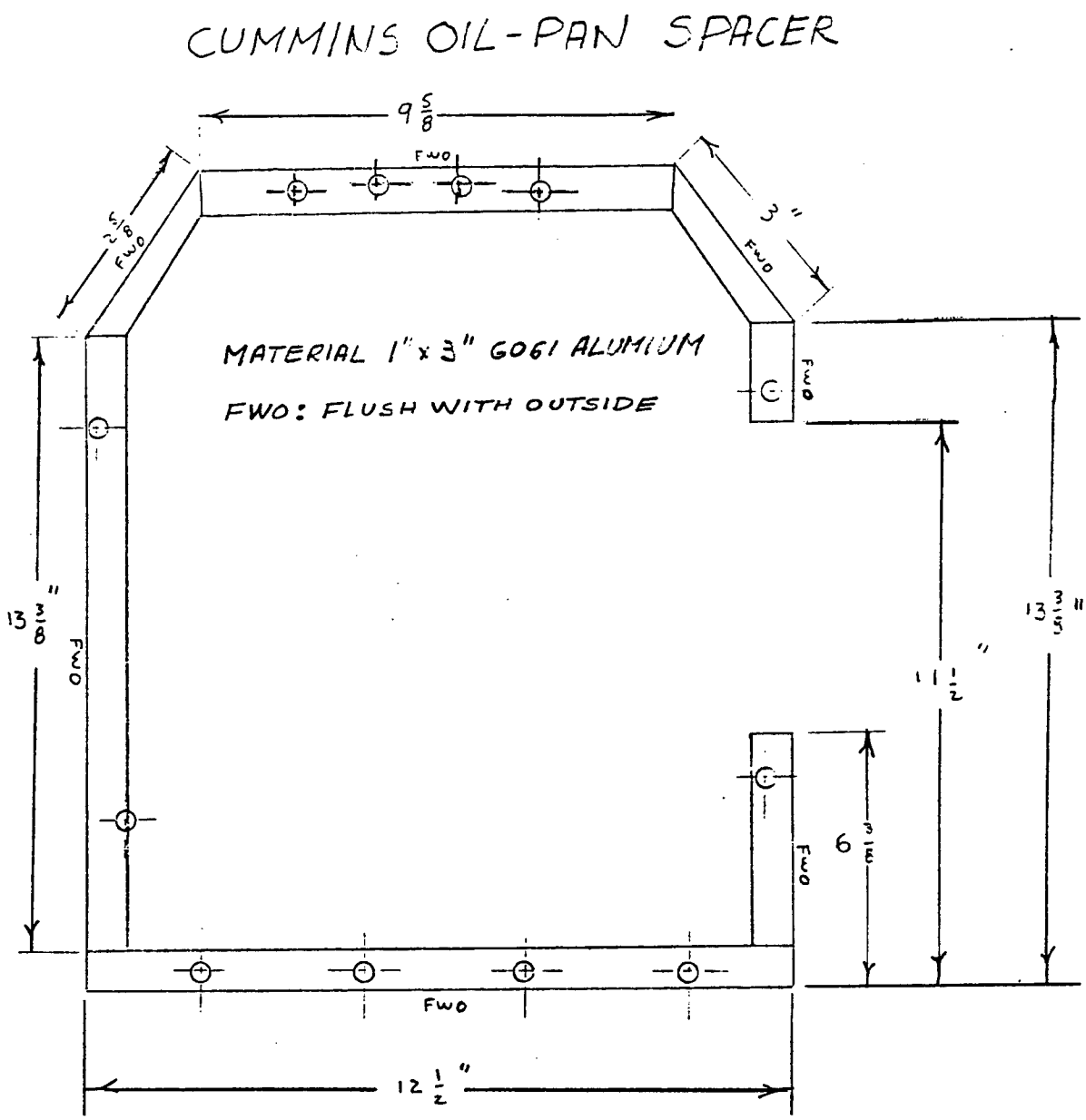

Figure 5-13. Oil-Pan Modifications

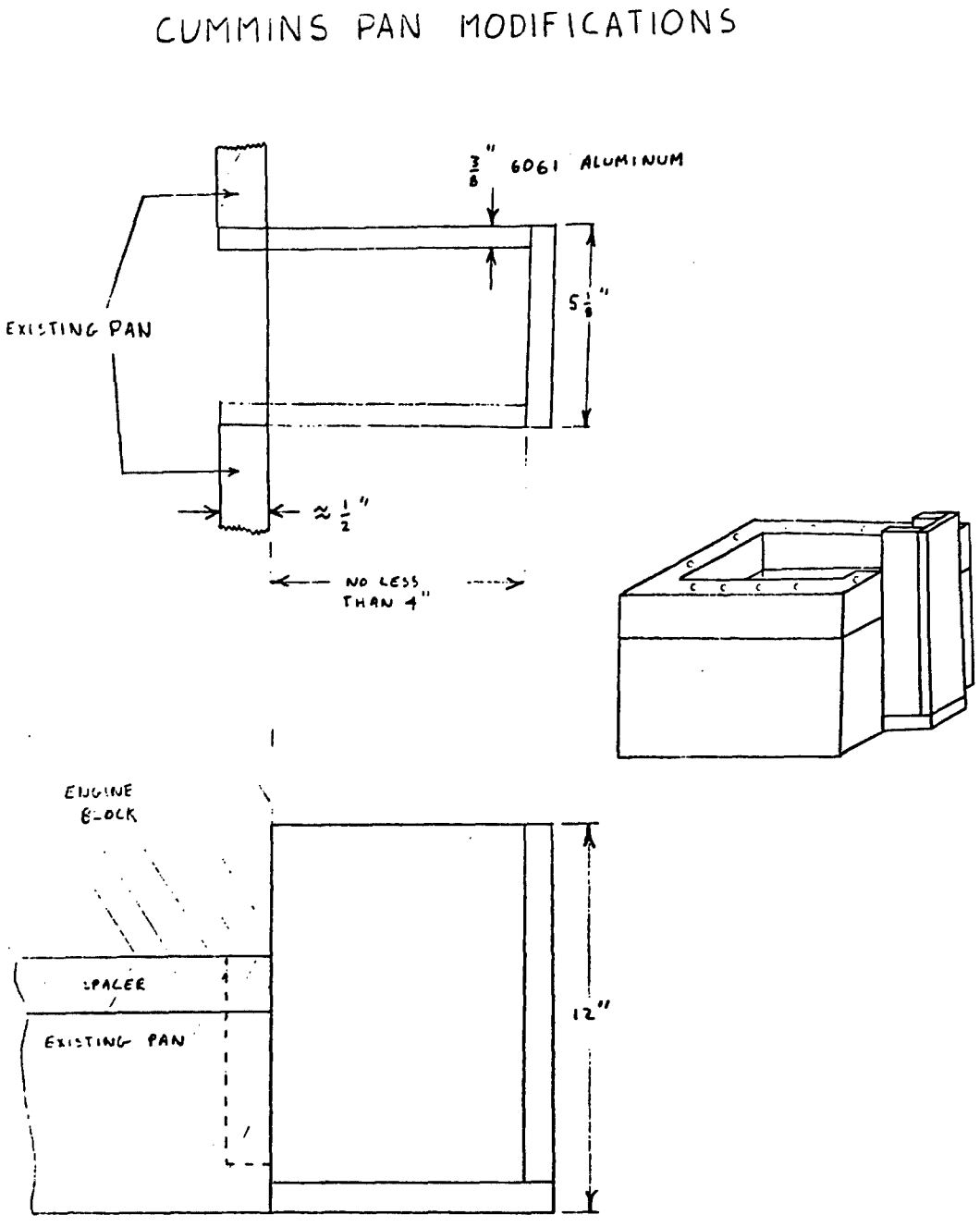

Figure 5-14. Oil-Pan Spacer

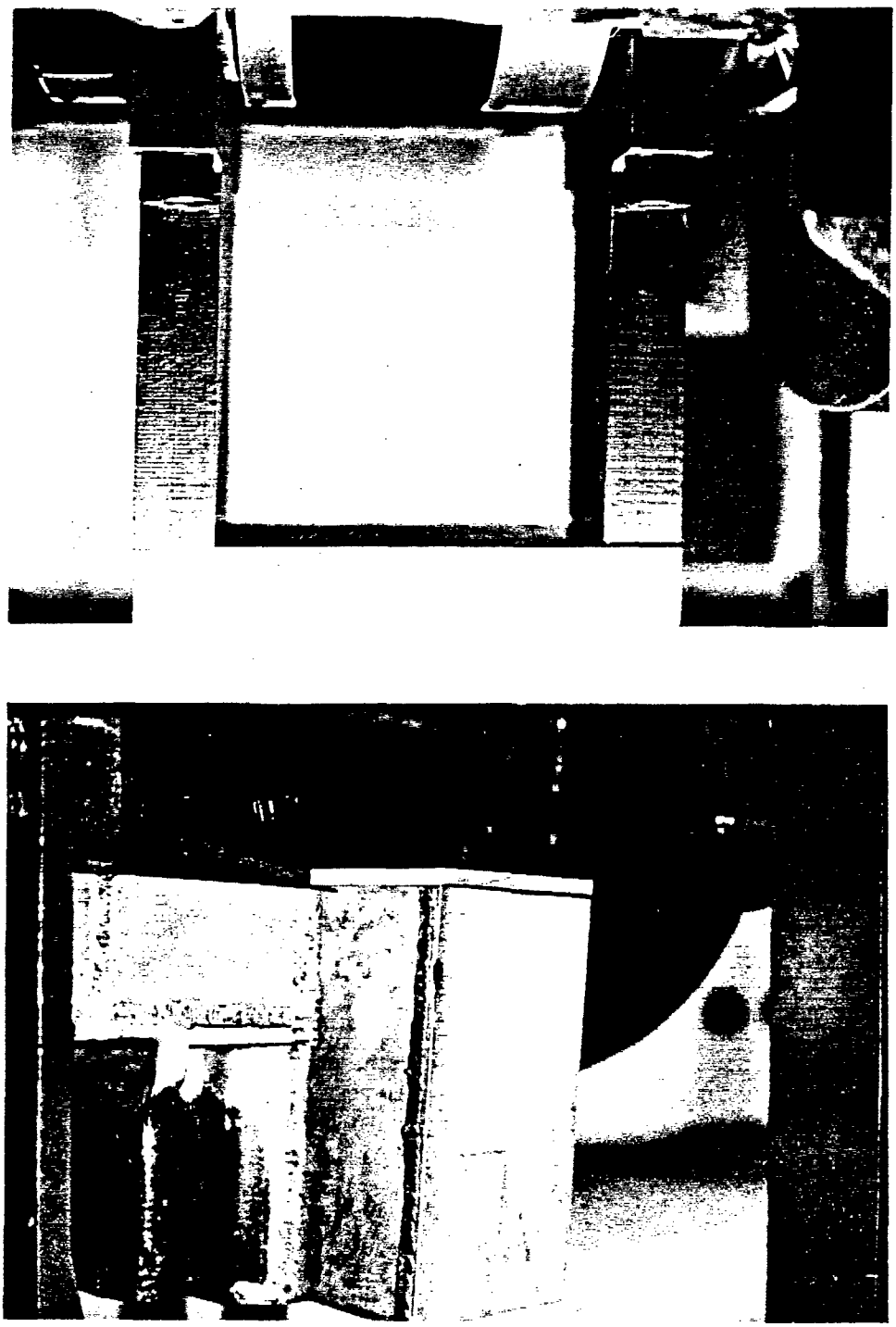

Figure 5-15. Photographs of Lower-End Bracket (upper) and Oil-Pan Modifications (lower)

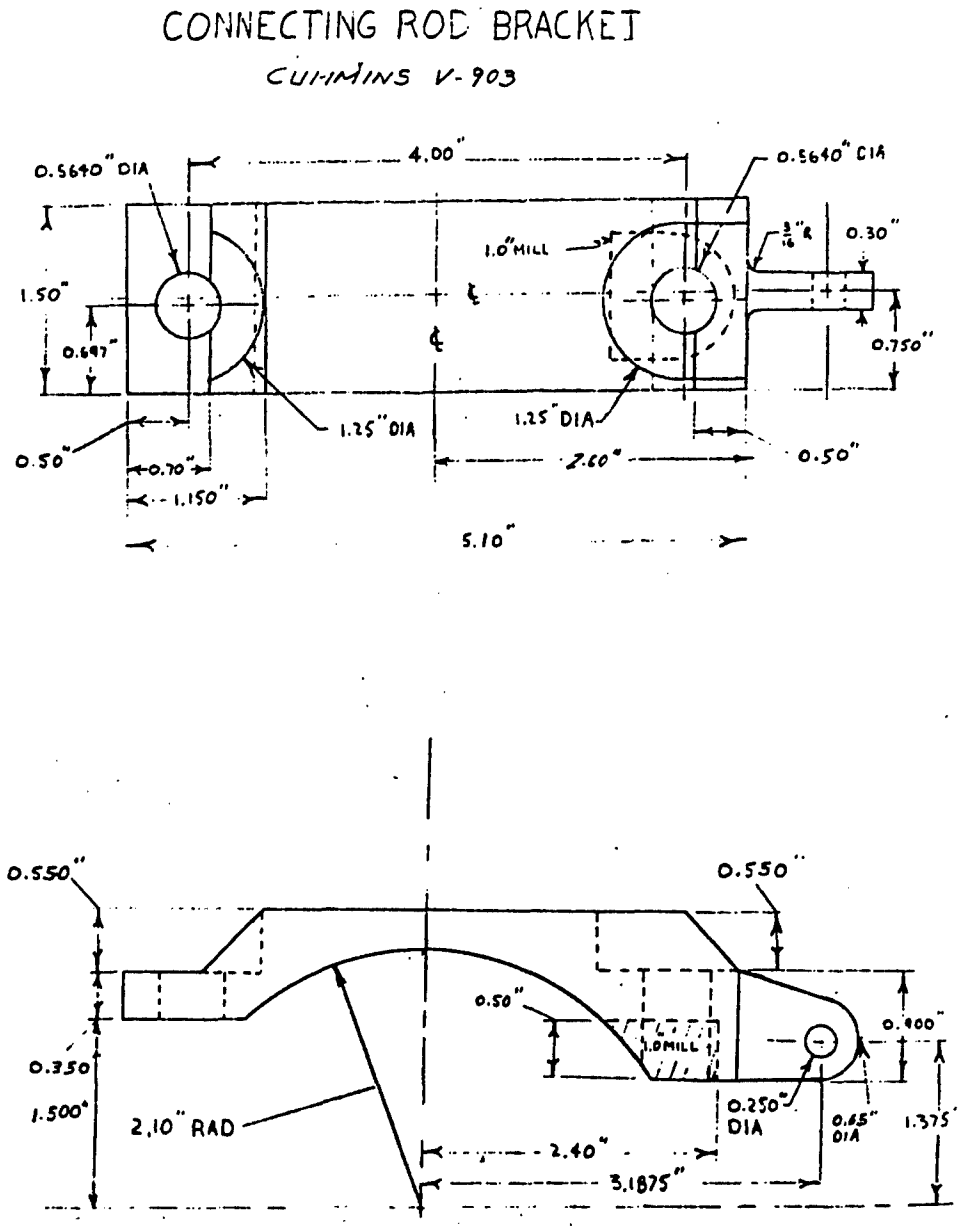

Figure 5-16. Grasshopper to Connecting Rod Attachment Bracket

The final Grasshopper linkage design parameters were:

Top member length	6.90"
Bottom member length	6.00"
Swing angles a1	65 deg
a2	57 deg
a3	56 deg
Upper pivot pin relative to connecting rod big end centerline (rod vertical)	X = +3.188" Y = -1.375"
Bottom pivot pin relative to crank center	X = +2.15" Y = -11.96"

This linkage was satisfactory in that it never broke, and the wires it carried never broke.

5.3.1.3. Cylinder Pressure-Transducer. A key aspect of the Instantaneous IMEP method is the correct measurement of the cylinder pressure at each crank angle. Our experience indicates that the Kistler 7061 transducer is the best available. This is a water-cooled unit, requiring a 14 mm installation hole. The transducer was installed in a virtually flush mounted manner in the Cummins 903 cylinder head. The transducer was contained in a 303 stainless steel sleeve. This prevented engine oil and coolant from contacting the transducer and cable connections. A copper compression washer provided a seal against cylinder pressure. The transducer installation, including sleeve, are shown in Figures 5-17 to 5-19. Figure 5-20 presents photographs showing the installation of the pressure transducer into the cylinder-head.

A Ruska Model 2400 HL dead weight tester was used to calibrate the pressure-transducer. Six calibration pressures up to 300 psi were applied. The procedure was repeated several times. Finally, the curve of calibration voltage versus pressure was fit by the least squares method. Subsequently, the pressure-transducer was used to calibrate the strain-gauges applied to the connecting rod. This gave an internally consistent calibration between the cylinder pressure and strain-gauge signals. The Kistler Model 504E10 charge amplifier was used with the Kistler transducer.

5.3.1.4. Strain-Gauged Connecting Rod. An integral part of the Instantaneous IMEP method is to measure the compressive stress in the connecting rod. This requires machining flats on the connecting rod. Figure 5-21 shows the machined rod prior to application of the gauges. The intent of the machining is to provide smooth surfaces which are symmetric about the neutral axis of the rod. Micromeasurements strain

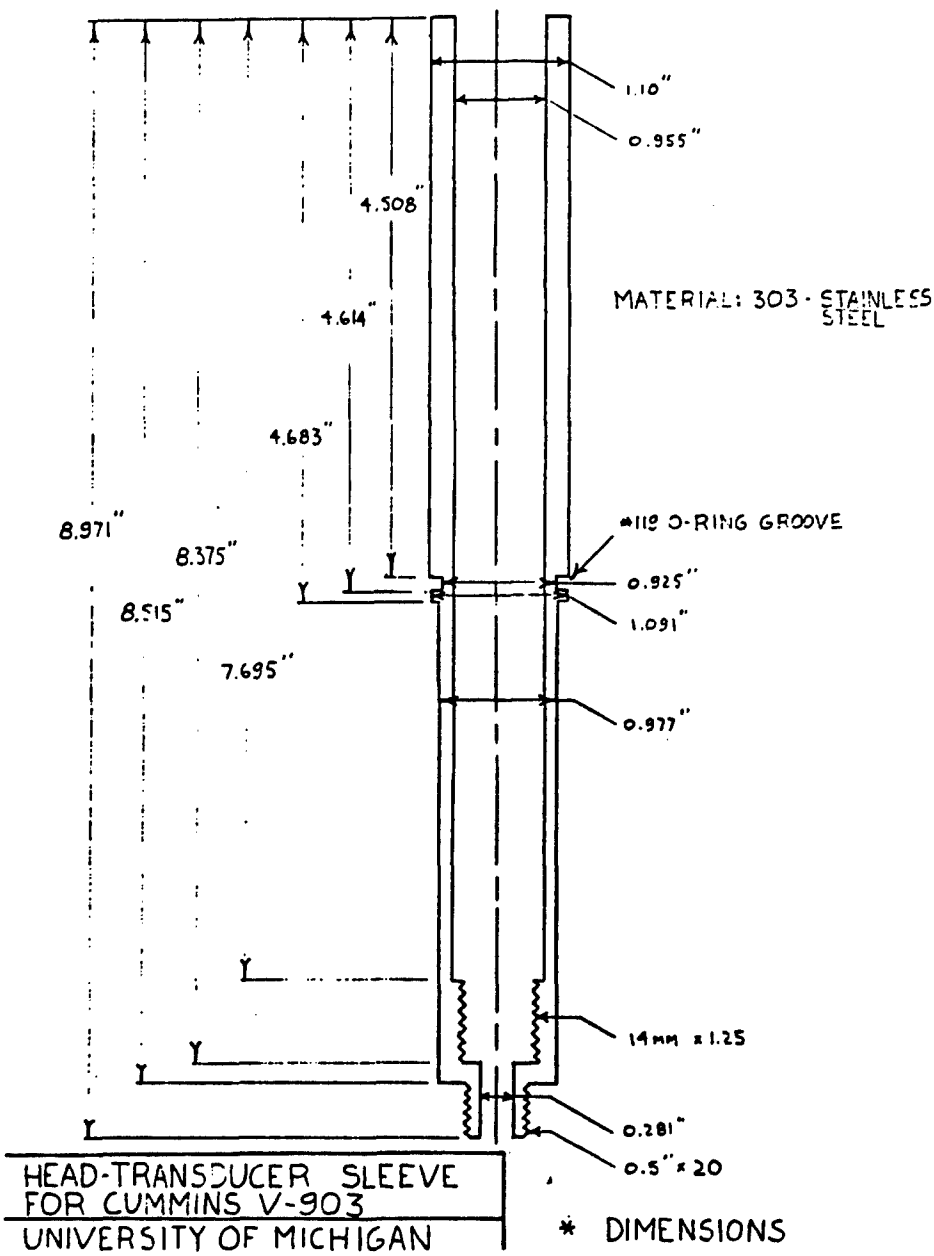

Figure 5-17. Pressure-Transducer Sleeve

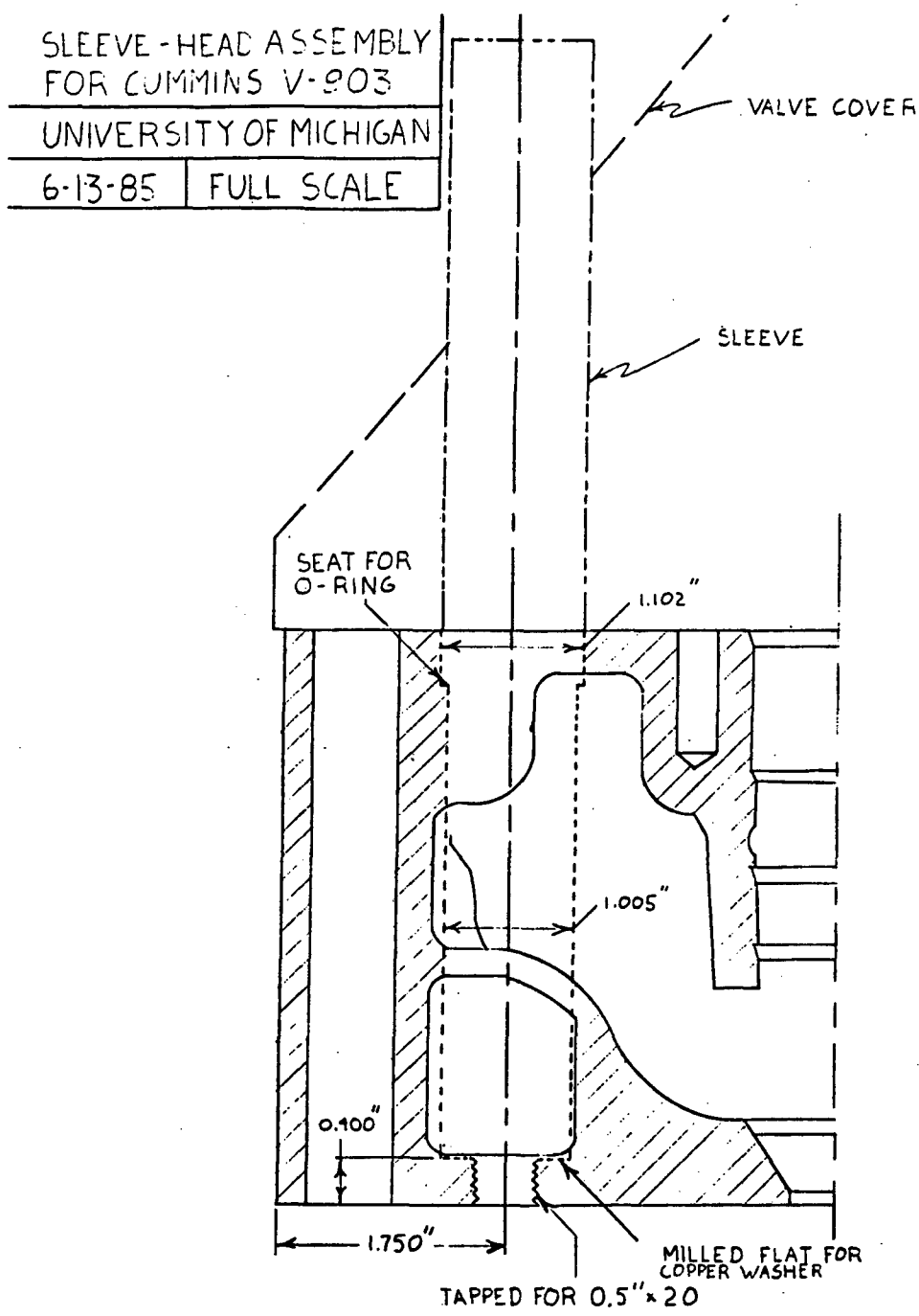

Figure 5-18. Sleeve and Head Assembly

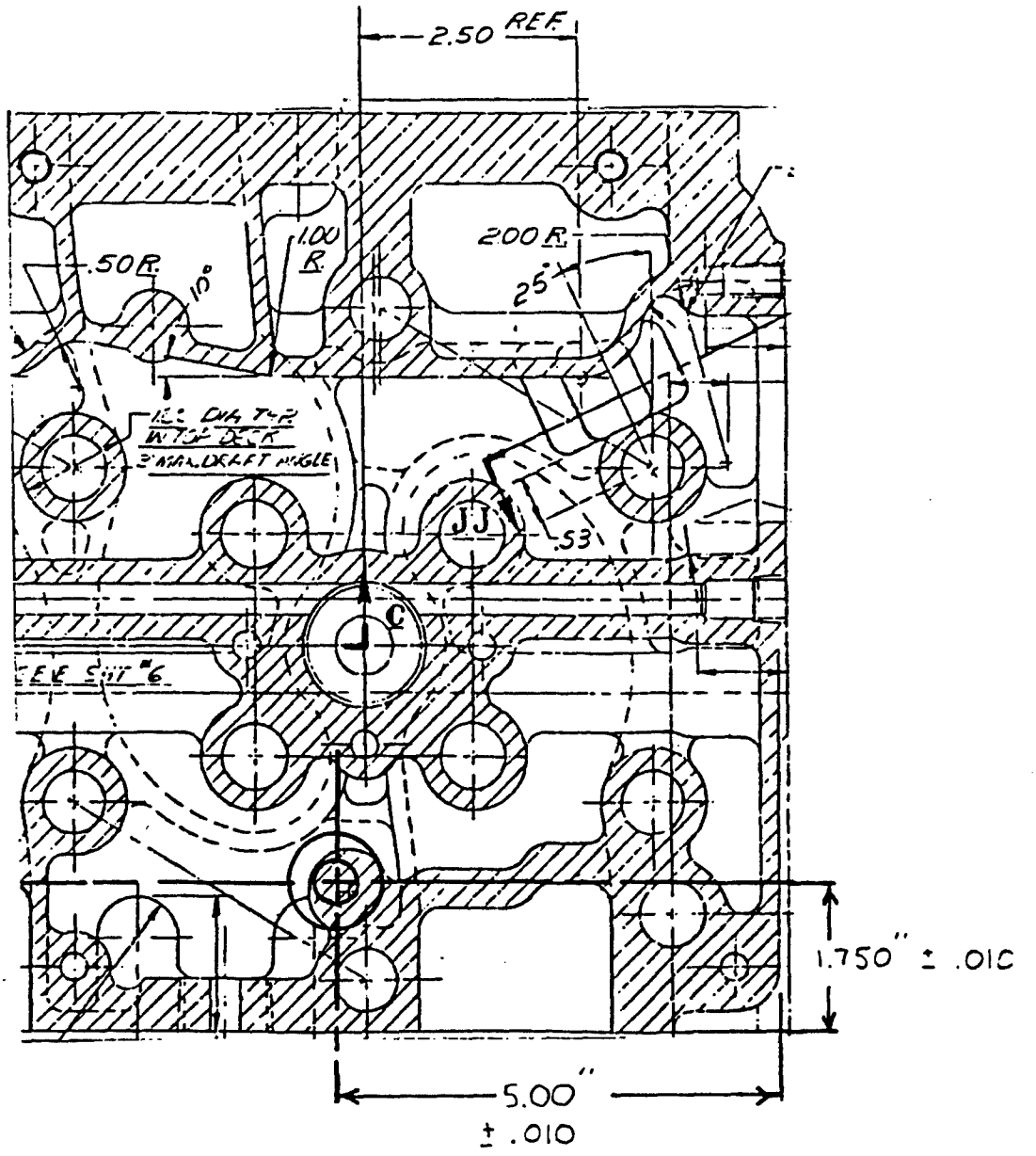

Figure 5-19. Pressure-Transducer Location in Head

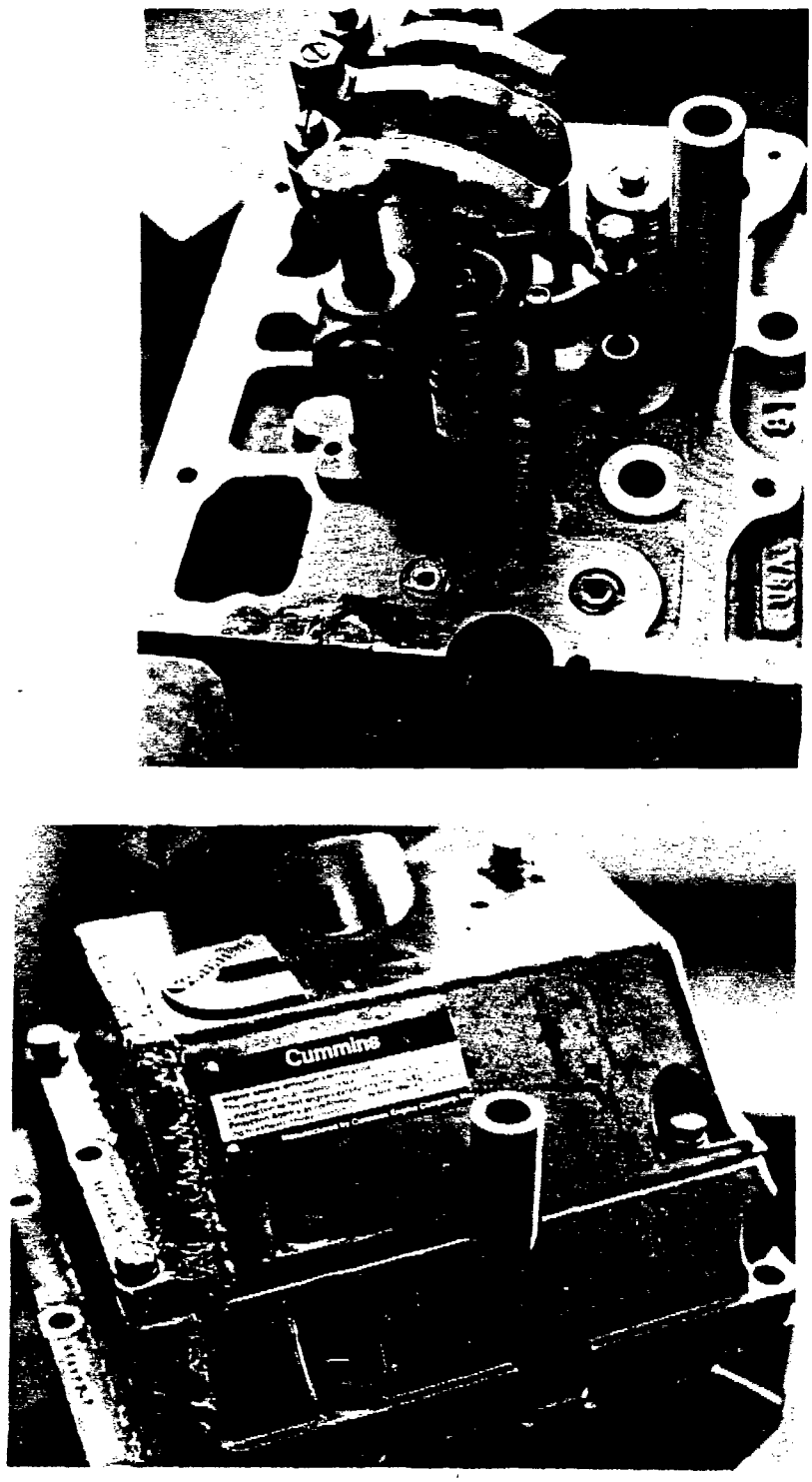

Figure 5-20. Photographs of Pressure-Transducer Installation

Figure 5-21. Photograph of Machined Connecting Rod

gauges Model WK-06-062TT-350 with resistance of 350 ohms were used. These are pairs of gauges mounted at right angles.

After the gauges were applied and the rod installed, the engine was motored for a few hours, in order to age the gauges. Then the strain-gauges were calibrated twice as follows. A one-inch thick flat plate with two 14 mm tapped holes and one-inch spacer was bolted to the cylinder block deck to allow introduction of calibration pressure and mounting of the pressure-transducer. Steam heated coolant was circulated to control temperature during calibration. The crankshaft was locked at two different crank angles using brackets on the flywheel, and a nitrogen bottle was used to apply continuously increasing and decreasing pressure to the piston. Stain-gauge and pressure-transducer outputs were recorded simultaneously, and then calibration constants were calculated from this data. These constants are the relationship between applied force and voltage output, which together with bending and temperature corrections are described in References 1 and 2. A Micromeasurements Model 2310 strain-gauge amplifier was used.

5.3.1.5. Data Acquisition. The Instantaneous IMEP method requires simultaneous measurement of cylinder pressure transducer and connecting rod strain-gauge voltages at one crank angle degree intervals. A data acquisition system was developed based on the IBM PC-XT, which enabled these measurements at engine speeds up to 3000 rpm, a computer data acquisition rate of 18 kHz. Ultimately, the data acquisition rate was 20 kHz. A 12-bit resolution system was used. At this resolution the error caused by a variation of one bit is 0.25 percent, well within the objective of 1 percent accuracy. That is one part in 4096. Data for nine consecutive engine cycles were stored in memory for transfer to a floppy disk. At the same time, the friction force as a function of crank angle, was calculated and periodically displayed on the a high-resolution (720 point up by 450 down) monochrome monitor display screen (Figure 5-22). In this manner, it was possible to determine if the data "looked right" as it was being acquired. A dot matrix printer with graphics capability allowed print out of test conditions, as well as the monitor display.

Two Techmar Labmaster 2009 option TM-40-PGH analog to digital conversion boards were installed in the IBM XT for the data acquisition. These were triggered by the optical encoder mounted on the engine crankshaft (Figure 5-23). In some engine tests, a commercial crank angle encoder, the Ledex Model RC23-DM-360-5SE-1B, was substituted. Sample and

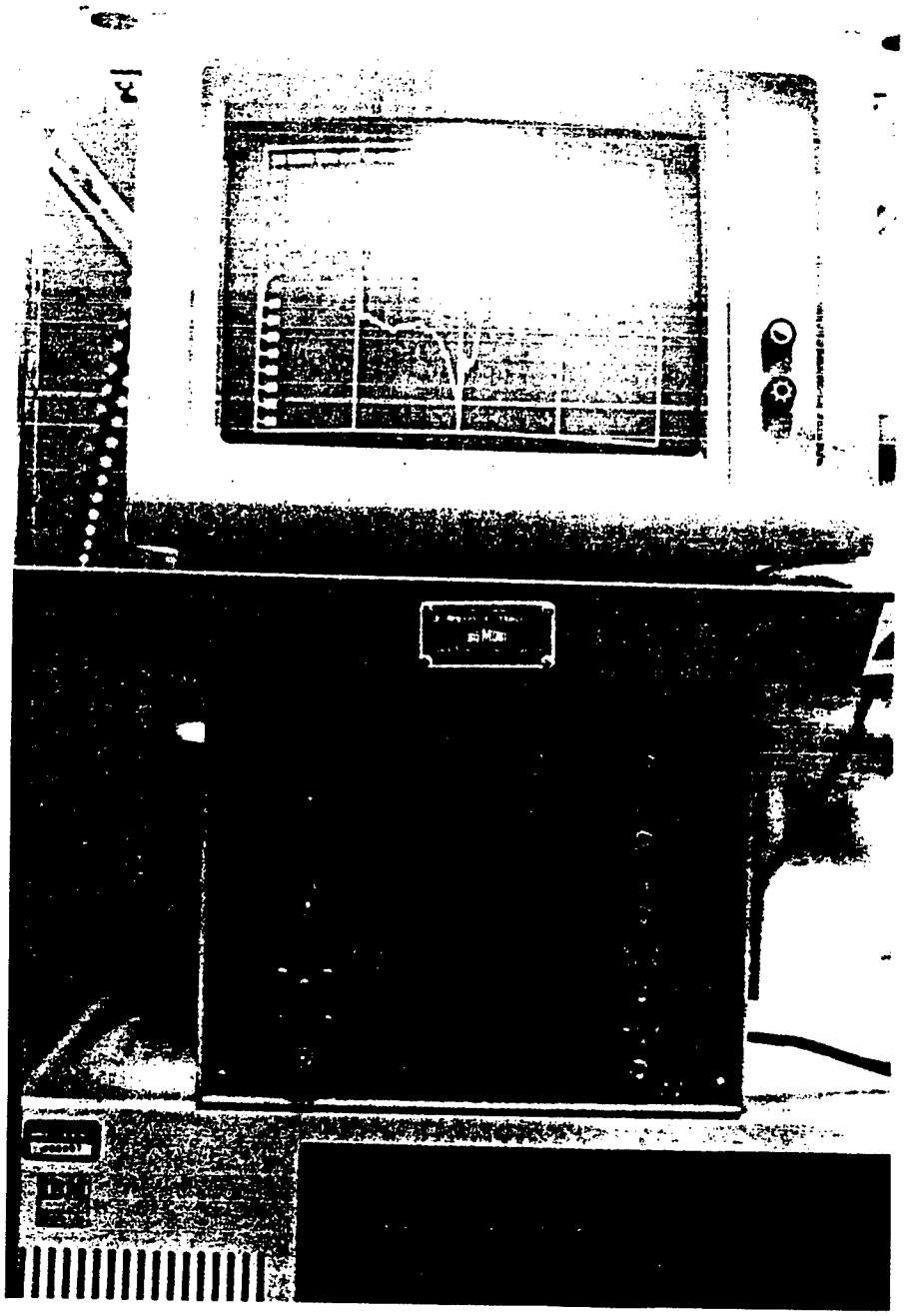

Figure 5-22. Data Acquisition System and Display

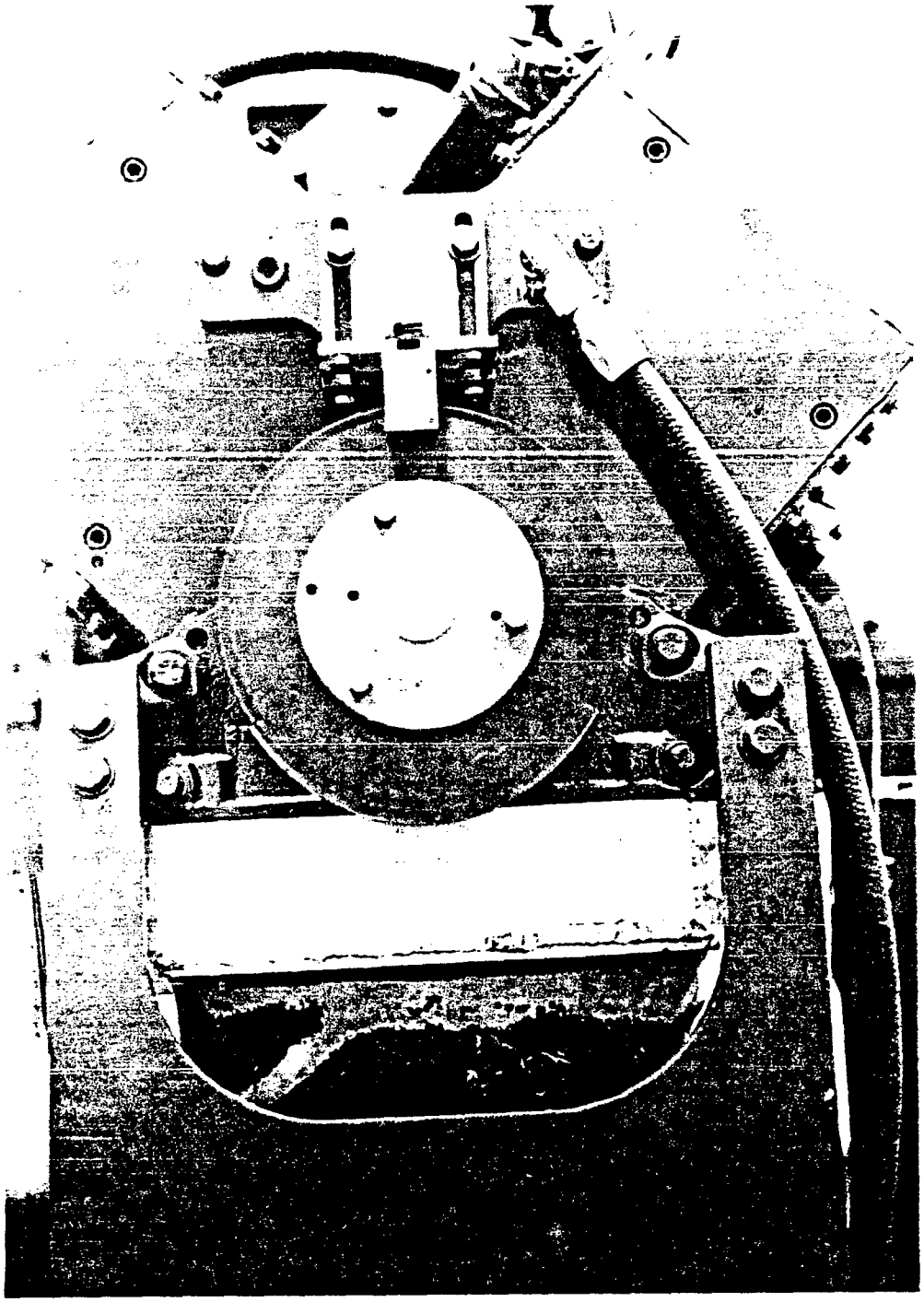

Figure 5-23. Crankangle Encoder Installed on Front of Engine

hold circuits on the A/D boards remember and hold the voltage until the next trigger signal, giving the computer time to acquire the data. The circuit of this data acquisition system is in Figure 5-24. Every other top dead-center pulse is removed, so that the crank angle pulses can be gated through, starting with TDC on the intake stroke. A block diagram of the system software is shown in Figure 5-25. The main programs were written in Fortran with an assembly language subroutine linked to the data collection program for fast data acquisition. This data acquisition system was further used for measuring the time interval between crank angles, for determining the speed variation of the crank, and in the data acquisition of the Fixed-Sleeve method.

5.3.2. Implementation of the Fixed-Sleeve Method.

5.3.2.1. Implementation on the 4.1-Litre Engine. This gasoline engine is unique in that it is comprised of a die cast-aluminum block into which are inserted cast-iron liners. It presented a very convenient vehicle to implement the Fixed-Sleeve method. In the Fixed-Sleeve method the cylinder-head is not modified, except that a flush mounted, water cooled, Kistler 7061 pressure-transducer was installed in a manner similar to that described in 5.3.1.3., except that it was installed through the front of the cylinder-head in number 1 cylinder.

The cylinder block was modified in that a sleeve was inserted within a modified steel replica of the removable production liner. Acting on this sleeve are both the friction force of the piston and rings and the combustion gas-pressure force acting on the upper rim of the sleeve. That gas force, acting on about 6.5 square cm of rim area, is then subtracted from the total, leaving the friction force as a function of crank angle.

The combined gas and friction forces are measured by full-strain-gauge bridge circuits uniformly spaced on both inside and outside of the slender section (1.5 mm thick) of the tailpiece of the outer liner. The gauges and method of application are similar to that described in 5.3.1.4. for the Instantaneous IMEP method. In this design, a total of 16 active and 16 dummy gauges were used. The arrangement provided temperature and bending compensation and enough sensitivity to resolve better than one-pound force. The production cylinder-head and gasket seal against the outer liner as in the production engine. A smaller 80 mm piston, provided by Cadillac engineering, and specially built cast iron liners, provided by SPX Corporation, were used with an otherwise production engine, except that a carburetor and

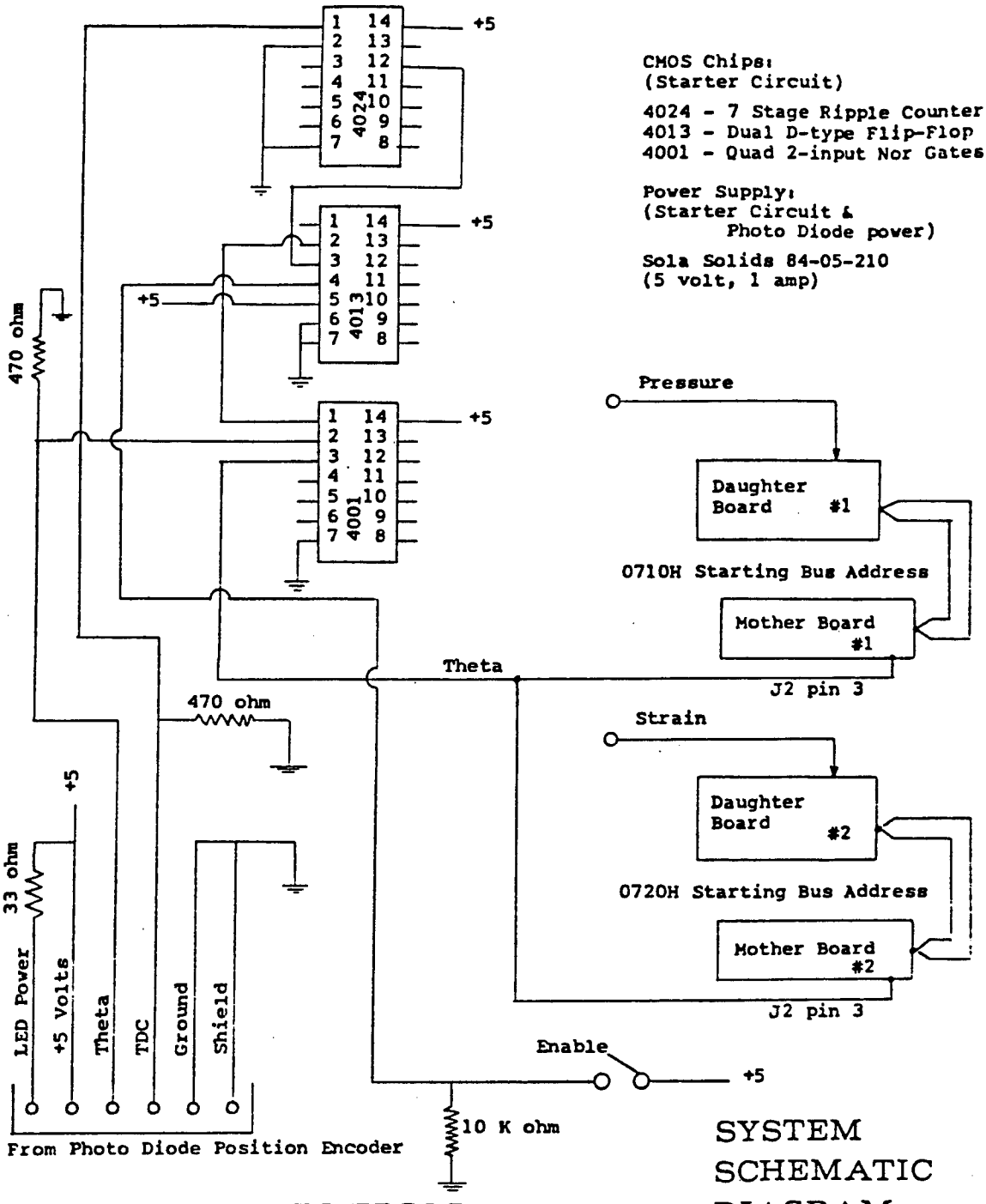

Figure 5-24. Schematic of Data Acquisition System

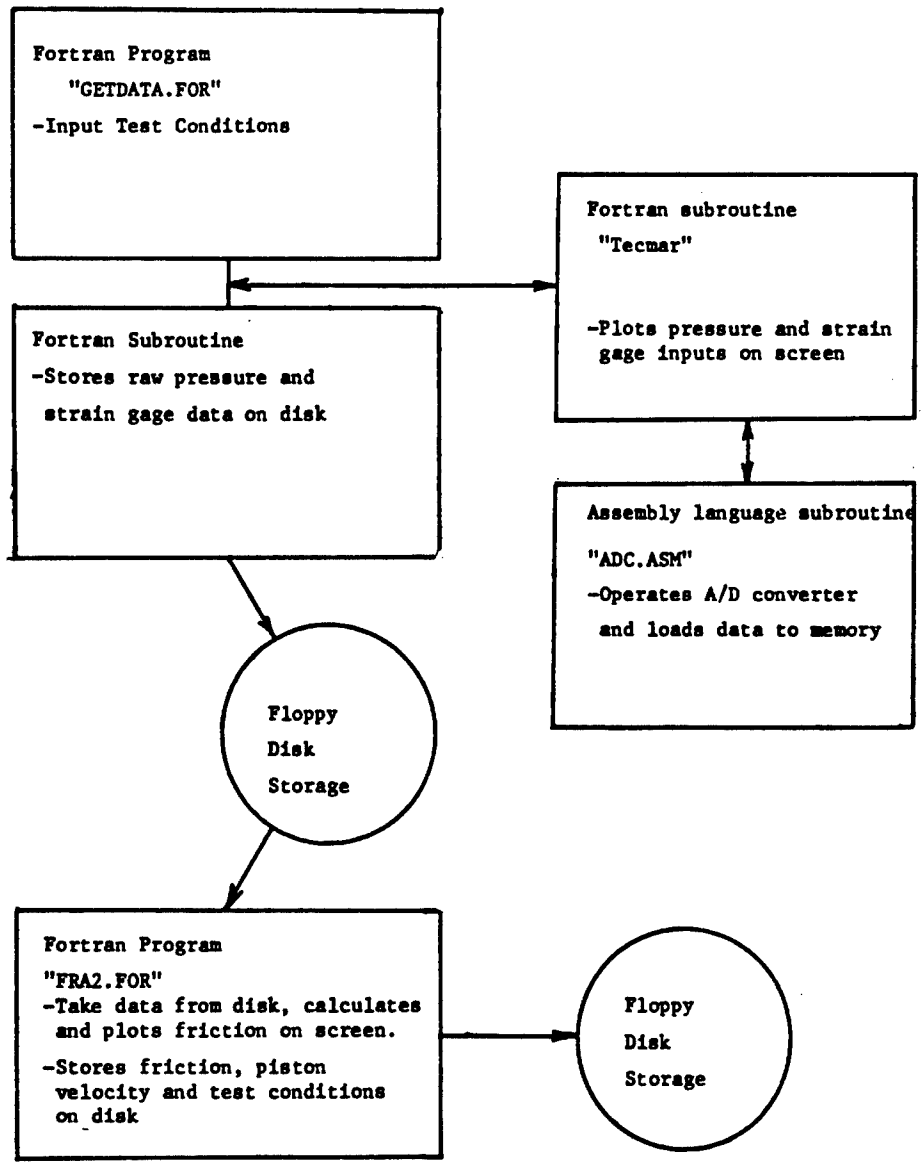

Figure 5-25. Block Diagram for Data Acquisition System

mechanical distributor were used for experimental convenience. All cylinders were fired for the tests.

5.3.2.2. Additional Details. Referring to Figure 5-6, other features of the design are: tensioned piano wire (0.5 mm dia) near the maximum side thrust region, to pilot the inner sleeve and keep it from contacting the outer liner (which gives no axial restriction.); soft silicon O-rings for isolating the cooling water and combustion gases; and several holes between inner and outer sleeves, to admit cooling water. The top of the inner sleeve was shaved slightly to avoid any contact with the head. The two sleeves were held together by a pair of lock nuts at the base of the assembly. With this design, both piston and liner can be changed without disturbing the instrumentation. Figure 5-26 shows a photograph of the Fixed-Sleeve assembly components.

5.3.2.3. Implementation on the Cummins 903 Engine.

Basic Design and Instrumentation. A second single-cylinder Cummins 903 engine was set up in Room 246, for the implementation of the Fixed-Sleeve method. In all respects the instrumentation and procedures were identical to those described for the 4.1-litre engine. Each engine presents a different challenge insofar as designing and applying the Fixed-Sleeve method. Figure 5-27 shows a photograph giving an exploded view of the design created for the Cummins 903. At the left is a collar which is rigidly attached to the underside of the block. That collar has a necked-down section with strain-gauges mounted inside and outside. The collar and liner bottom are both threaded. The liner is then inserted into the block and screwed into the collar, which supports it rigidly at the bottom. The top of the liner is specially prepared as a separate piece, shown on the right in the figure. This piece is clamped to the block by the cylinder-head in the same manner as the production engine. The liner and the top piece have a concentric step and are allowed to slip relative to each other. Sealing is accomplished by two O-rings. Combustion gases are sealed by a metal O-ring. A rubber O-ring is located just below the metal ring.

Similar to the 4.1-litre engine, the collar was instrumented with 16 pairs of high-temperature strain-gauges. Each bridge consisted of eight gauges, four of which were equally spaced on the inside surface and the other four on the outside. The bridges were wired so that the gauges measuring the circumferential, or hoop stresses, provide temperature compensation. The gauges were wired to minimize the effects of bending loads. The gauges and wires were

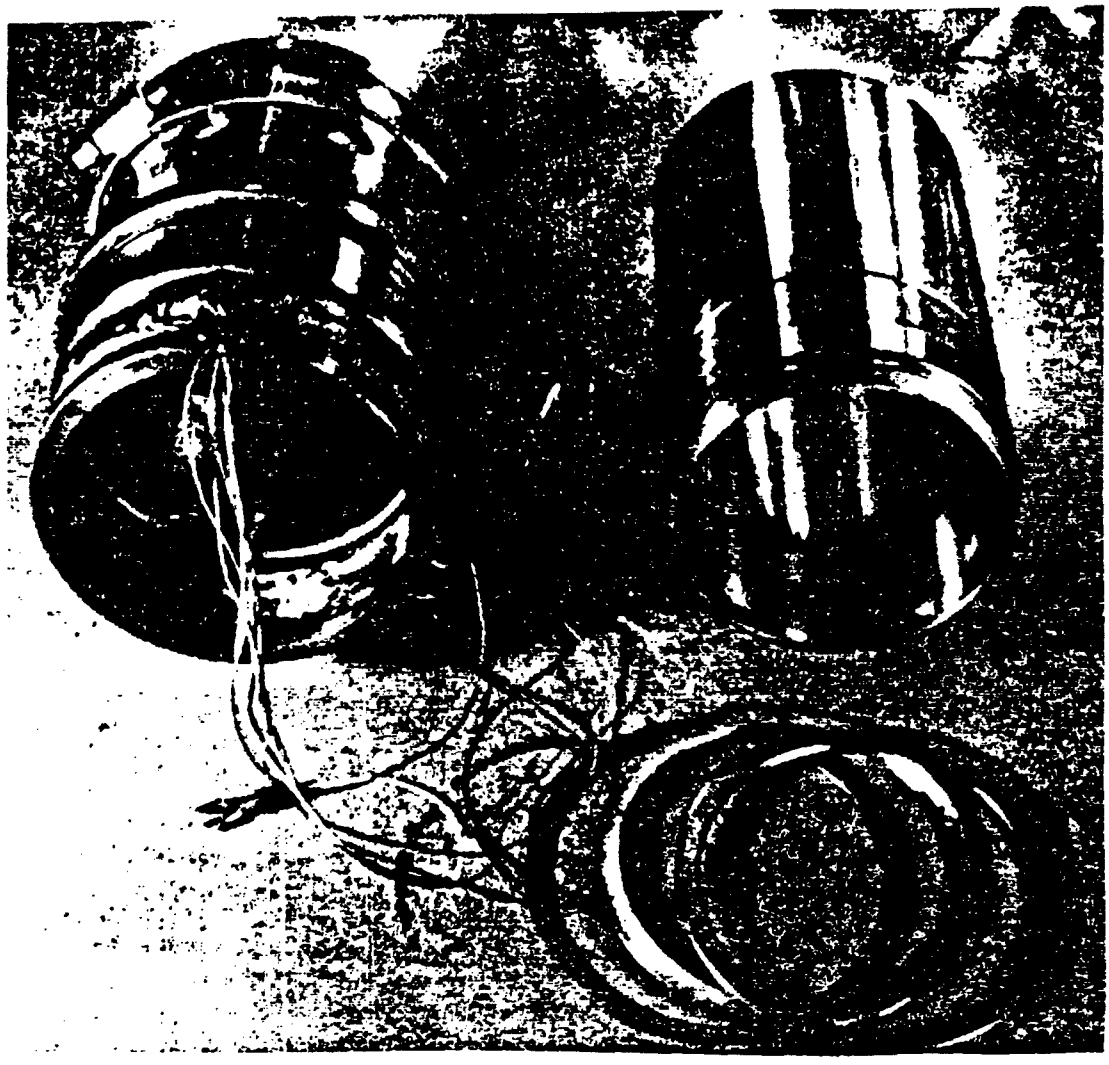

Figure 5-26. Photograph of Fixed-Sleeve Assembly for 4.1-Litre Gasoline Engine

covered with a thin layer of epoxy to protect them from damage and temperature variations due to hot oil.

Calibration. The purpose of calibrating the fixture was to determine the following information:

1. Signal to noise ratio
2. Causes of noise
3. Repeatability
4. Linearity
5. Gauge factor
6. Magnitude of hysteresis caused by O-rings

Signal to Noise Ratio. Figure 5-28 shows the noise present with no excitation. Figures 5-29 and 5-30 show the same conditions, except that the excitation is applied, and 10-(Figure 5-29) and 2-lb weights (Figure 5-30) are alternatively placed on the collar. It can be seen in Figure 5-30 that with no filtering, the noise level is about 1-2 lbf. Figures 5-31 and 5-32 show the same signal (2-lb weight) when 10 kHz and 30 kHz low-pass filters are used.

Causes of Noise. Figure 5-33 is the same as Figure 5-32 except, no load is applied. Figure 5-34 shows a spectral distribution plot of Figure 5-33 obtained with a fast Fourier transform (FFT). This plot is used to detect any 60 Hz component. It is seen that 60 Hz and its harmonics represents a sizable portion of the noise. Figure 5-35 is an spectral distribution of the same signal, but with the sampling rate adjusted so that the FFT would include much higher frequencies. The figure shows the presence of a 1700 Hz signal and its harmonics. After some investigation, it was determined that the IBM monitor was the source. Figure 5-36 shows the signal with the monitor unplugged.

Repeatability and Linearity. Repeatability is excellent, with no observable difference from run to run. Linearity was assessed by putting successively heavier weights on the collar. Figure 5-37 shows the result. The strain-gauges are quite linear, and no correction is anticipated.

Hysteresis. The hysteresis of the O-rings at the liner/top-ring interface has been investigated at atmospheric pressure and room temperature only. No hysteresis was observed, a very desirable result. Subsequently, it was found that the sleeve could not be inserted with the lower cavity seals in place. It was then decided to cool the running engine with engine oil, and eliminate the seals. Thus water was eliminated and no rubber seals used.

Figure 5-27. Components of the Fixed-Sleeve Method for the Cummins 903 Engine

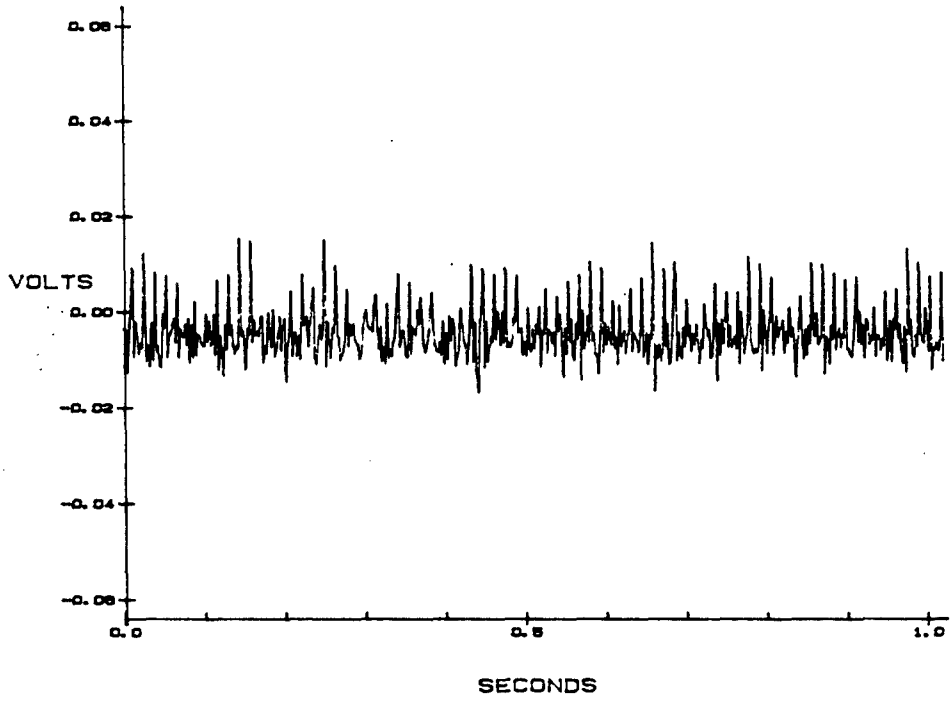

Figure 5-28. Original Strain-Gauge Bridge Noise, No Bridge Excitation

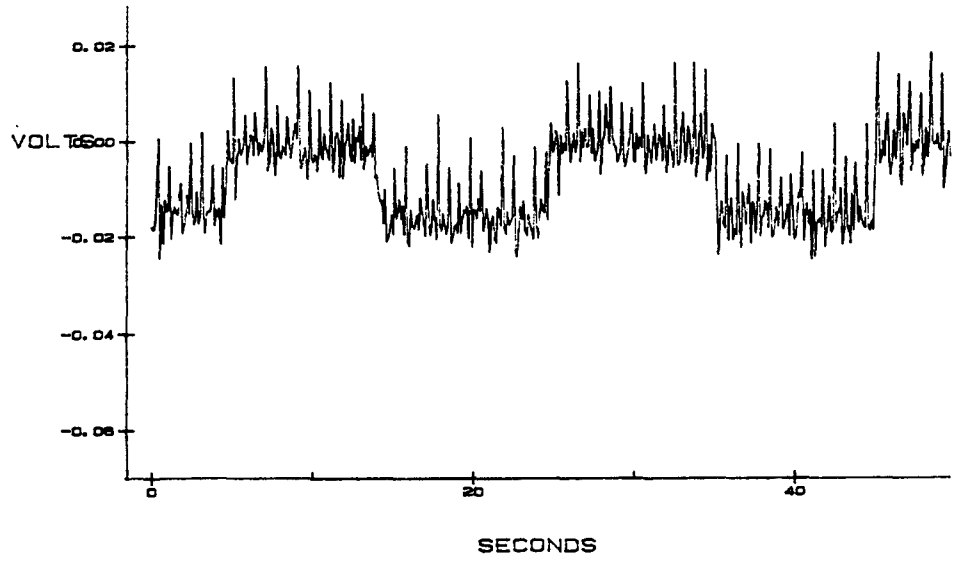

Figure 5-29. Same as Figure 5-28 Except with Excitation, 10 lbm Weight Applied Intermittently

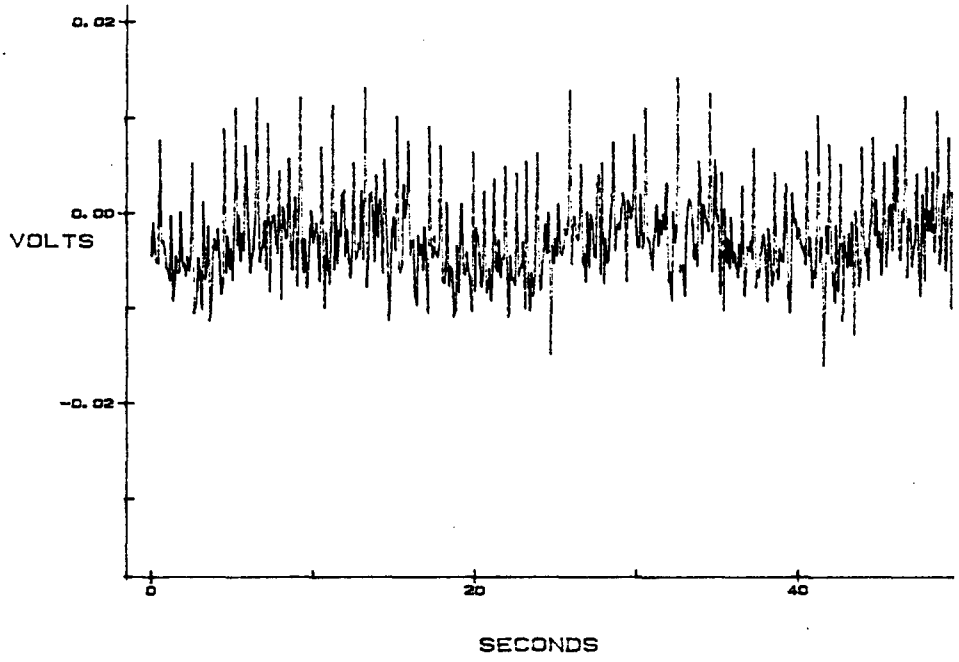

Figure 5-30. Same as Figure 5-28, Except 2 lbm Weight Added

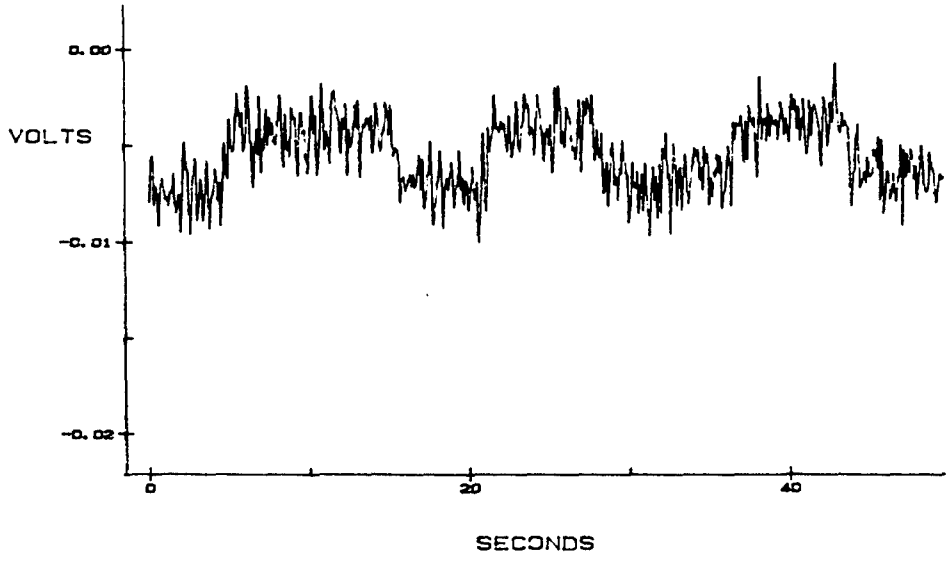

Figure 5-31. Same as Figure 5-30, Except 10 kHz Filter

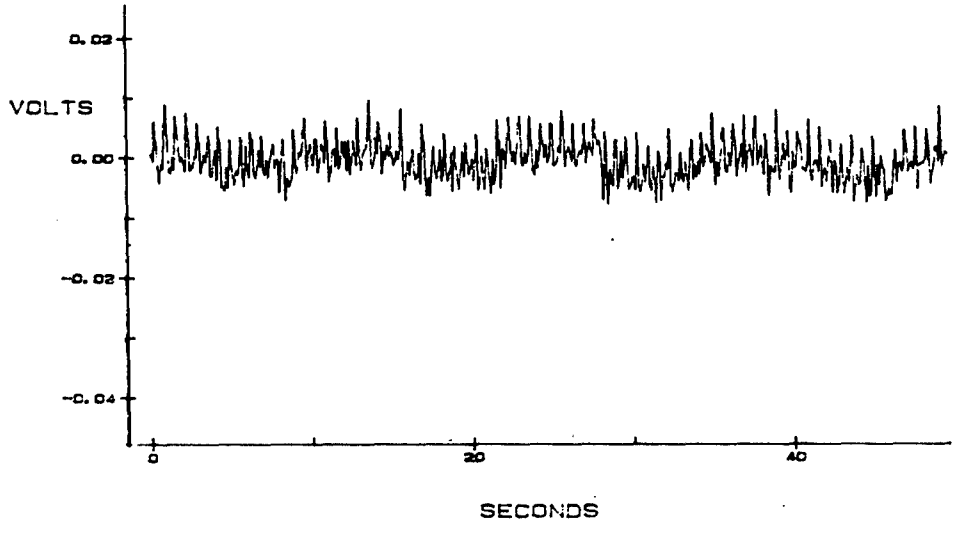

Figure 5-32. Same as Figure 5-30, Except 30 kHz Filter

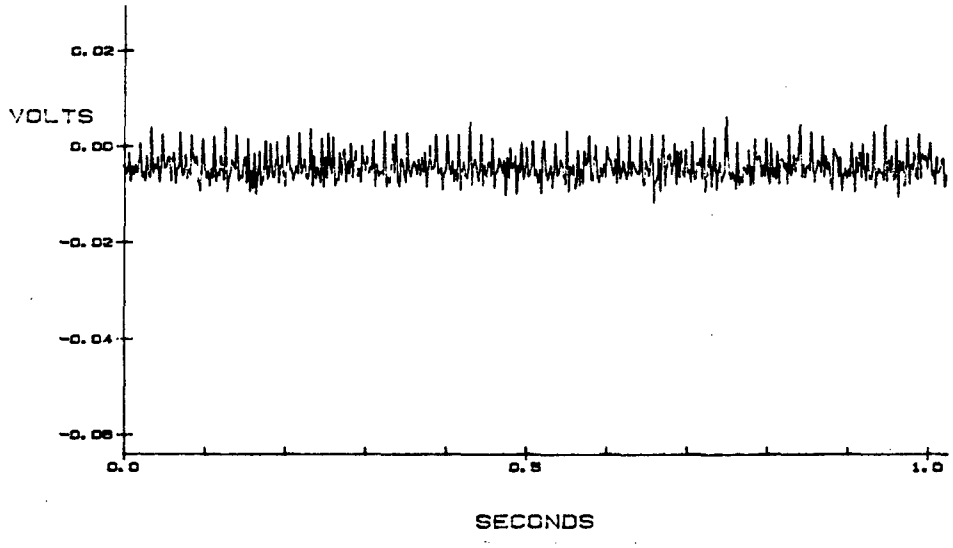

Figure 5-33. Same as Figure 5-32, Except No Load Applied

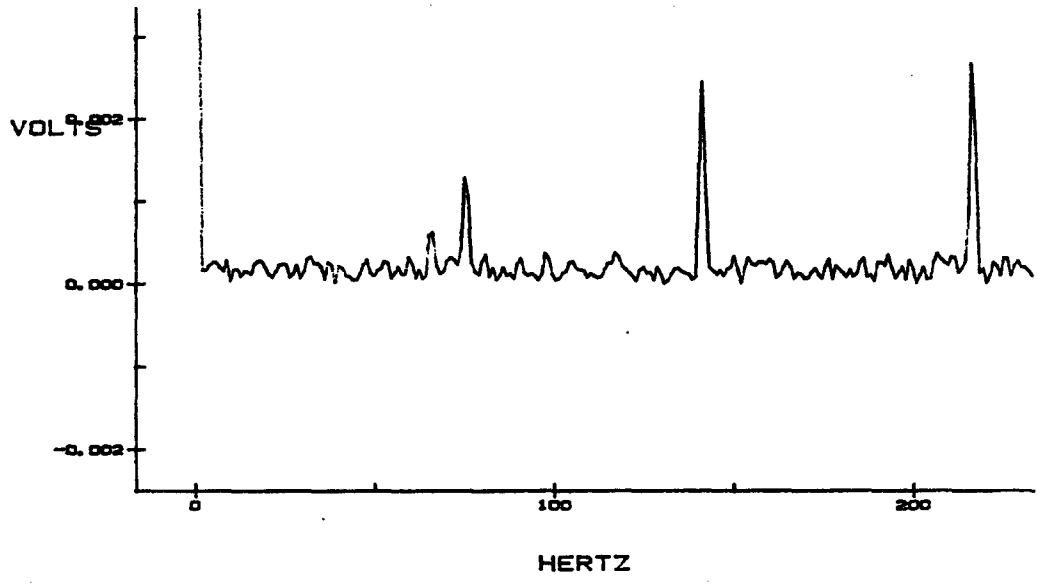

Figure 5-34. Fourier Transform of Figure 5-33

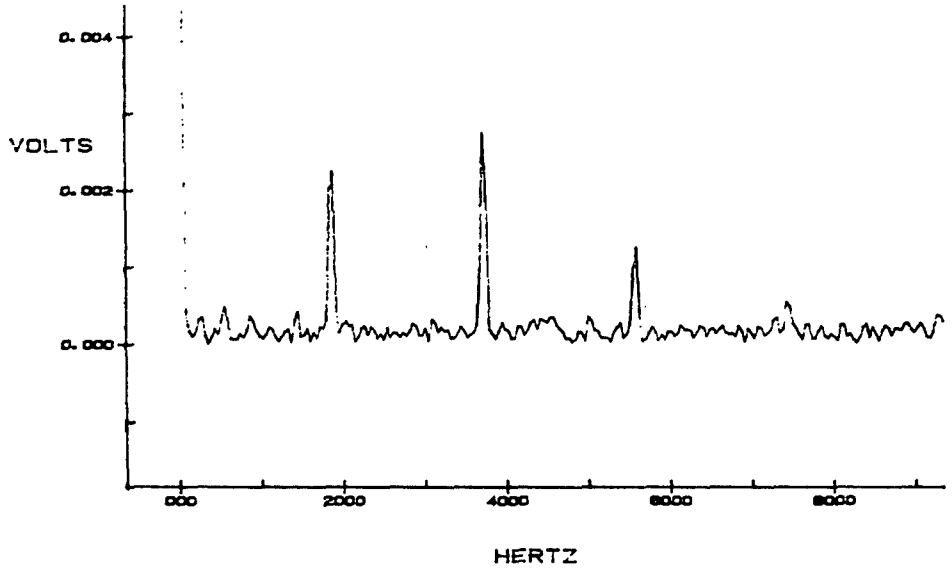

Figure 5-35. Fourier Transform of Figure 5-33, Higher Frequencies

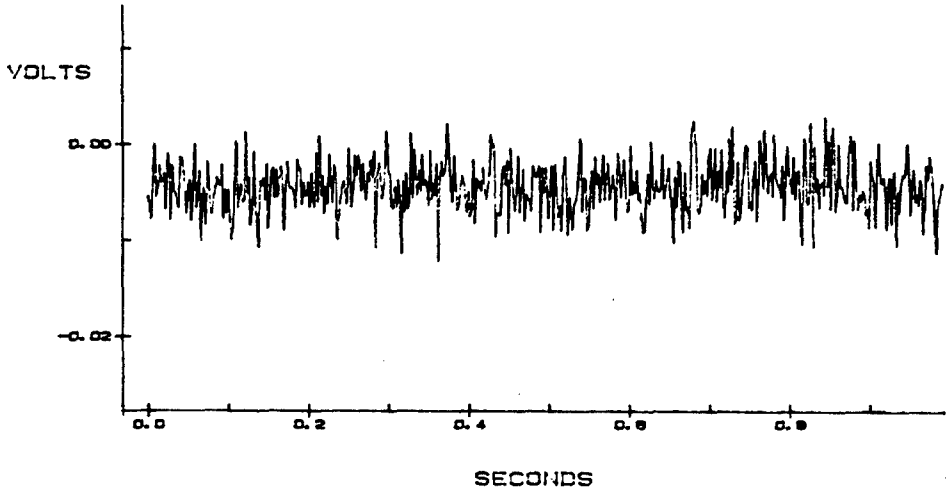

Figure 5-36. Original Signal, Except IBM Monitor Unplugged

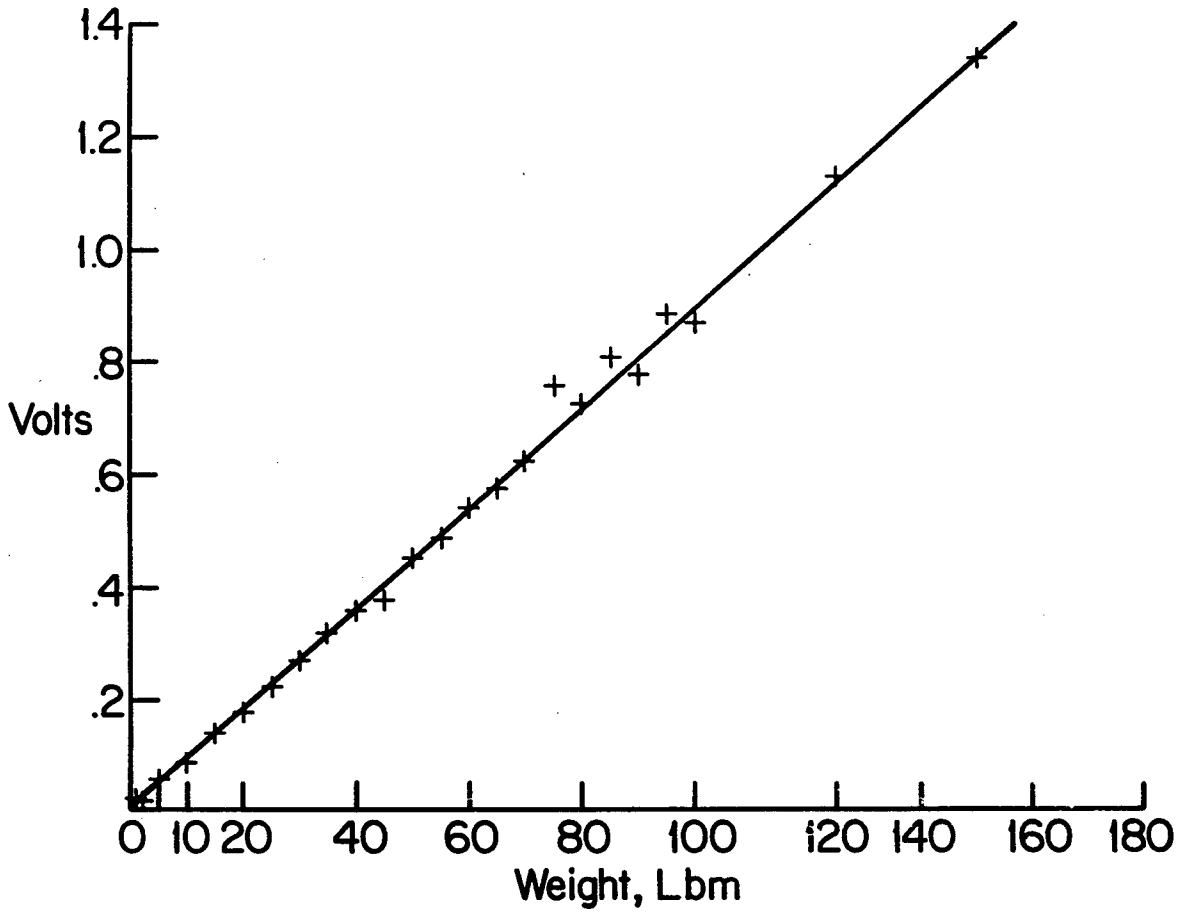

Figure 5-37. Bridge Calibration, Volts Versus Weight Applied to Strain-Gauged Collar

5.3.3. Ring and Liner Bench Test. The implementation of the ring and liner bench-test involved not only the calculation of friction coefficient as a function of crank angle, as well as average coefficient for the cycle, but also implementing various process control tasks. Friction coefficient is determined by dividing the friction force transduced by the strain-gauges, by the normal load provided by the air cylinder. Friction coefficient is calculated and stored every 1.4 degrees of crank rotation. The friction coefficient is also averaged over one revolution. The average coefficient, as a function of crank angle, is displayed on the monitor screen for both right and left sides and may be recorded on a floppy disk at predetermined intervals. Three cycles are averaged prior to plotting and storing. Upon completion of the test, ring and liner profiles may be measured to determine wear volume, weight loss, and surface roughness, as part of an overall assessment program. In the present study, liner and ring roughness profiles were taken in the axial direction of the liner and liner weight loss determined. Ring weight loss is difficult to determine, since only a small portion of the ring is worn.

For process control, as well as data acquisition and analysis, a computer system is employed. Speed, load and test temperature, as a function of time, are input for the process control function. The simulator is capable of unattended operation over the prescribed cycle. While the results presented herein are for tests of 2 and 4 hours duration, tests of up to 20 hours have been conducted. Automatic shut-down occurs if variables exceed preset limits. Periodically, friction data is taken, displayed on the screen, and stored on a flexible disk. Table 5.3 gives a list of the computer controlled features.

5.4. Testing

Below is discussed the testing of the various experimental methods conducted within this program. These are:

1. Instantaneous IMEP Method
2. Fixed-Sleeve Method
3. Ring and Liner Bench Test

5.4.1. Testing With the Instantaneous IMEP Method.

5.4.1.1. Procedures. In testing with the Instantaneous IMEP method both motoring and firing tests were run. Some motoring tests were run without compression, by installing a one inch thick steel plate with a hole the size of the cylinder bore. Typically two data runs were taken at each

Table 5-3. Automated Features of Simulator

Measurement and Control Features	
Strain Gauge Force	- Friction force stored digitally as a function of angular crank position - Unit stops if friction coefficient exceeds specified value (Important for scuffing tests)
Motor Speed	- Speed monitored by angular position sensor and recorded - Speed Controlled from 50 to 700 rpm - Independent measurement for overspeed protection
Loading Force	- Air cylinder pressure monitored and recorded - Pressure regulator motorized - Load constant or ramped up to about 650N
Oven Temperatures	- Sample block temperature monitored for control, and recorded - Heaters cycled on and off based on control equations - Oven air sensed independently for over-temperature protection - Temperature up to 650°C
System Integrity	- Automatic shut-down after 10 seconds if no signals received from controller

engine speed. Each run contained two sets of nine consecutive cycles and each set was taken about 1 minute apart. Prior to tests the engine was stabilize at the test condition. Pressure and strain-gauge signals were recorded simultaneously using the data acquisition system described in 5.3.1.5. Results are presented in Figure 5-41 through 5-48, and are the average of 18 cycles. The use of an 18 cycle average arose from the characteristics of the data acquisition system, and did not reflect additional considerations. Eighteen cycles did provide very repeatable friction results, and there appeared to be no reason to acquire additional data.

5.4.1.2. Results on the Cummins 903 Engine. Below is a discussion of the test results and some problem that were encountered in conventionally cooled engine tests and with SAE 40 lubricant. This is followed by results from a cooled test with ceramic-coating on rings and liners, and SDL-1 lubricant.

Baseline Engine Data. Data taken during the break-in of the single-cylinder Cummins 903 engine are shown in Figures 5-38, 5-39 and 5-40, and summarized in Table 5-4 together with the test conditions. Looking at Figures 5-38 and 5-39 it is seen that the bsfc increased about 0.01 units (2.5 percent), and the motoring torque increased about 4 lbf. ft. (13 percent) during the break-in. This indicated a problem resulting in friction increase. Subsequently, it was found that a large steel ring bolted to the top of the dummy balance piston had worked its way against the cylinder wall. This caused some light scuffing and friction increase. The steel ring was modified and reinstalled, which solved the problem. A further problem is evident in Figure 5-40. Fuel pressure increased during break-in. Ultimately, this was traced to swelling of the rubber fuel return line, which was incased in a flexible stainless braided covering. The line was replaced. After the initial problems were corrected, no new problems arose. The engine installation was judged satisfactory, since the performance was similar to other 903 single-cylinder engines built by Cummins previously.

Piston Assembly Friction Without Compression. Figure 5-41 shows friction force, as a function of crankangle, under a low-speed engine condition of about 200 rpm without compression. There is no pressure force across the piston and, thus, the curves reflect the strain in the connecting rod which gives the friction forces almost directly, since the inertia forces are small at this speed. Results are presented for a relatively cool oil and water temperature of 102 F and also a relatively hot oil and water temperature of approximately 200 F. An SAE 40-grade oil was used.

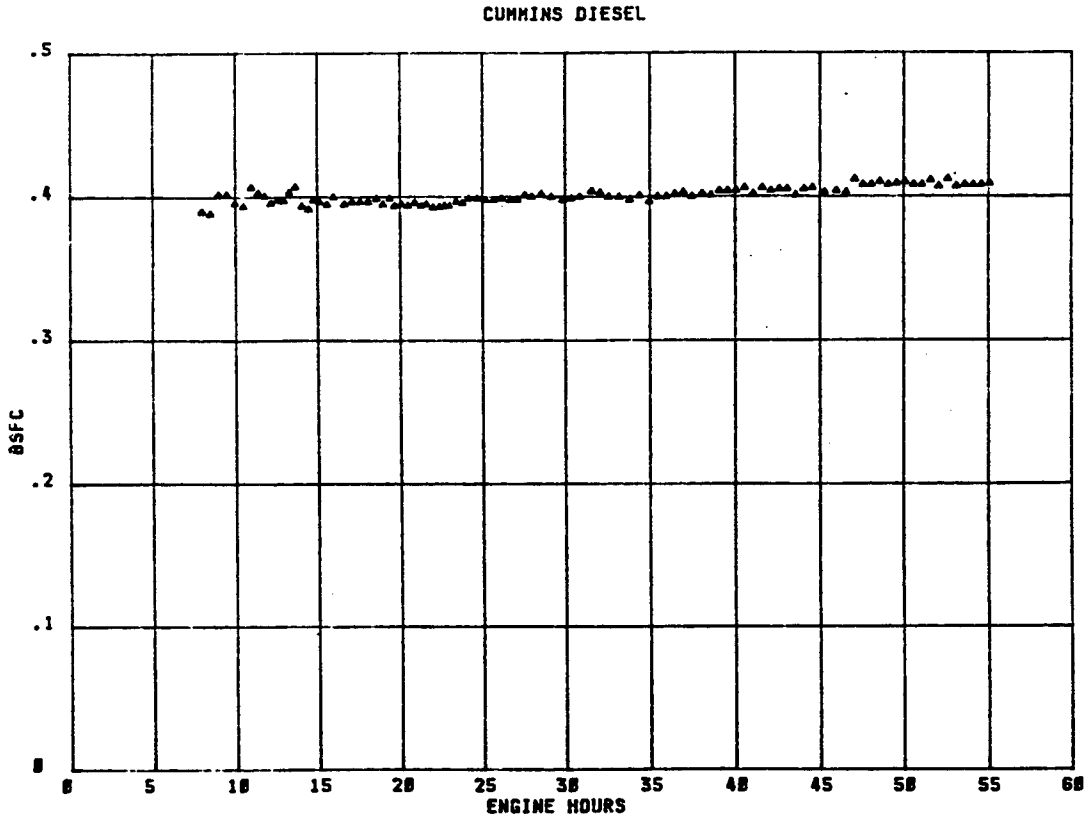

Figure 5-38. Brake Specific-Fuel Consumption During Break-In: BSFC units, lbm/bhp-hr

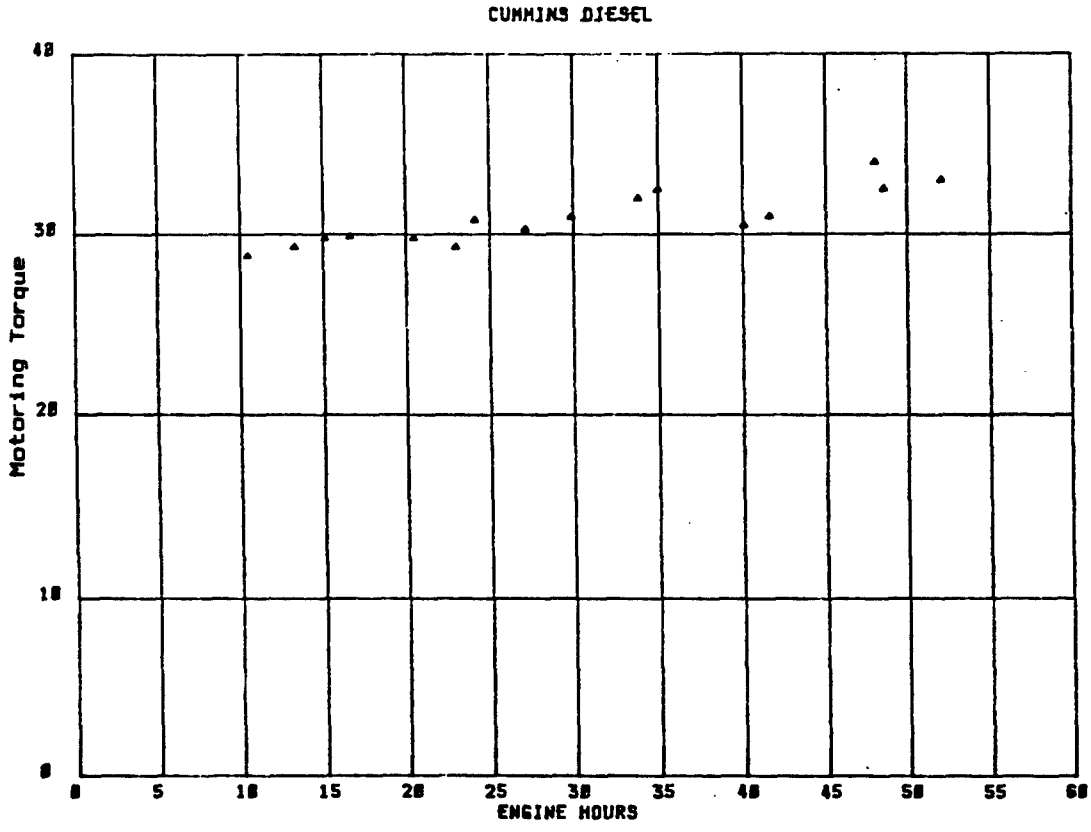

Figure 5-39. Motoring Torque During Break-In

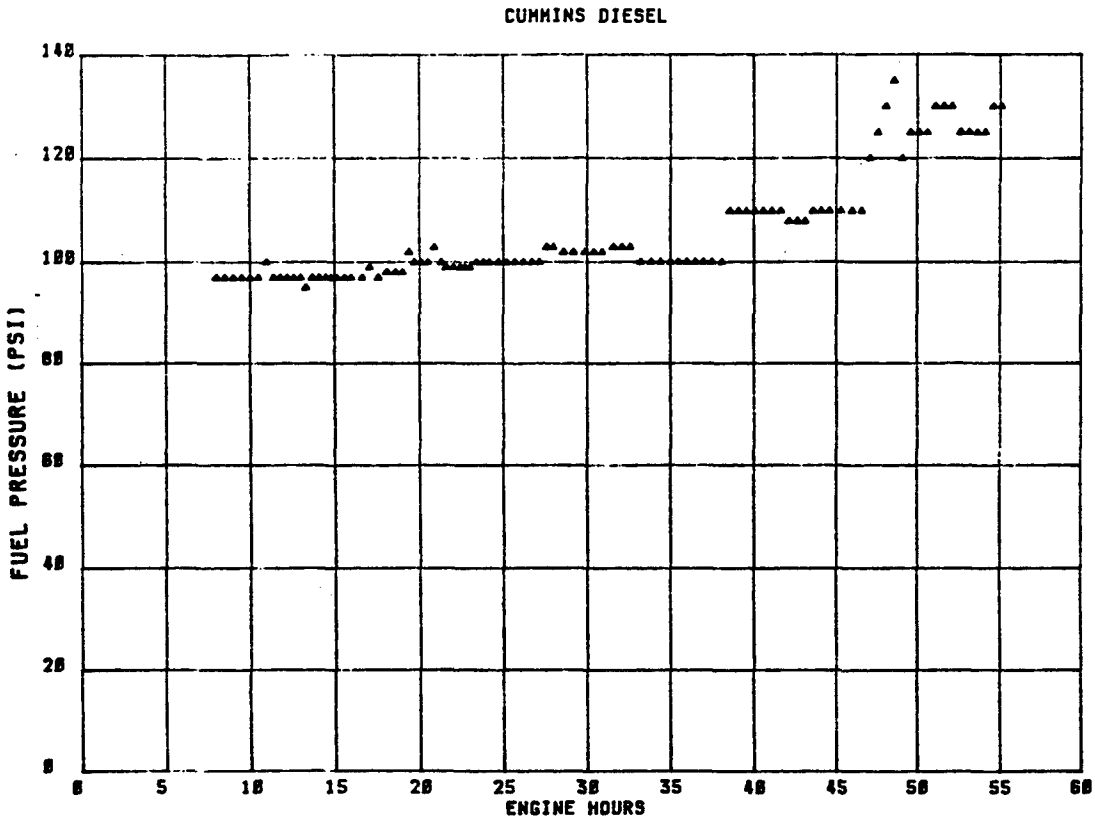

Figure 5-40. Fuel Injector Inlet Pressure During Break-In

Table 5-4. Summary of Average Break-In Data

SCE V903 performance Data	Baseline
Speed (rpm)	2600
Torque (ft-lbs)	135
Brake Hp	66.83
BSFC (lb/bhp-hr)	0.400
Fuel Rate (lb/hr)	26.85
A/F Ratio	30.50
In/Ex Mfld Press (in Hg)	50.5/50.5
Ex Mfld Press/In Mfld Press	1.00
Fuel Press (psi)	100-125
Oil Rifle Press (psi)	35
Oil Temp (-F)	240
Intake Mfld Temp (-F)	140
Ex Mfld Temp (-F)	810
Water Out of Cyl Head (-F)	185
Water Into Cyl Head (-F)	176
Blowby-in H2O	3.0
Fuel Out of Cyl Head (-F)	135
Fuel Into Cyl Head (-F)	75

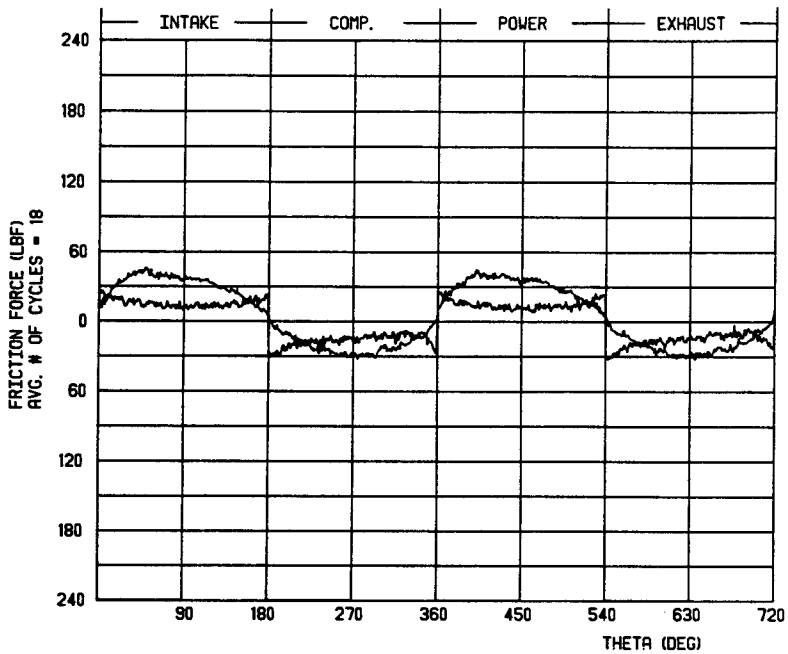

Figure 5-41. Friction Force with Low (102 F) and High (200 F) Oil and Water Temperatures, SAE 40 Oil, 200 RPM, Normally Aspirated

It is evident that the greater viscosity in the lower temperature test produced a much more hydrodynamic character to the resulting friction. With the higher water and oil temperatures, the friction trace exhibits considerable mixed lubrication and may be viewed as essentially a square wave of amplitude approximately plus or minus 20 lb force. The piston and ring assembly friction mean effective pressure was was 4.8 psi cold and 2.37 hot. The nearly two-to-one difference in friction results mainly from lower friction forces during the midstroke where the product of friction force times velocity is especially high.

Occurrence of Magnetic Interference. At the University of Michigan, we have had considerable experience applying the Instantaneous IMEP method to various gasoline engines. The application to the diesel engine was not expected to present a large problem, at least under motoring conditions. Consequently, friction traces, such as that shown in Figure 5-42, were entirely unexpected. Figure 5-42 shows friction force as a function of crankangle at 1200 rpm, motoring for the 903 engine. In spite of our best efforts, the data appeared to be nonsense. After making a number of changes in engine hardware and instrumentation, it was finally realized that the strange result was coming from magnetic fields of the rotating crankshaft. The crank of this engine had been magnetized either during manufacture or inspection. Strain-gauges and lead wires, including the wires on the grasshopper linkage, constitute conductors moving in that magnetic field.

Figure 5-43 shows the strain-gauge bridge output signal before and after reduction of the magnetic field, with no bridge input. The voltages generated by the magnetic field were dominating the signal. A number of steps were taken to minimize this magnetic field effect, which are summarized in Table 5-5. The extraneous signals were minimized primarily through a combination of degaussing of the crankshaft and magnetic shielding. As a result, the extraneous voltage became a relatively minor portion of the signal, which could be measured at each engine speed without bridge excitation, and the resulting noise subtracted from the strain-gauge signal. The relatively smooth curve shows the noise after all reduction methods were implemented.

Results After Elimination of Magnetic Noise. Having resolved the magnetic field problem, both motoring and firing data were taken on the Cummins 903 engine. Figure 5-44 shows motoring results at 1200 rpm with one atmosphere boost pressure. In part, the remaining noise on the trace resulted from the relatively high amplifier gain required to amplify the strain-gauge signals from the rather massive

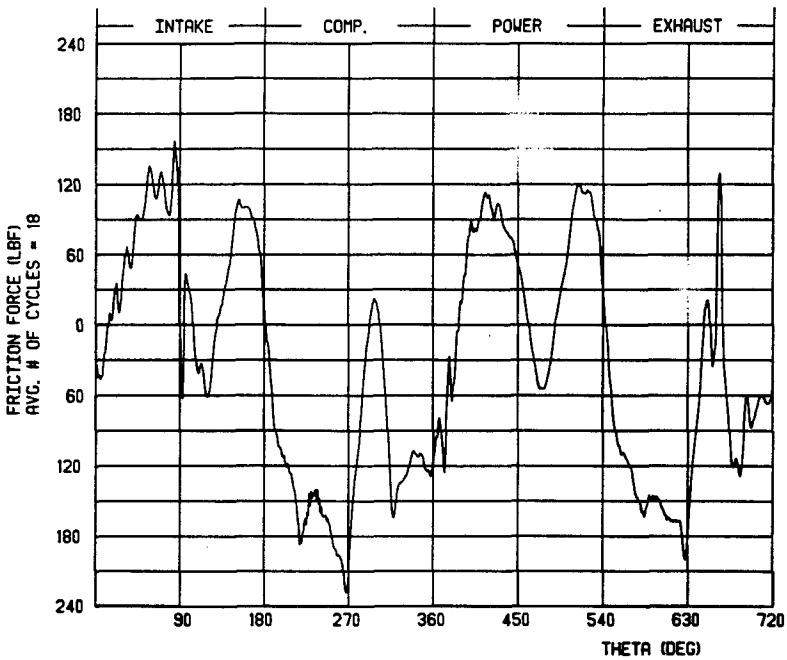

Figure 5-42. Friction Force Trace Including Error From Crankshaft Magnetism - 1200 RPM, 200 F Water and Oil, Naturally Aspirated

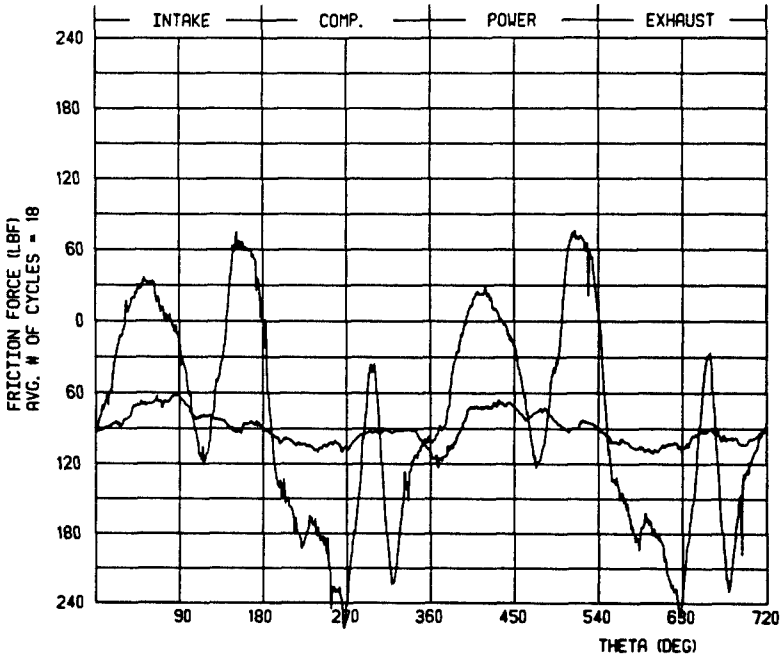

Figure 5-43. Strain-Gauge Signal Without Bridge Excitation Before and After Reduction of Magnetic Interference, 1200 RPM

Table 5-5. Steps Taken to Minimize Magnetic Noise

1. Install Mu Metal (high permability iron) shielding over all connecting rod wiring and connector.
2. Change wiring on connecting rod to give pairing of sense wires and excitation wires to remove loops.
3. Twist pairs of copper braid shielding on grasshopper wires.
4. Demagnetize crankshaft as much as possible with hand- held degausser.
5. Smooth sharp edges on crankshaft to remove field concentrations near grasshopper/connecting rod.
6. Measure signal at each speed without strain-gauge excitation, so that any remaining noise can be subtracted from strain-gauge signal.

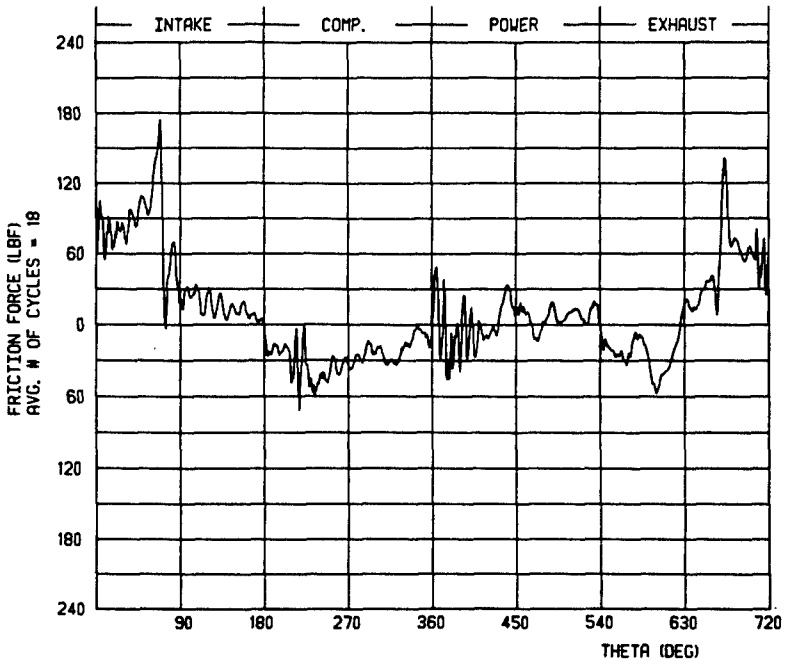

Figure 5-44. Motoring Piston and Ring Friction, 1200 RPM, 29.17 PSIA Manifold Pressure, 200 F Water and Oil, Friction MEP = 3.03 PSI

connecting rod of this engine. Compared to gasoline engine experience, the jumps at the dead centers are not as predominate. All in all, the friction appears to be relatively hydrodynamic throughout the 720 degree stroke. Figure 5-45 shows results of firing at 1200 rpm with one atmosphere pressure boost. Compared to motoring in Figure 5-44, large differences may be noted around top dead-center compression. This large change between motoring and firing suggests that the technique will be useful for identifying lubrication problems in a low-heat rejection engine, where the friction forces at top dead-center combustion might become very large. This firing curve exhibits some problems, which are artifacts of the measurements. In particular, on the power stroke, the friction force drops to a negative level, which is incorrect.

Accounting for Instantaneous Crank Speed. The inertia forces of Figures 5-44 and 5-45 were calculated based on measured instantaneous crankshaft speed. Figure 5-46 shows a trace of instantaneous speed at 1200 rpm firing with 30 inches of mercury boost pressure. The more than 50 rpm variation in speed over the cycle of this one-cylinder engine affects the inertia force significantly. Thus, consideration of the effect of instantaneous crank-speed is necessary in this case. The friction trace is distorted, as shown in Figure 5-47, if this is not done. Considering the instantaneous crank-speed of the engine is essential to obtaining good friction results, if there is significant speed variation such as might be expected in engines with few cylinders and heavy reciprocating inertias.

Results With SDL-1 and Uncooled Operation. Figures 5-48 and 5-49 show motoring and firing results with synthetic lubricant SDL-1 at 1200 rpm, intake manifold pressure of 30 psia, about 40 psi bmep, and without cylinder block cooling. These curves may be compared to Figures 5-44 and 5-45, in which SAE 40-oil was used in the conventionally cooled engine. The tests with SDL-1 were run using chrome oxide ring and liner coatings, whereas the data with SAE 40 used production chrome-plated iron rings and Lubrited gray iron liner. In comparing these results with those of the SAE 40 lubricant, it is noticed that the PR FMEP is about the same (2.97 versus 3.03 psi) motoring, but is lower for the SDL-1 (1.55 versus 2.25 psi) firing. Note that near TDC compression, the SDL-1 gave higher friction in the mixed or boundary friction regime, which is characteristic of the lubrication there, even for motoring. It is not known why the SDL-1 gave significantly lower firing friction with uncooled operation. The result may be real, or it be due to measurement inaccuracy. More study on this is needed.

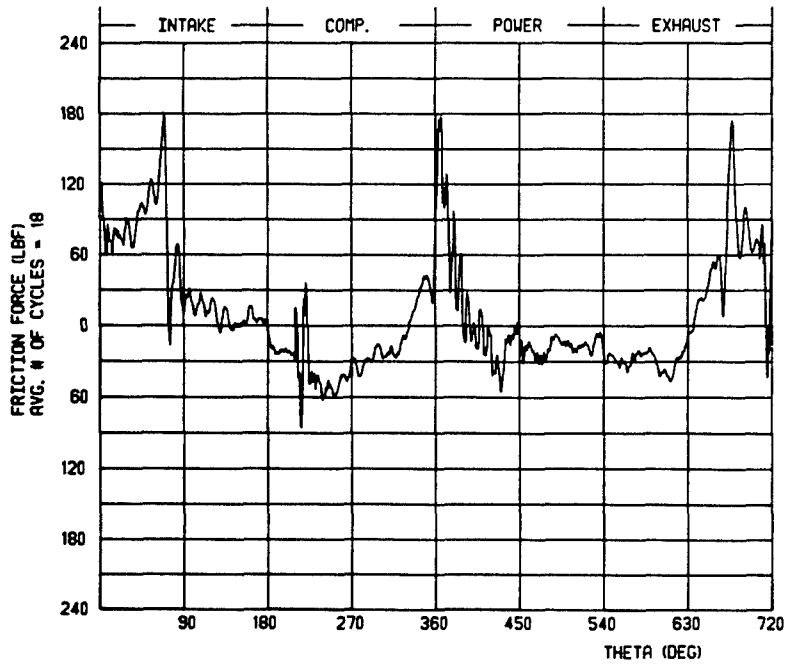

Figure 5-45. Firing Piston and Ring Friction, 1200 RPM, 29.17 PSIA Manifold Pressure, 200 F Water and Oil, Friction MEP = 2.25 PSI

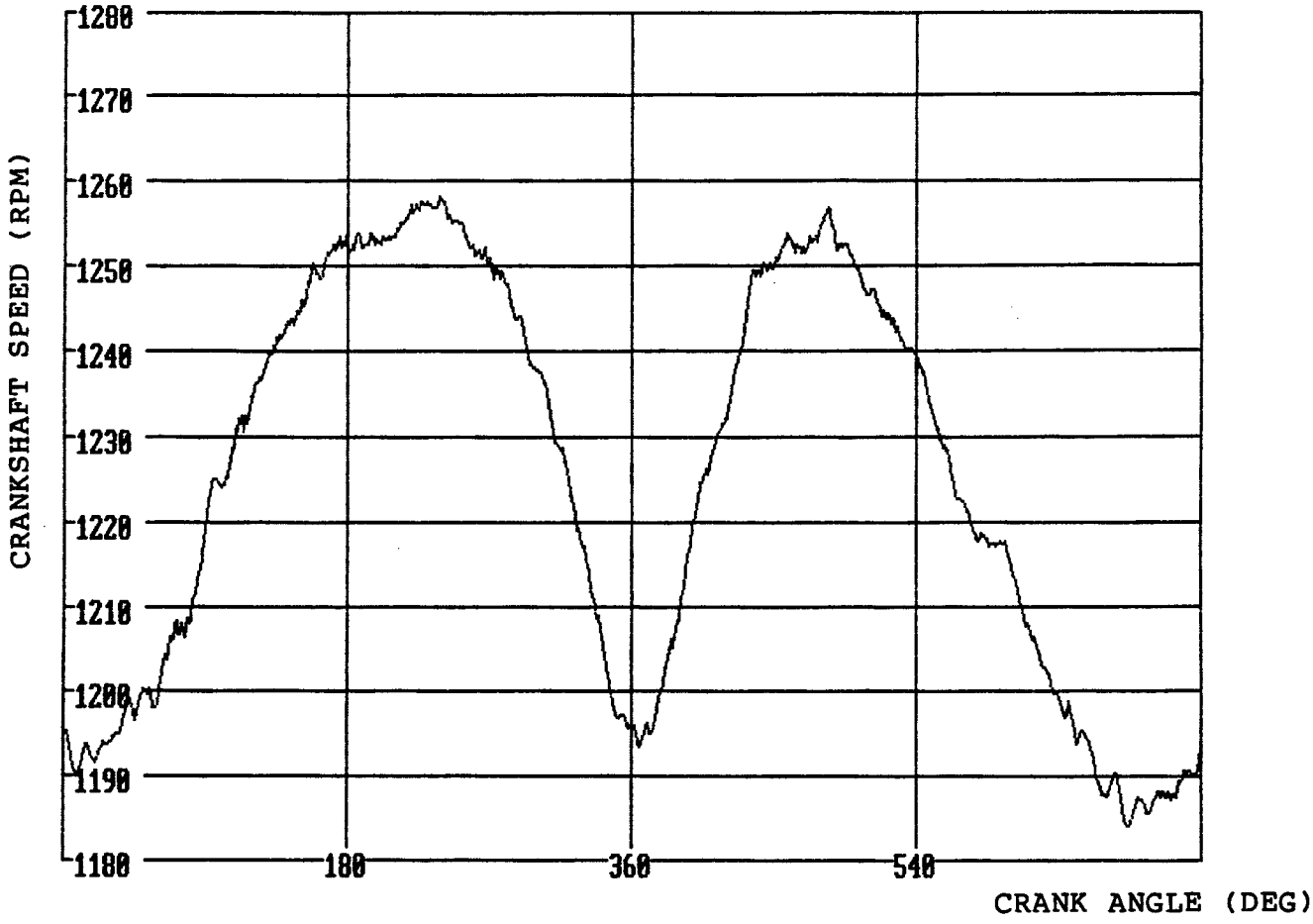

Figure 5-46. Instantaneous Crank Speed at 1200 RPM, Firing, 30 In. Hg. Boost

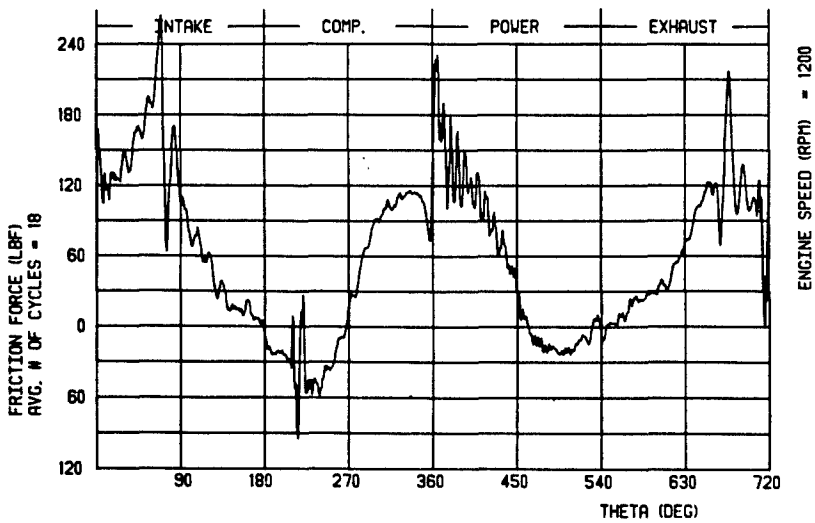

Figure 5-47. Results shown in Figure 5-45 Before Corrected for Instantaneous Speed Variation

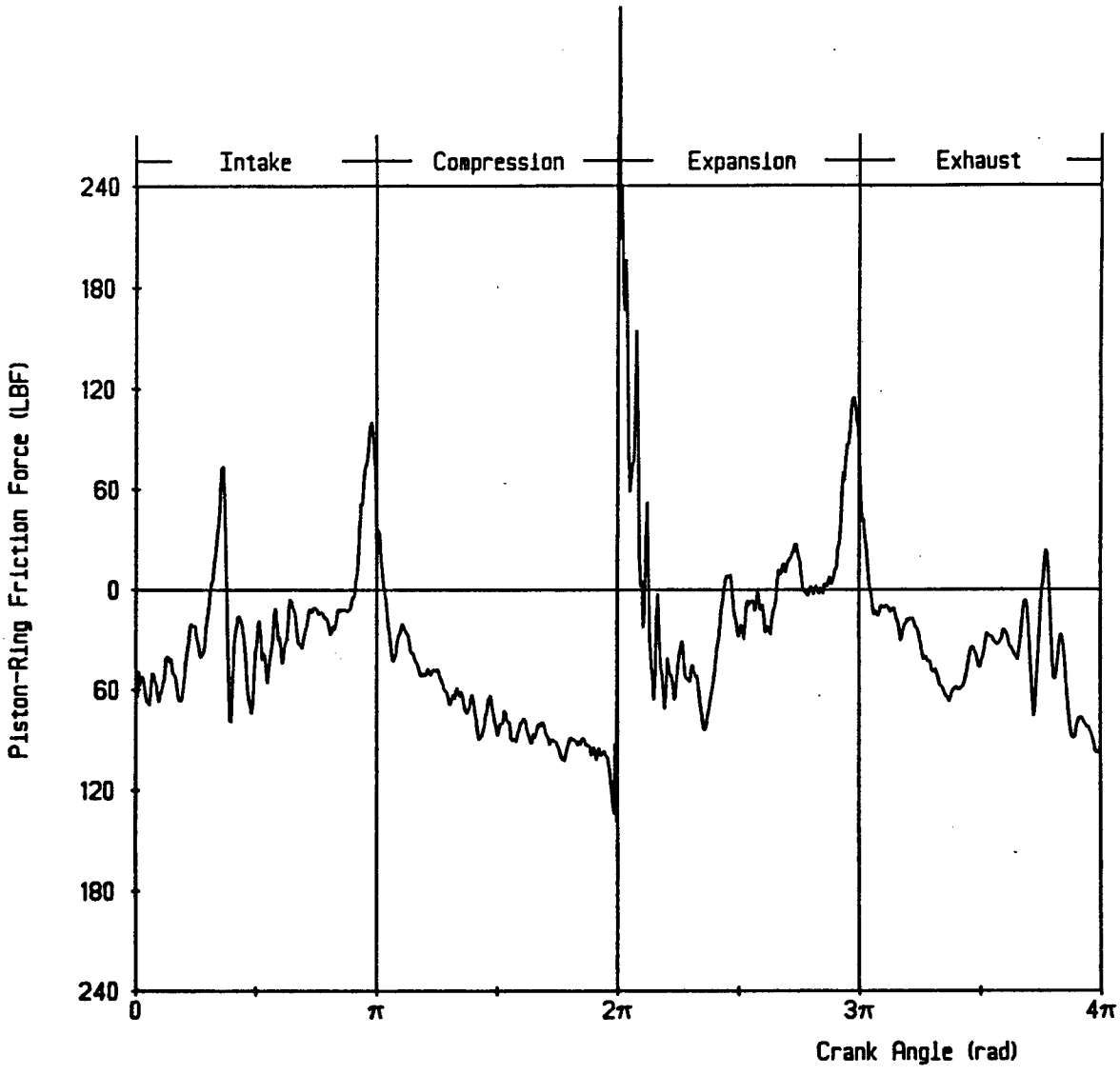

Figure 5-4 Motoring Piston and Ring Friction, 1200 RPM, 30.01 PSIA Manifold Pressure, Uncooled Operation, Friction MEP = 2.97 PSI, Synthetic Lubricant

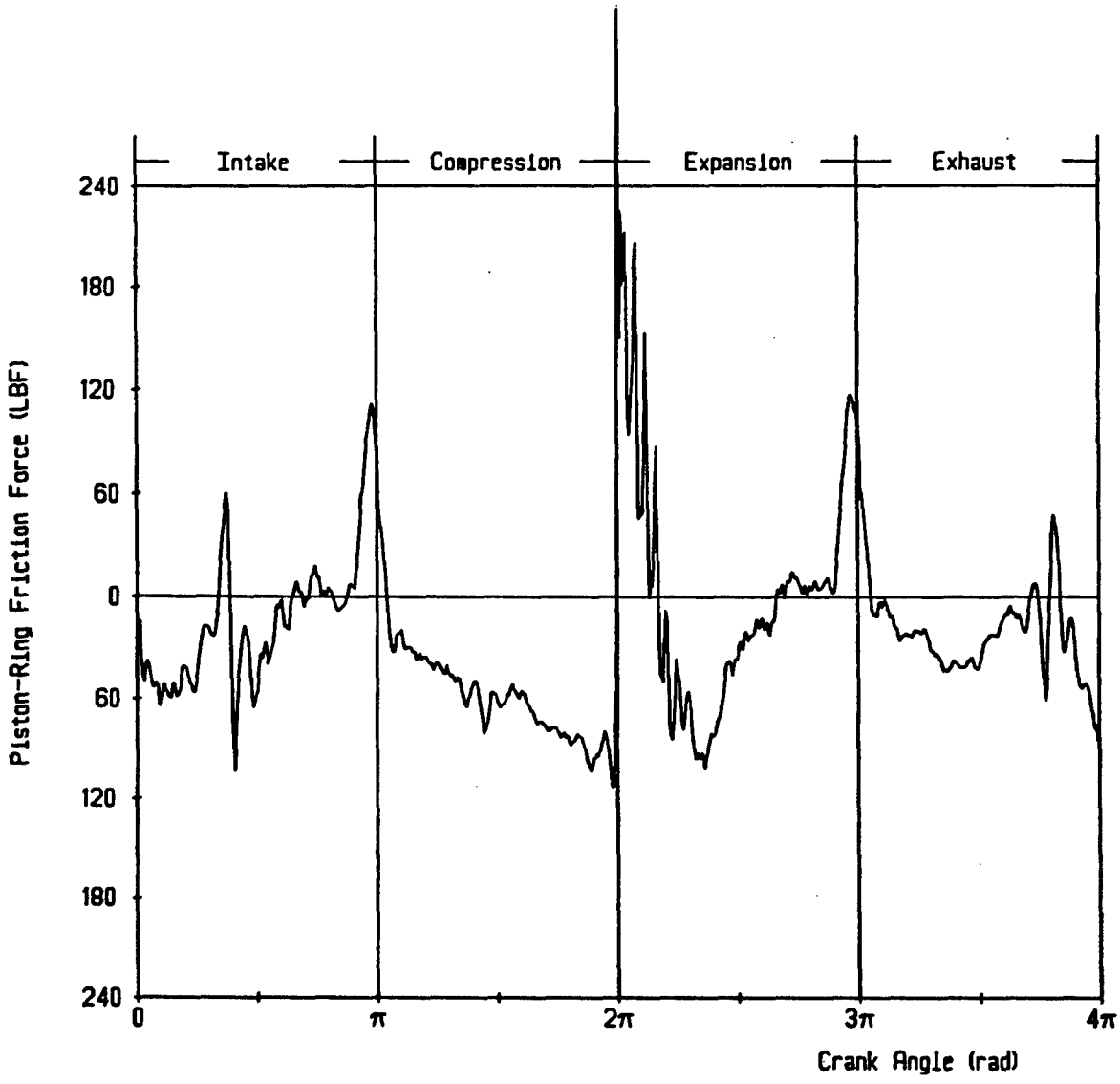

Figure 5-49. Firing Piston and Ring Friction, 1200 RPM, 29.91 PSIA Manifold Pressure, Uncooled Operation, Friction MEP = 1.55 PSI, Synthetic Lubricant

General Comments on the Instantaneous IMEP Method. The Instantaneous IMEP method, when properly implemented, has the potential of determining piston and ring assembly friction with good accuracy over a large portion of the full cycle. It is estimated that about 90 percent of the cycle is reported with good accuracy. At the very highest pressures and combustion temperatures the uncertainties become greater. Thus about 10 percent of the crank angles of the cycle, around top dead-center combustion, have relatively high uncertainty with respect to friction forces.

The method is projected to be able to assess changes in friction coming about from engine or lubrication failures. The foregoing statement is very significant, since often one wishes to anticipate a problem as it develops. Therefore, even if the absolute values with the Instantaneous IMEP method are less than perfect, the indication of a relative change is useful. A major plus for the Instantaneous IMEP method is that essentially no engine structural modifications are required. Our overall experience with this method, in both gasoline and diesel engines, shows that it has very good repeatability. Even with uncooled engine operation, there was no indication that the technique would not work.

Unfortunately, this program terminated just at full implementation of the method on the Cummins 904 engine with ceramic-coated rings and liner, and uncooled operation. It is believed that with relatively little additional work, a variety of coatings, lubricants, and engine operating conditions could have been evaluated.

5.4.2. Testing With the Fixed-Sleeve Method.

5.4.2.1. Procedures. Several motoring and firing tests were run at speeds between 500 and 2000 rpm and up to full load on the 4.1-litre engine. This somewhat limited speed range should not be interpreted to suggest any known speed limitation in the method. We were simply proceeding with caution using a new experimental rig. The voltages from pressure-transducer and strain-gauges were digitally recorded at one crank angle degree intervals, using either a Nicolet Model 602 Digital Oscilloscope interfaced with an IBM PC for friction force calculation, or the data acquisition system described in Section 5.3.1.5.

5.4.2.2. Calibration. The Kistler Model 7061 pressure transducer was calibrated using the Ruska dead weight tester as in Section 5.3.1.3. Calibration of the fixed sleeve assembly strain-gauges was done either by placing weights on the rim of the inner sleeve, or by pressurizing the cylinder

after assembly using the spark plug hole with the piston at tdc. The strain-gauges used were the same as those described in Section 5.3.1.4. The cylinder pressure acting on the end of the fixed sleeve provided the calibration force. The result was to use the pressure-transducer to establish the strain-gauge calibration. The latter method was normally used, since it was relatively easy and gave very consistent results. Both increasing and decreasing pressure were applied. A small difference was noted, probably due to hysteresis of the O-rings and the piston rings. A different calibration curve was then used for increasing and decreasing pressures. This curve is shown is Figure 5-50. In the future, it is planned to quantify how much of the hysteresis is due to the O-ring and how much due to the rings. Of course, it is desirable to minimize, or eliminate the hysteresis.

5.4.2.3. Fixed-Sleeve Results on 4.1-Litre Engine.

Description of Typical Motoring Results. Figure 5-7 showed some typical cylinder pressure and strain-gauge signals. These were averages of 2 engine cycles for such motoring traces. (All results shown for firing traces are averages of 18 cycles.) The engine was motored at 1000 rpm, wide-open throttle with manifolds removed. Shown also is the resulting friction force as a function of crank angle. The friction trace is obtained by subtracting, at each crank angle, the product of cylinder pressure and rim area from the force experienced in the fixed sleeve by the strain-gauges.

It may be noted that the strain-gauge signal mimics the cylinder pressure, except that the friction force distorts the signal mainly at the dead centers. In other portions of the cycle, the shape of the curves are very similar. At the dead centers, the reversal of static friction is seen as an abrupt jump in friction force. Clearly, mixed or boundary lubrication predominates at the dead centers. At tdc compression, the jump is greatest, and this is consistent with the presence of high gas pressure in the cylinder at that time. The small amount of noise on the friction trace results, in part, from the discrete character of the digital data acquisition system and, in part, from structural vibrations. At this point, no effort has been made to impute any significance to that noise. Figure 5-51 shows four consecutive strain-gauge traces under WOT motoring conditions. The signals are virtually identical.

Comparison of Motoring with Firing Friction. There is always interest in determining to what extent motoring and firing friction are similar. Figure 5-52 shows a comparison

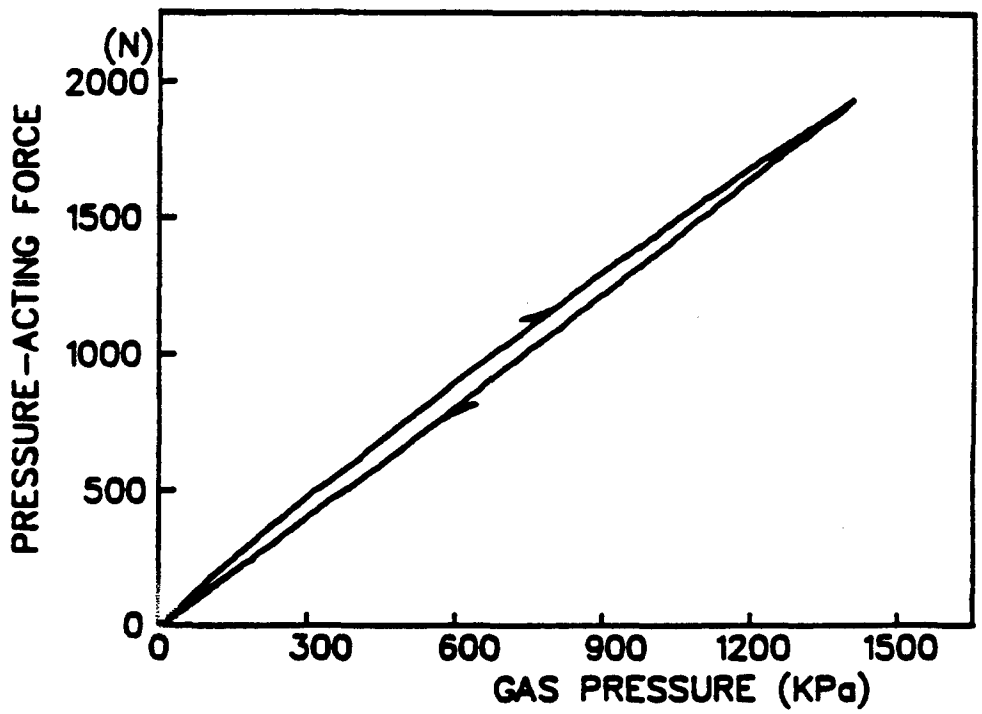

Figure 5-50. Calibration Curve Showing Increasing and Decreasing Pressure

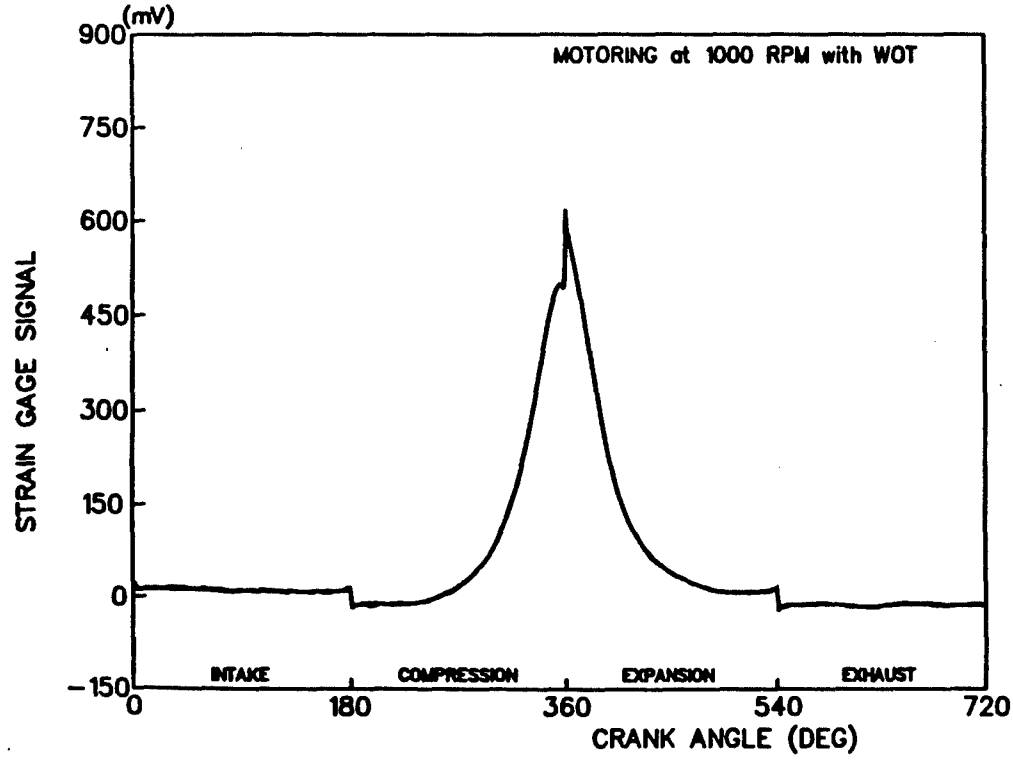

Figure 5-51. Strain-Gauge Signals Overlapped for Four Consecutive Traces, 1000 RPM, Motoring, WOT

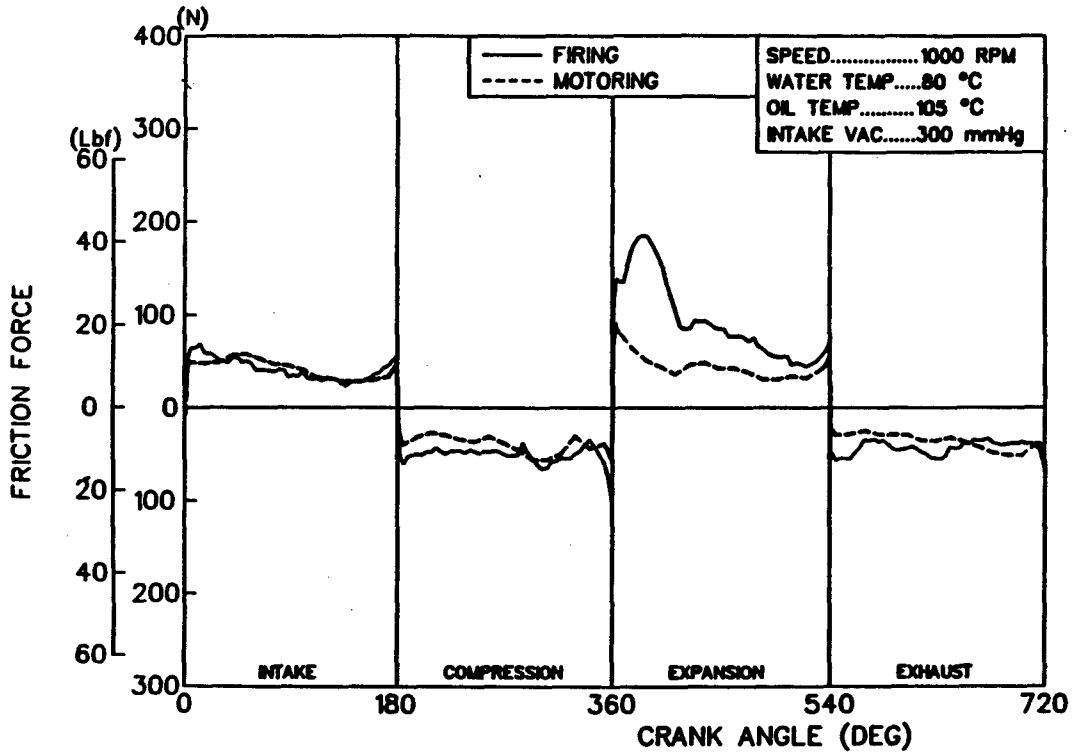

Figure 5-52. Friction Force Versus Crank Angle Motoring and Firing, 1000 RPM, Part Load: Note Major Difference After TDC Firing

at 1000 rpm and 300 mm Hg manifold vacuum. The engine vacuum and temperatures were maintained the same motoring and firing. As might be expected, the firing friction differs and is much larger than motoring friction during the expansion stroke. Elsewhere, the differences are more minor. Virtually identical results were published for a different engine in Reference 3, using the Instantaneous IMEP method. It is evident that the traces have various primary and secondary features. In the future, it is hoped to correlate some of these to specific engine design characteristics.

Engine Speed Effects. Figure 5-53 shows the effect of engine speed on piston and ring friction. Four speeds ranging from 850 to 2000 rpm are shown at a constant brake torque of 89 Nm. It is interesting to note that the four curves are quite similar in shape and, in fact, the integrated friction mean effective pressure only varied from 42.8 to 45.1 kPa across the set. The exact vertical relationship between the curves can not be determined, due to the inability to set an absolute zero for each curve. This is due mainly to the zero shift in strain-gauge signals. The crank angle of maximum piston velocity is indicated. In this region, one would expect hydrodynamic lubrication, especially at the higher engine speeds.

Engine Temperature Effects. The influence of water and oil temperatures are shown in Figure 5-54. The temperature variations were made by varying the coolant temperature. Oil temperatures varied from 35 to 91 C, and coolant temperature from 25 to 80 C. At the lower oil temperature, higher friction is noted at mid-strokes where the more viscous oil caused more hydrodynamic drag. The situation at the dead centers is opposite, in that the more viscous oil reduced the magnitude of the jumps. These observations are consistent with predictions based on Stribeck diagram characteristics and the behavior of the friction coefficient in the mixed versus the hydrodynamic regime. Noted on the Figure are transition points where the friction changes from mainly boundary to mainly hydrodynamic. Because the curves reflect the contribution of three rings and a piston, these transition points are blends of four different elements. An analogy may be made with resistors in series, the largest frictional resistance at any crank angle dominates the result. A discussion of friction results, with various piston rings removed, can be found in the upcoming section entitled "Effect of Ring Removal."

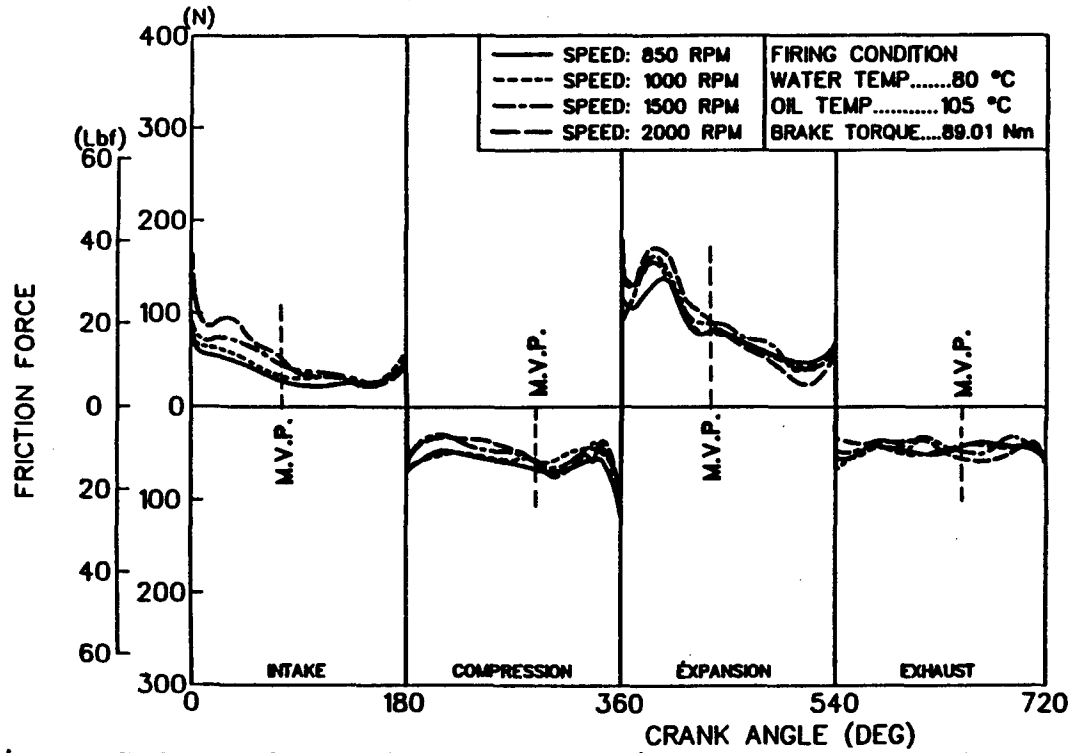

Figure 5-53. The Influence of Engine Speed Under Firing Operation, 1000 RPM, WOT: M.V.P. Indicates Maximum Piston Velocity Crank Angle

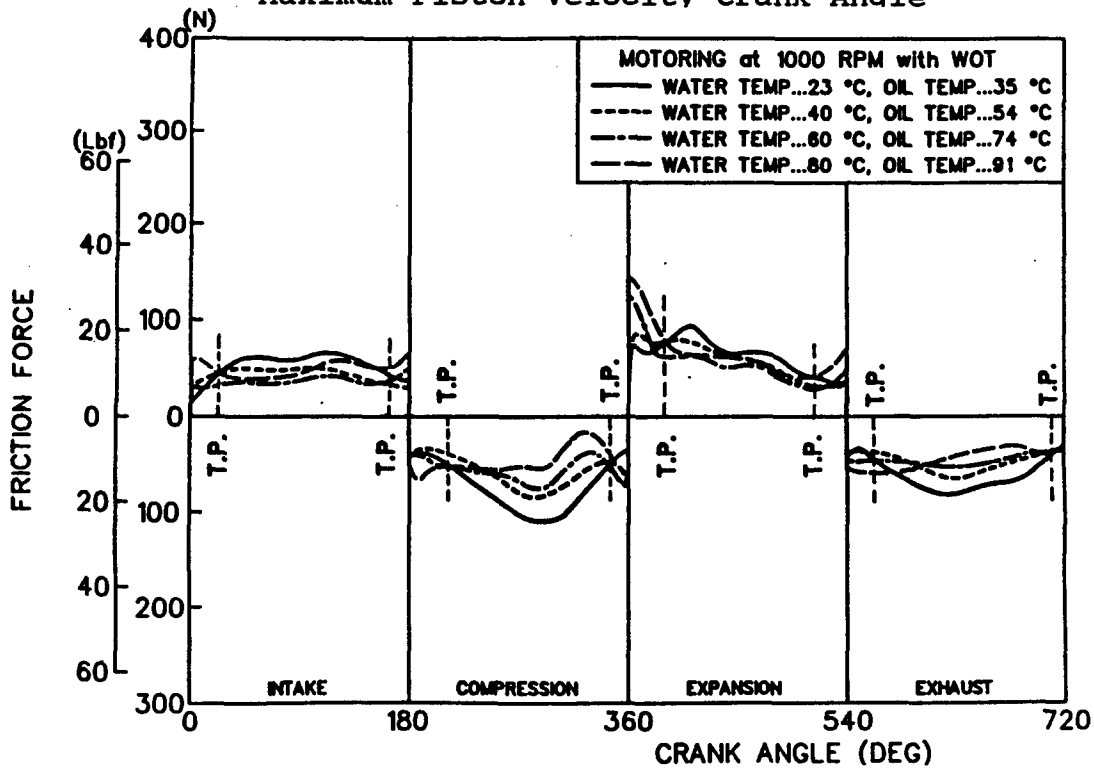

Figure 5-54. The Effect of Water and Oil Temperatures Under Motoring Operation, 1000 RPM, WOT

Comparison Between Honed and Machined Liners. One experimental difficulty experienced in the tests was to "properly" hone the liner. These relatively thin liners defied honing into perfectly straight, round cylinders. Figure 5-55 shows a comparison between a machined liner and a honed liner under WOT motoring conditions at 1000 rpm. Neither were broken-in, thus results are under green, as-received conditions. Note that at top dead-center compression, the machined liner produced much higher friction than the honed liner. The machined-only liner had a surface roughness of 0.351 micro-meter Rq (root mean square roughness). The honed liner had 120 degree crosshatching and a roughness of 0.239. Further studies are needed to understand just how shape and surface variables affect friction. It is under mixed or boundary lubrication conditions where surface variables should be most important, and tdc compression is where such friction predominates. The Fixed-Sleeve method appears to be an ideal tool for exploring bore distortion and bore finish variables.

Effect of Piston Mass. In recent years, there has been much interest in reducing piston weight. In Reference 5, it was reported that there was no change in friction when weight was added to the piston pin. In that study, the Instantaneous IMEP method was used. That test was repeated using the Fixed-Sleeve method, and the results were the same; that is, the friction force versus crank angle was identical, when 170 g was added to pin of the 80 mm piston. This increased total reciprocating mass from 658 to 828 g, or 25.8 percent. At 1000 rpm motoring, the maximum side thrust was increased from 51.2 N to 64.4 N. No change would be expected in the ring friction. The fact that the overall friction did not change suggests that the change in reciprocating mass did not affect the piston skirt friction. Apparently, the decrease in friction coefficient with increased load in the hydrodynamic regime virtually offset the increase in normal load itself, at least within the limited speed range investigated.

Effect of Ring Removal. The final set of experimental data given are for the piston and ring friction with various rings removed. Engine conditions are 500 rpm, motoring, and without cylinder pressure. These are shown in Figures 5-56 and 5-57. Data with the oil ring removed are shown in Figure 5-56 for various combinations of top and second ring. Similar results are shown in Figure 5-57 for the oil ring installed. Clearly, the oil-ring friction dominates the ring pack. Note that the incremental friction of each compression ring is higher when the oil ring is installed. Apparently, the large quantity of oil flooding the cylinder wall, when the oil ring is removed, dominates the results.

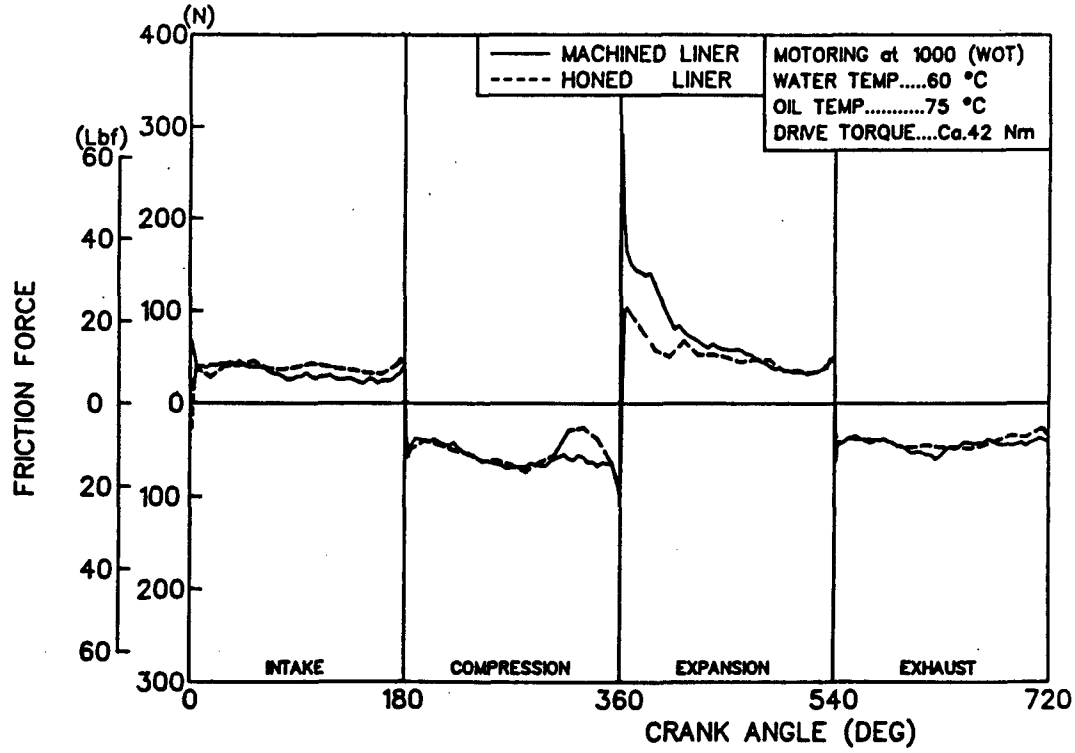

Figure 5-55. Comparison Between Honed and Machined Liners, 1000 RPM, Motoring, WOT

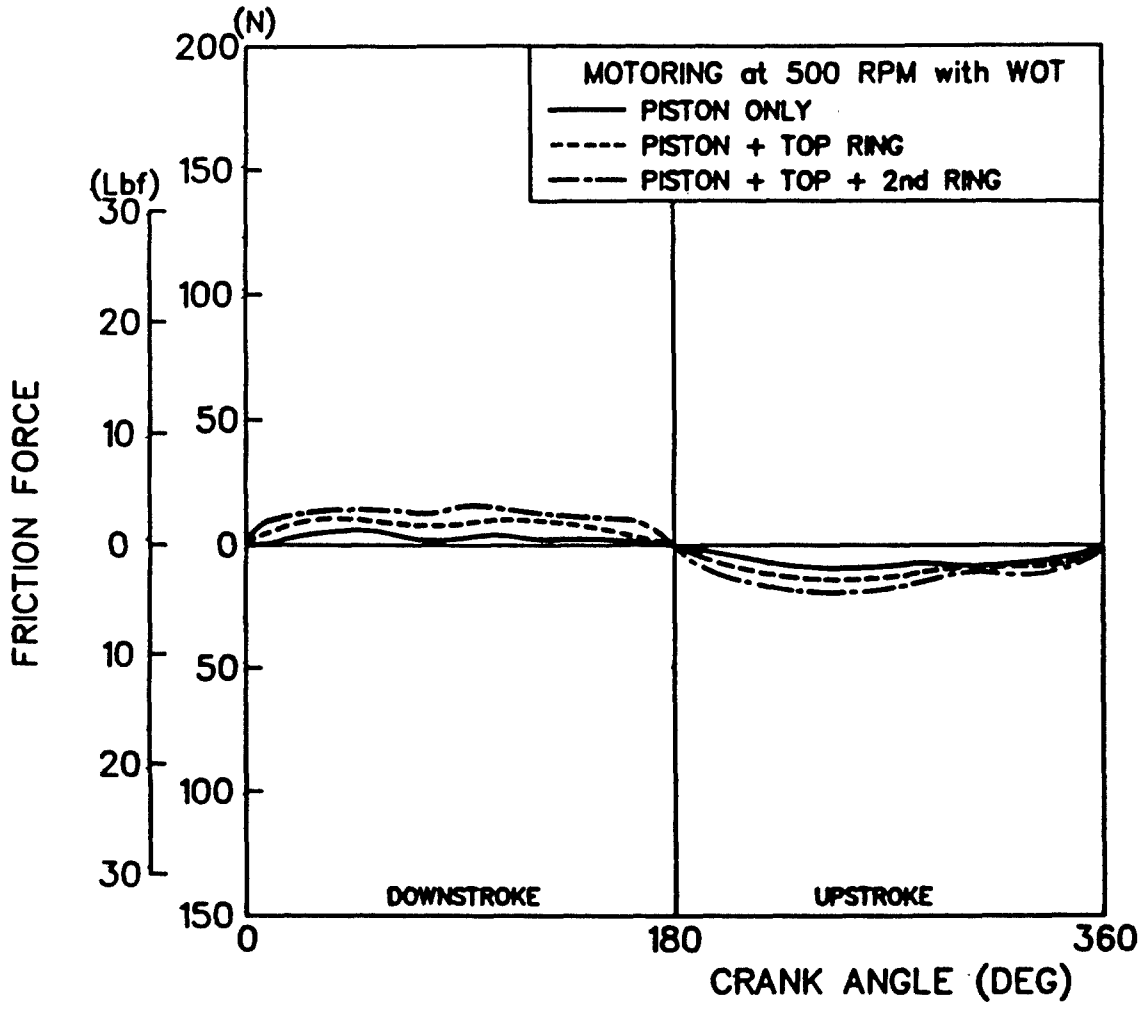

Figure 5-56. Friction Without Oil Ring, Various Compression Rings Removed, 500 RPM, Motoring, WOT

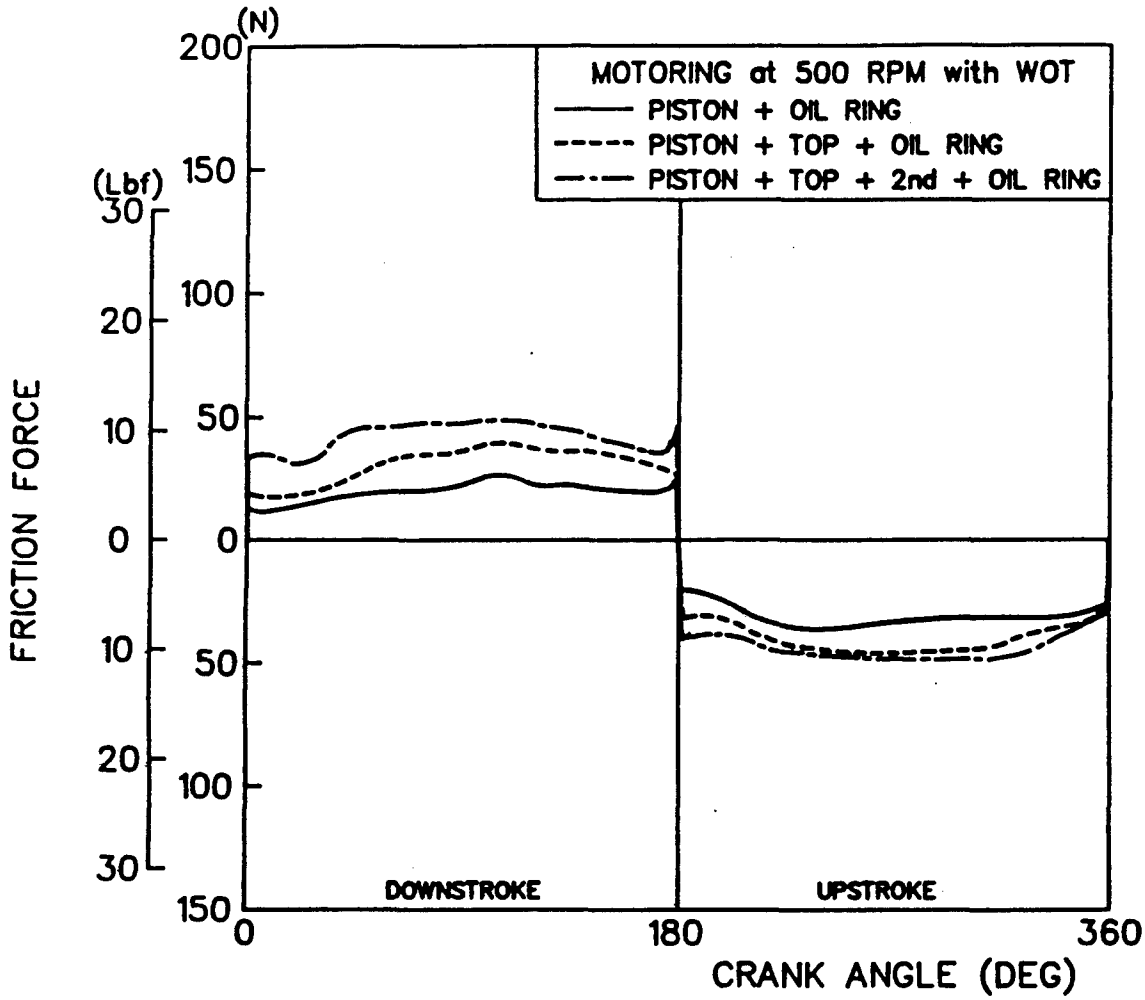

Figure 5-57. Friction with Oil Ring, Various Compression Rings Removed, 500 RPM, Motoring, WOT

This also gives a hydrodynamic characteristic to the friction, in that the jumps at the dead centers are eliminated.

Figure 5-58 summarizes the comparison. Quantities are shown as piston and ring fmep. The fmep is calculated by integrating the product of friction force and piston velocity over 720 crank-angle degrees, and dividing the result by the displacement of one cylinder. The fmep varies from a low of 4 without rings to a high of almost 40 kPa with the full ring pack, a factor of 10. The results of this series of tests, in which rings are removed, demonstrate the experimental difficulty of determining the correct friction contribution of individual rings and the interactive effects which exist with a full-ring pack.

A large friction reduction with the two-ring piston is suggested in the center group of Figure 5-58. Probably the absence of the second ring permitted excessive oil on the bore, which lowered the friction. Neither oil consumption or blow-by were investigated in this study. As a result, any friction benefit of the two-ring piston cannot be confirmed until the other parameters are controlled within specifications.

General Comments on 4.1-Litre Engine Results. Based on the experience with the 4.1-litre engine, the Fixed-Sleeve method looks very promising. Repeatability and the ability to differentiate small friction differences appear excellent. On the other hand, a special liner is required and, thus, engine modifications are necessary, which themselves modify base engine friction characteristics. The method appears to be readily adapted to engines with liners.

The Fixed-Sleeve method permits relatively rapid change of piston, ring, and liner variables; and calibration is relatively straight forward. As a result, variables can be investigated relatively quickly.

In particular, this method is expected to be very useful for evaluating bore roundness, straightness, and surface finish effects. It will also be useful for evaluating new piston or ring designs. The location of the strain-gauges, away from the heat and cylinder stresses, suggests that this method could be adapted to measure friction in uncooled engines.

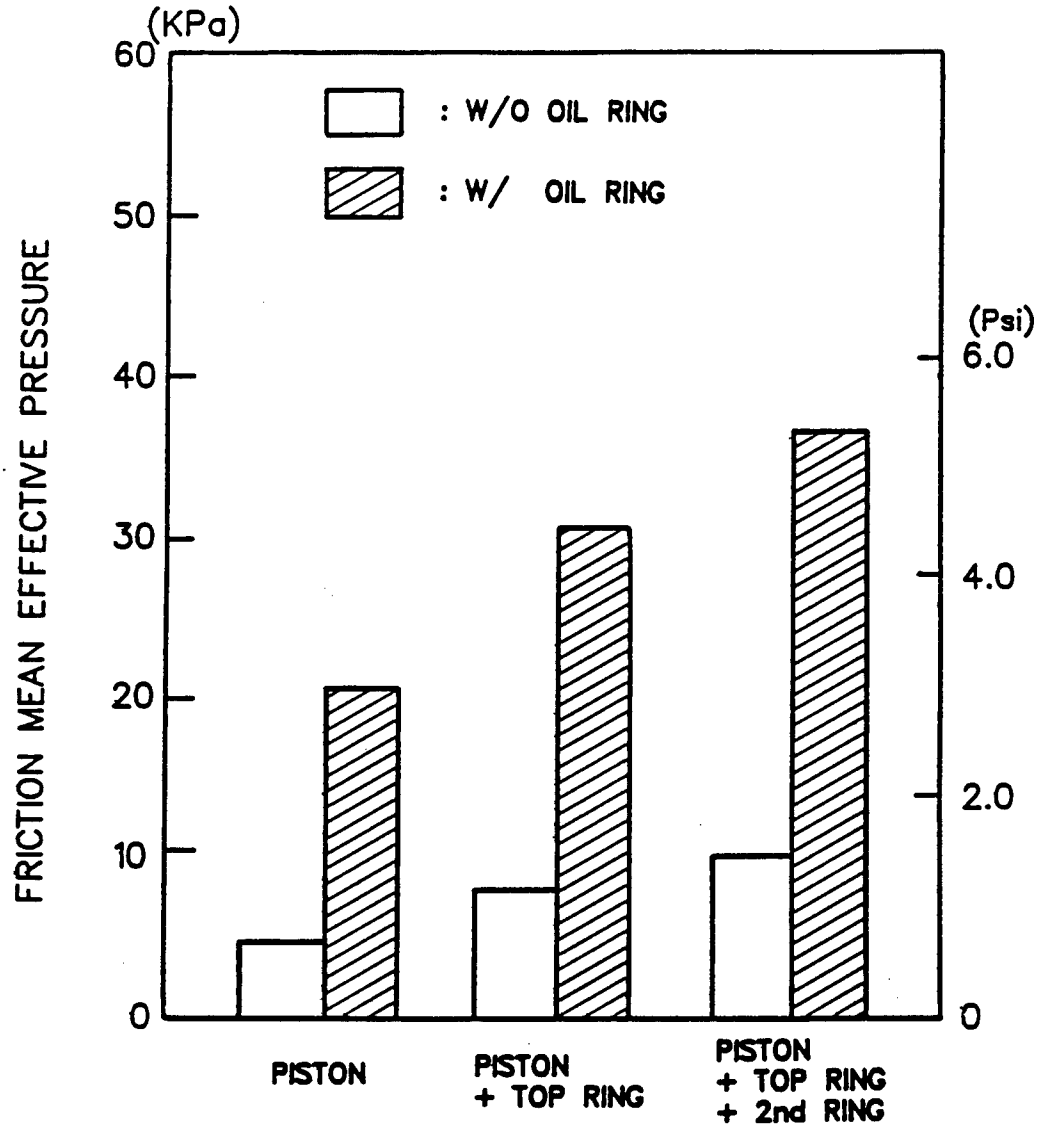

Figure 5-58. Histogram of Friction Mean Effective Pressure for Various Ring Combinations, from Data of Figures 5-55 and 5-56

Comparison of the Fixed-Sleeve and Instantaneous IMEP Methods on the 4.1-Litre Engine.

Introduction. Having developed two techniques for measuring piston and ring assembly friction, it is of interest to see how they compare. Minor differences might be expected, since the Fixed-Sleeve method does not include the piston pin friction, whereas the other method does. The comparison was conducted using cylinder 1. The engine was further modified for the Instantaneous IMEP method. This involved a strain-gauged connecting rod, grasshopper linkage, and modified oil-pan for dry sump operation.

Results. For this comparison, the engine was both motored and fired at 1000 rpm. A variety of tests were run in which oil and water temperatures were varied between 100 and 200 F. Figure 5-59 shows the comparison at relatively low water and oil temperatures of 104 and 130 F, respectively, part-load operation. The upper trace is the Fixed-Sleeve method, the lower the Instantaneous IMEP method.

Both techniques gave similar results. The friction was strongly hydrodynamic with the low temperature, viscous oil. The PR FMEP's were 9.7 psi (Fixed-Sleeve) and 8.5 psi (IMEP), a difference of about 12 percent. The major difference occurred abound TDC compression. Here, the cylinder pressure is the major term in the calculation for both methods. The error is believed to be due to the distortion (lowering of output) of the pressure-transducer as the hot compressed gases act on the transducer diaphragm. It is thought that the lesser dependence of the Fixed-Sleeve method on cylinder pressure by about a factor of 10 (rim area versus piston area) is the reason. Also note that the IMEP method is distorted in the opposite direction from the Fixed-Sleeve method, due to the location of the measurement (piston versus liner). The size of the jumps at the dead centers, another measure of friction, is equal for both methods.

Figure 5-60 gave a similar comparison firing, with relatively high water and oil temperatures of 176 and 220 F respectively. There is more boundary or mixed friction at this condition as can be seen by the nearly flat friction trace throughout the intake, compression, and exhaust strokes. The beginning of the expansion stroke, however, is quite different between the two methods. There, the IMEP method shows relatively low friction compared to the Fixed Sleeve method. It is possible that this discrepancy could be due to incorrect piston or liner rim area measurement, but it is more likely due to output shift as the flame front passes over the pressure-transducer. When calculating

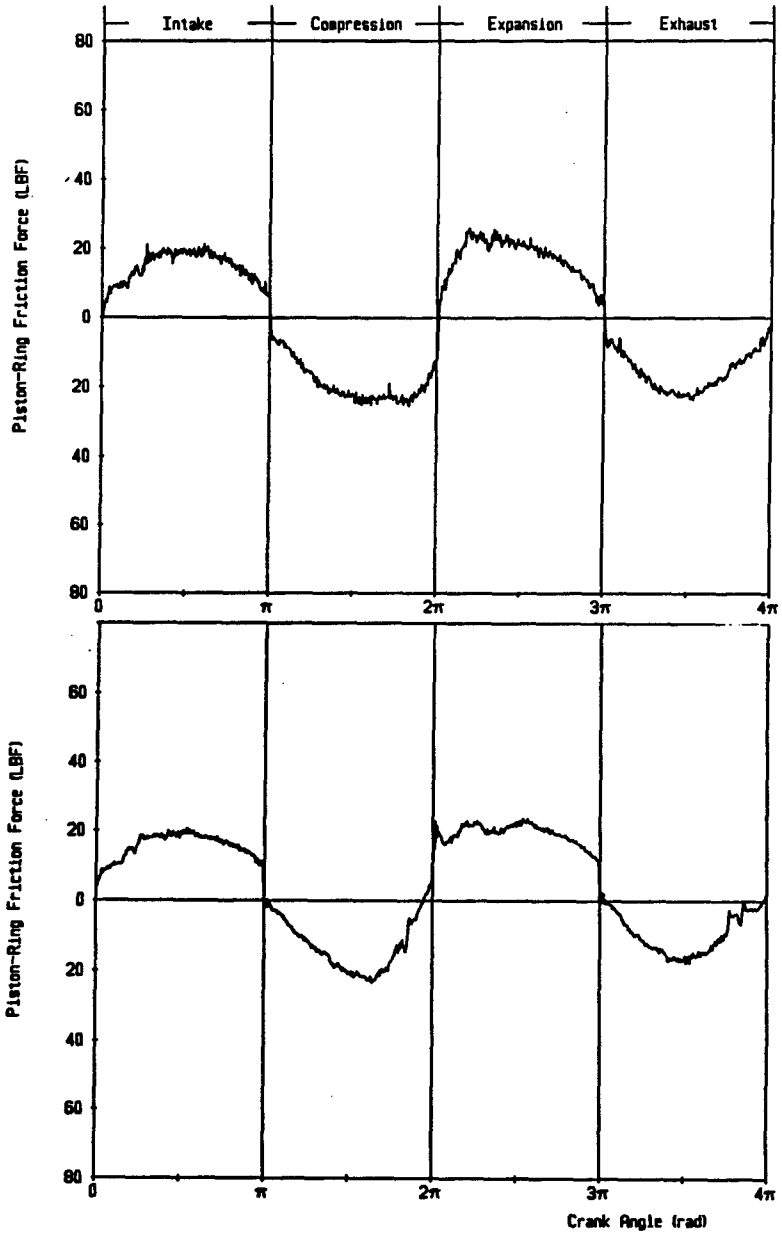

Figure 5-59. Comparison of Fixed-Sleeve (upper) and Instantaneous IMEP (lower) Methods, Motoring, 1000 RPM, SAE 50 Oil, 14.39 PSIA Manifold Pressure, 104 F Water, 130 F Oil

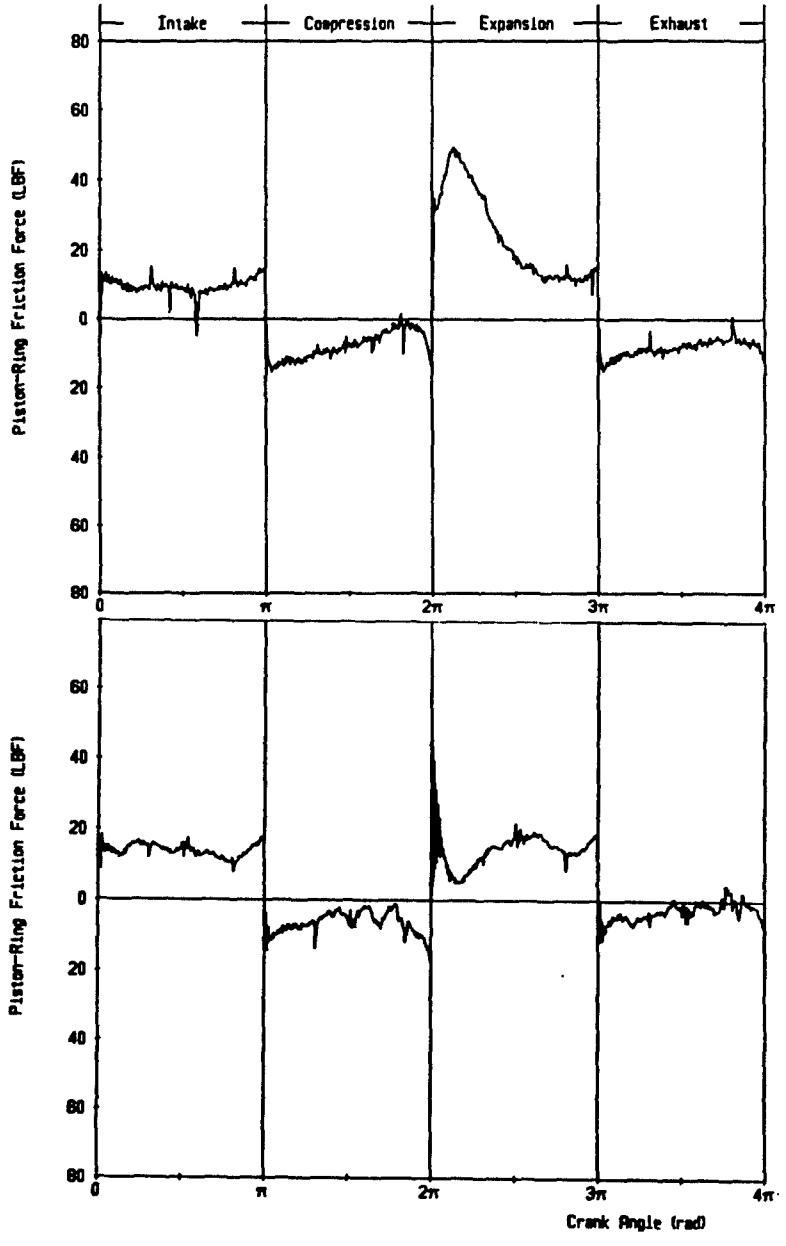

Figure 5-60. Comparison of Fixed-Sleeve (upper) and Instantaneous IMEP (lower) Methods, Firing, 1000 RPM, SAE 30 Oil, 8.39 PSIA Manifold Pressure, 176 F Water, 220 F Oil

friction near TDC expansion, both methods must differ large forces to get a relatively small friction force. The Fixed-Sleeve method is less sensitive to pressure-transducer error, as discussed above. Subjectively, the Fixed-Sleeve trace "looks" more correct. The PR FMEP differed, 6.18 psi for the Fixed-Sleeve and 4.64 psi for the IMEP method.

A variety of additional PR FMEP results are plotted in Figure 5-61. The Fixed-Sleeve results are consistently higher. In light of the fact that the Fixed-Sleeve method does not account for piston pin friction, the higher result for the Fixed-Sleeve method suggests that there is a systematic difference between the two methods.

Comments. As noted, there seems to be some differences and many similarities between the two methods. The points of agreement strengthen confidence in the overall friction results by either method. An important fact to note is that the Instantaneous IMEP method does not require engine modifications that affect friction, whereas the the Fixed-Sleeve method does. (In the present comparison, both methods were applied to the modified engine simultaneously.) Probably, the Fixed-Sleeve method is more precise but may not provide as true a picture of the friction of the original unmodified engine. More comparisons of this type are needed in the future, to strengthen confidence in the measurements.

5.4.2.4. Testing With the Cummins 903 Engine.

Fixed-Sleeve Results - Motored. The Fixed Sleeve method was evaluated under motoring conditions on the 903 engine. Some results are discussed below. Figure 5-62 show the friction force motoring at 100 rpm. PR FMEP was 4.08 psi. This is a believeable value at this low speed, where the friction is mainly boundary or mixed. This engine set-up was also bothered by magnetic noise, mainly from the crankshaft. This noise, reported as friction, is shown in Figure 5-63. Clearly, it is a significant noise with respect to the signal. The motoring friction, with the magnetic noise subtracted, is shown in Figure 5-64. This improved the appearance of the trace (less hydrodynamic in appearance) and lowered the PR FMEP to 3.73 psi.

At 1000 rpm motoring, the magnetic noise predominated, Figure 5-65. Figure 5-66 shows the motoring friction, at 1000 rpm, corrected for the magnetic noise. It is uncomfortable to work with data to which such a large correction is applied, although the curve does not look incorrect in its general shape. The PR FMEP was -4.85 psi, obviously incorrect.

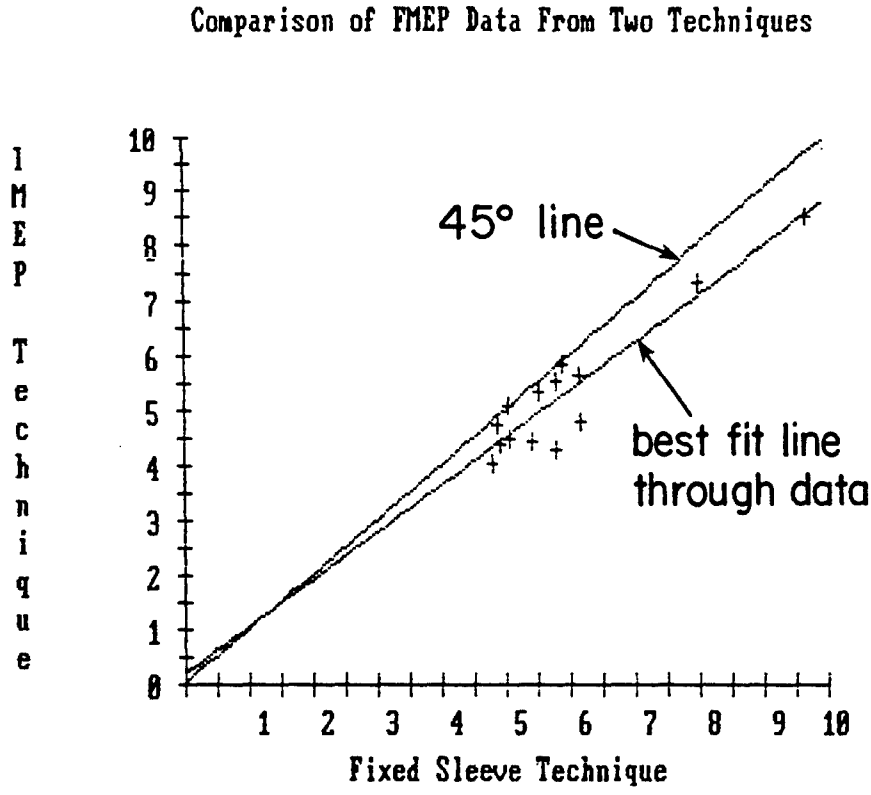

Figure 5-61. Comparison of PR FMEP Results for the Two Methods: (The Fixed-Sleeve Results are Consistently Higher)

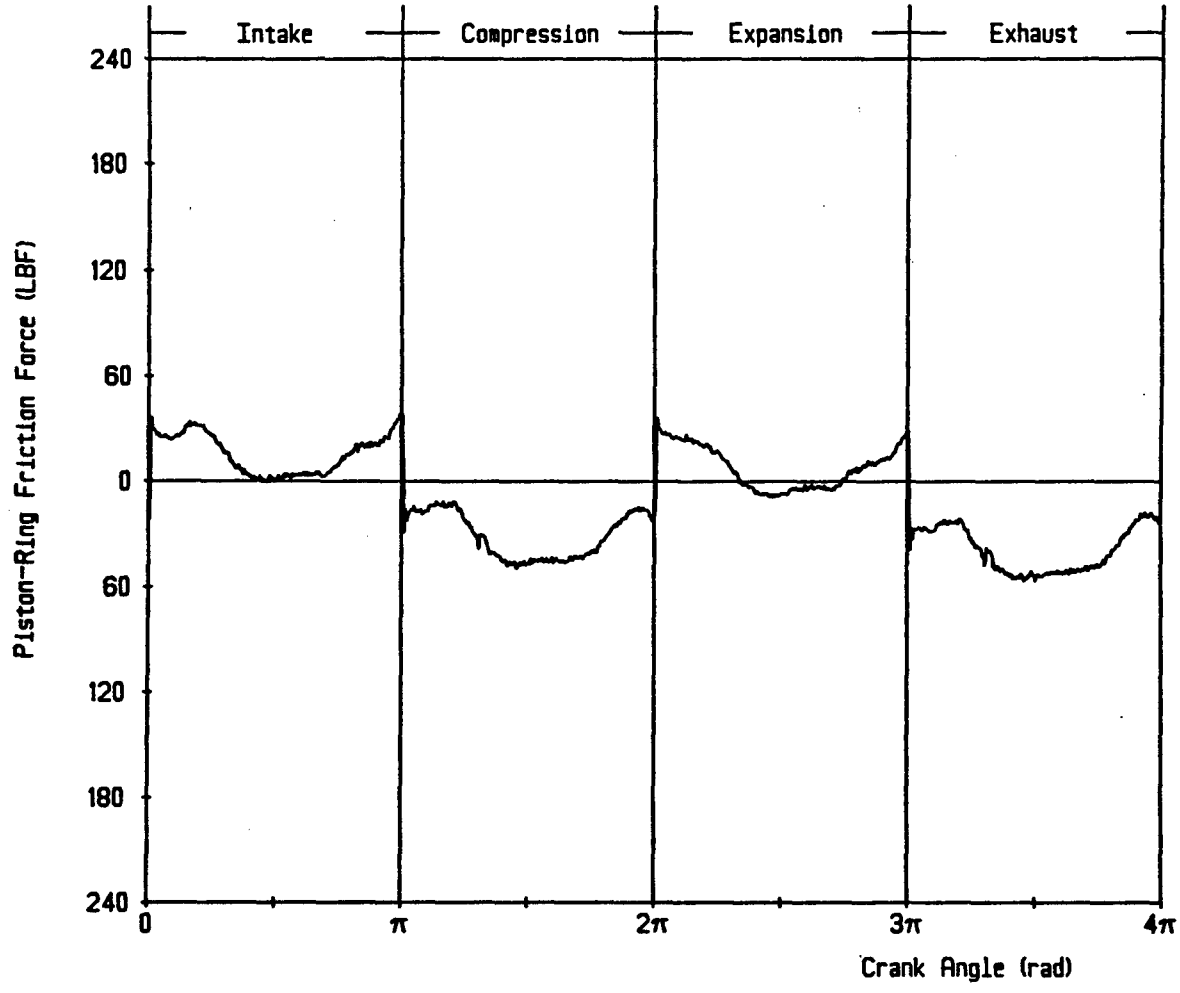

Figure 5-62. Piston and Ring Friction by Fixed-Sleeve Method, Cummins 903 Engine, 100 RPM, SAE 40 Oil, Motoring, 175 F Water, 195 F Oil, Friction MEP = 4.08 PSI

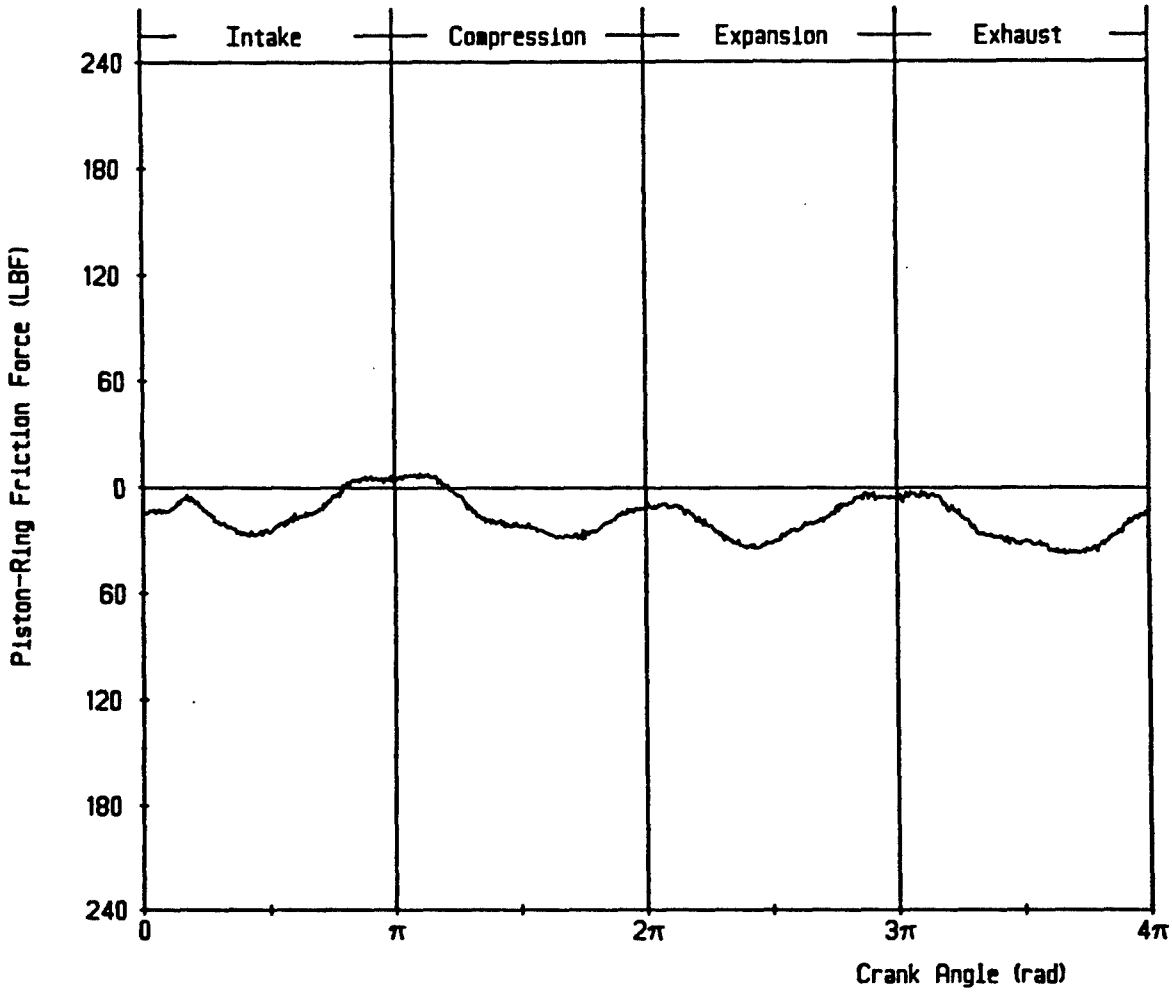

Figure 5-63. Noise Generated by Magnetic Fields, No Bridge Excitation, 100 RPM

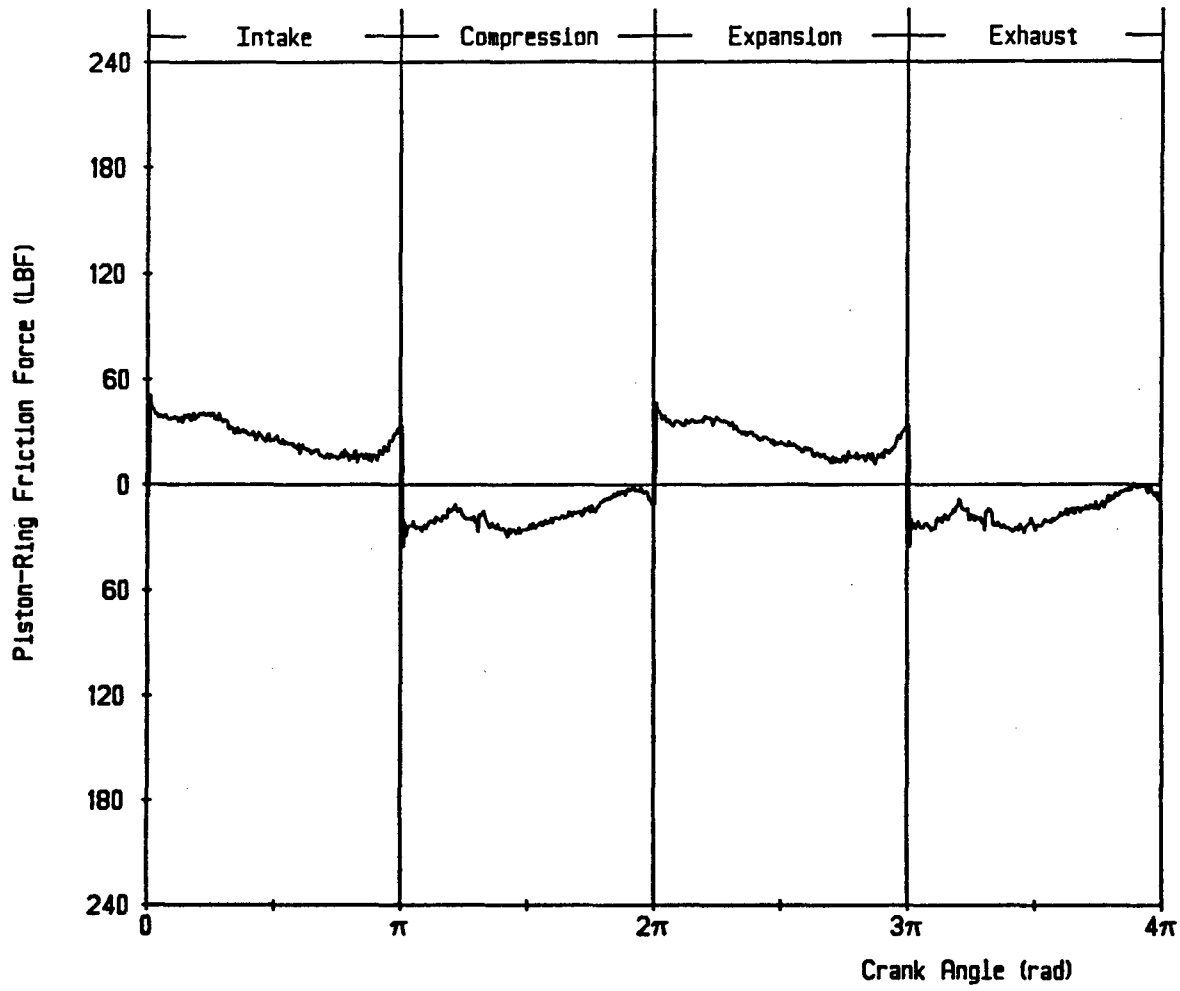

Figure 5-64. Data of Figure 5-62 Corrected for Magnetic Interference

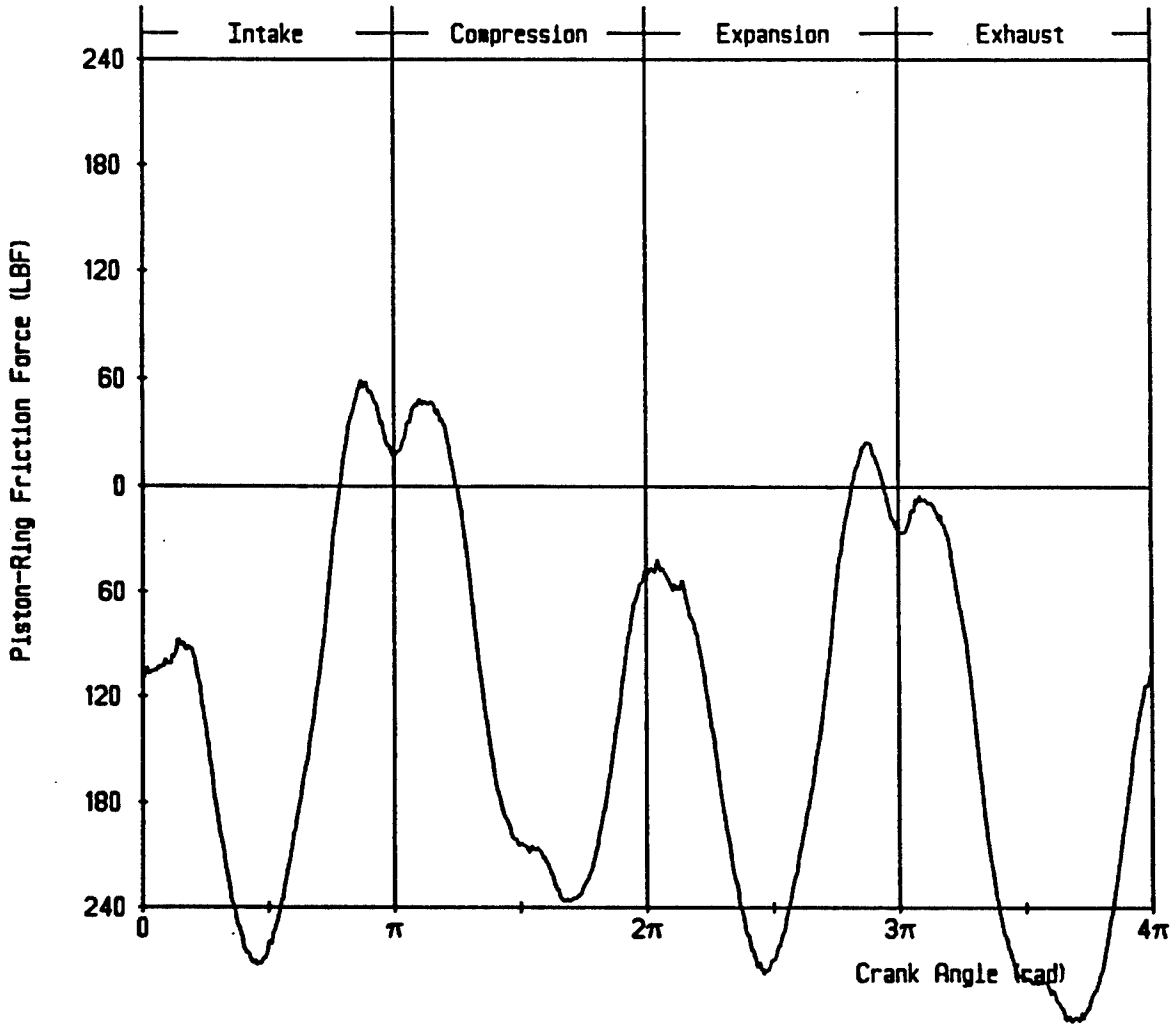

Figure 5-65. Noise Generated by Magnetic Fields, No Bridge Excitation, 1000 RPM

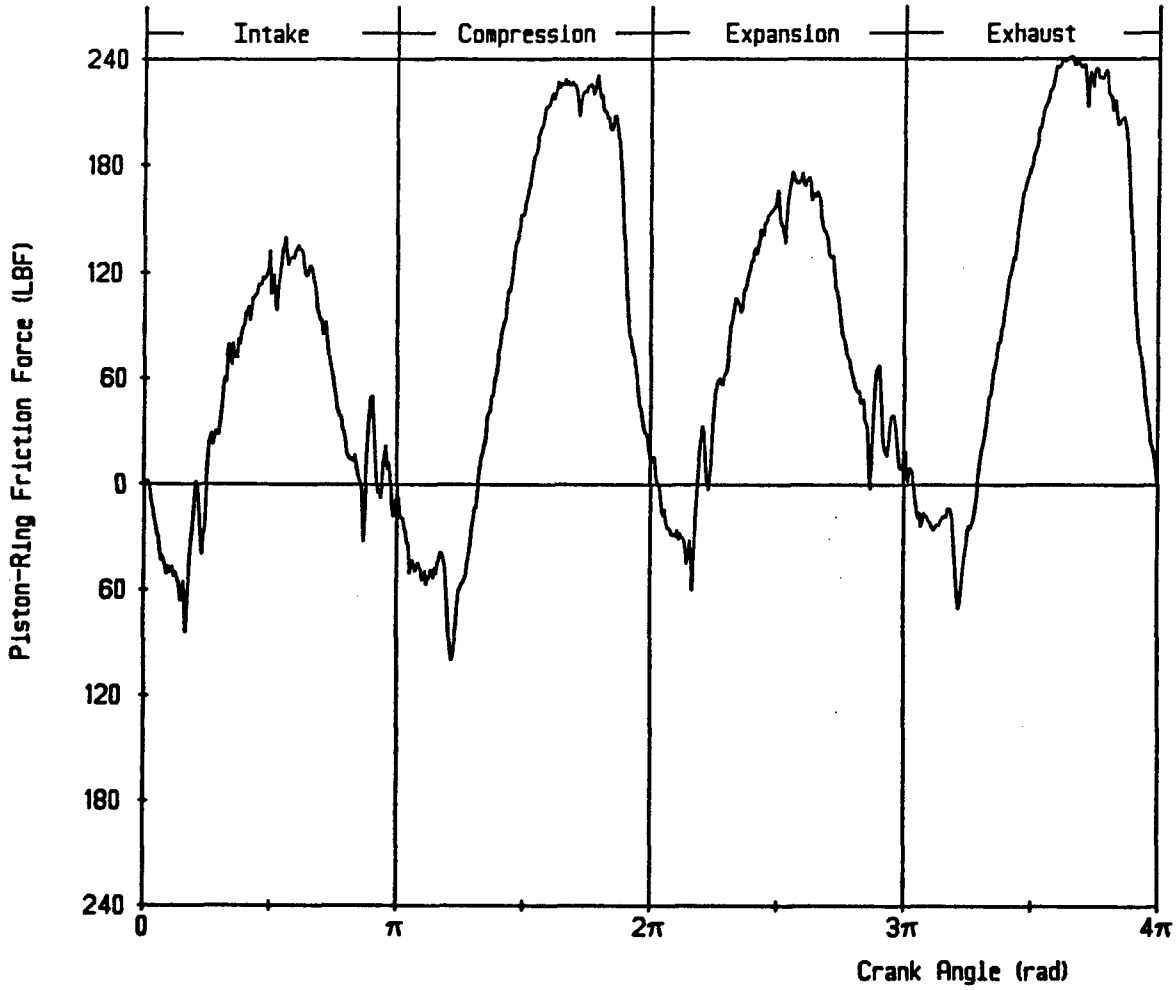

Figure 5-66. Piston and Ring Friction by Fixed-Sleeve Method, Cummins 903 Engine, 1000 RPM, SAE 40 Oil, Motoring, 175 F Water, 195 F Oil, Friction MEP = 4.85 PSI, Corrected for Magnetic Noise

With such a large magnetic interference at meaningful engine speeds, it was decided to terminate the test, degauss engine parts, and rework the design and shielding of the instrumentation. One problem noted with the Fixed-Sleeve design was the inability to "screw" the liner into the block with the rubber O-rings in place. Another was that the steel sealing ring produced some hysterisis. The engine was not fired.

Part of the problem with the magnetic noise may have arisen from the manner in which the strain-gauges were wired. Apparently, large loops acted as antenna to pick up magnetic noise from the rotating crank and from the background electrical noise of the dynamometer. Some bending induced signal was also noted.

A new collar was built with a thinner strain-gauge region cross section (reduced from 0.1 to 0.05 inches), in order to improve signal to noise ratio, but it was not instrumented or tested prior to the end of the program. Thus, it is not known whether that would have helped the noise problem. The collar could not be thinned too much for structural reasons.

Comments on the Fixed-Sleeve Method. Measuring piston and ring friction in a boosted, uncooled diesel engine is a challenge. The Fixed-Sleeve method appears to be a promising approach. Its virtues are that the strain- gauge instrumentation is attached neither to the piston or liner, and consequently either piston or liner can be replaced without disturbing the instrumentation. Also the instrumentation is located away from the major heat source and can be cooled as required. This is expected to be a plus for the uncooled diesel. Finally, errors in the cylinder pressure measurement are less of a problem, since the pressure correction involves forces acting on the rim area, rather than the entire piston crown, as is the case in the Instantaneous IMEP method. This is a plus, no doubt, in an uncooled engine. Further, compared to the Instantaneous IMEP method, there are no inertia forces to take into account. Like the Instantaneous IMEP method, magnetic interference must be considered.

5.4.3. Ring and Liner Bench Test. Below are presented baseline test results for lubricated production chrome-plated ring and gray iron liner at 25 C. These results are compared with other material combinations which had been previously tested in an uncooled Cummins NTC 250 engine. These combinations were tested with and without lubrication at 427 C; a temperature which would rapidly fail production materials, especially without lubrication. Table 5-6 gives the five combinations reported and the test conditions under

Table 5-6. Simulator Material Couples and Wear

A. Simulator Data

	Ring	Liner	Lube	Temp	Liner Mean Wear Depth um	Liner Wear Coef mm3/mm/N	Fric Coef
1.	Chrome Plate	Gray Iron	Mineral	25 C	1.5	1.9xE-9	0.05
2.	Plasma Sprayed Cr2O3	Plasma Sprayed Cr2O3	None	427	<0.25	<3xE-10	0.55
3.	TiC/ CaF2	Cr3C2	None	427	35	4.5xE-8	0.58
4.	Plasma Sprayed Cr2O3	Plasma Sprayed Cr2O3	Syn A	427			0.15
5.	TiC/ CaF2	Cr3C2	Syn A	427			0.1

Test Conditions: Load - 124 N/cm
Speed - 266 rpm
Test Duration - 2 hrs
Oil Supply Rate - 1 ml/hr @ 25 C
- 10 ml/hr @ 427 C

B. Cameron Plint Data

	Ring	Liner	Lube	Temp	Speed rpm	Load N	Liner Wear Coef cu mm/mm/N	Fric Coef
1.	Chrome Plate	Gray Iron	Mineral	25 C	600	100 (8N/mm)	2.3xE-9	0.16
2.	Chrome Plate	Gray Iron	Mineral	25	1200	250 (20N/mm)	1.4xE-11	0.06
3.	TiC/ CaF2	Cr3C2	None	360	600	250 (20N/mm)	1.9xE-8	1.45

Note: Test speed very important at room temperature (EHD vs boundary transition) for Cameron Plint.

which they were run, including load. Comparisons with Cameron Plint and firing engine tests are made.

5.4.3.1. Baseline Ring/Liner Results. Figures 5-67, 5-68 and 5-69 show baseline results with the production chrome plated top-ring, Lubrited gray iron liner, and with mineral oil lubrication. Test temperature was 25 C and load was 85.4 N on the liner segment whose width was 0.69 cm. This provided a load of 125 N/cm. Figure 5-67 shows friction coefficient as a function of crankangle over the 360 deg stroke. The coefficient is the average of right and left sides. The oscillations seen on the trace arise from vibrations brought on by the relatively heavy mass of the reciprocating ring holder and the compliant structure of the reciprocating mechanism. The average friction coefficient over the cycle was approximately 0.04, which suggests that lubrication was predominantly EHD. Figure 5-68 shows the liner sample surface profile as a function of sample length. This measurement was made with a Sheffield Surface Proficorder, Model RLC 7. The recessed portion of the trace, which is the length of the 2.54 cm stroke shows the total wear. Note that the wear is greater near the dead centers and less near the center of travel, perhaps showing a transition from boundary to EHD/mixed lubrication as the ring velocity increased. Figure 5-69 shows how the average friction coefficient changed with time, as the test continued. There was a substantial drop as the break-in process occurred reaching a level of about 0.055.

5.4.3.2. Titanium Carbide Ring and Chrome Carbide Liner Coatings. For coated components, sample temperatures were set to 427 C and load maintained at 85.4 N/cm. Two-hour tests were run. Figure 5-70 shows average friction coefficient results for the titanium carbide ring on the chromium carbide liner without lubrication. This is combination 3 in Table 5-6. There was no change in friction coefficient, as the test progressed. The average value remained quite high at 0.58.

The friction coefficient dropped significantly with time when the synthetic oil was used (Figure 5-71). This is combination 5 in Table 5-6. After two hours, the friction coefficient dropped to about 0.1, indicating predominately boundary lubrication.

Figure 5-72 shows Proficorder surface roughness traces of the fresh liner surface, and for two worn samples after the two-hour test. One sample was worn dry, and the other with the synthetic lubricant. The unworn surface was relatively rough. The lubricated sample was smoothed considerably when worn, but the unlubricated sample was further roughened.

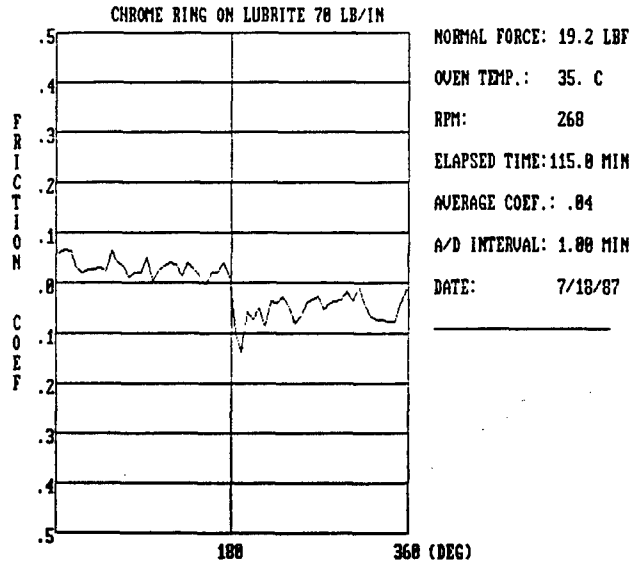

Figure 5-67. Friction Coefficient Versus Crank Angle for Base Engine Materials, Normal Force 85.4 N, 268 RPM, 35 C Test Temperature

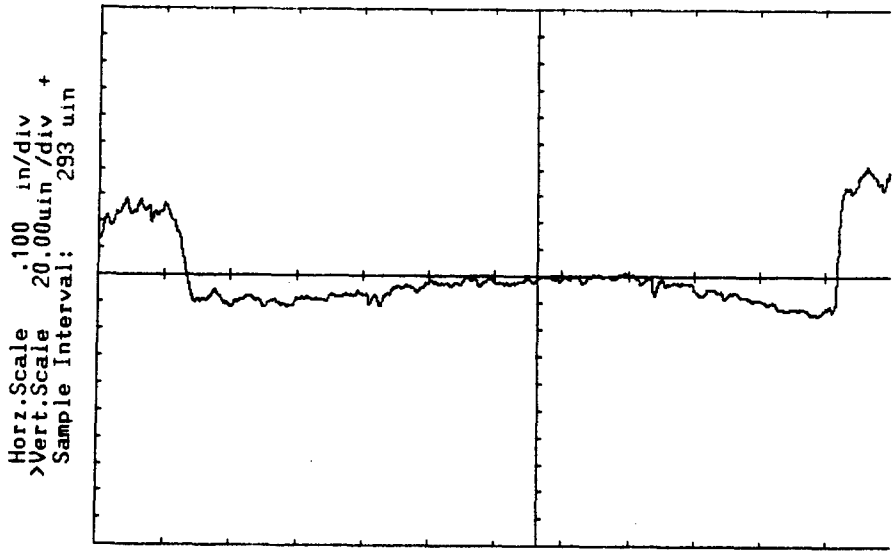

Figure 5-68. Proficorder Trace of Worn Baseline Liner Tested Against Chromium Plated Ring, Mineral Oil: Scale Vert = 0.51 um/div, Horiz = 2.5 mm/div, Sample Interval of 7.4 um

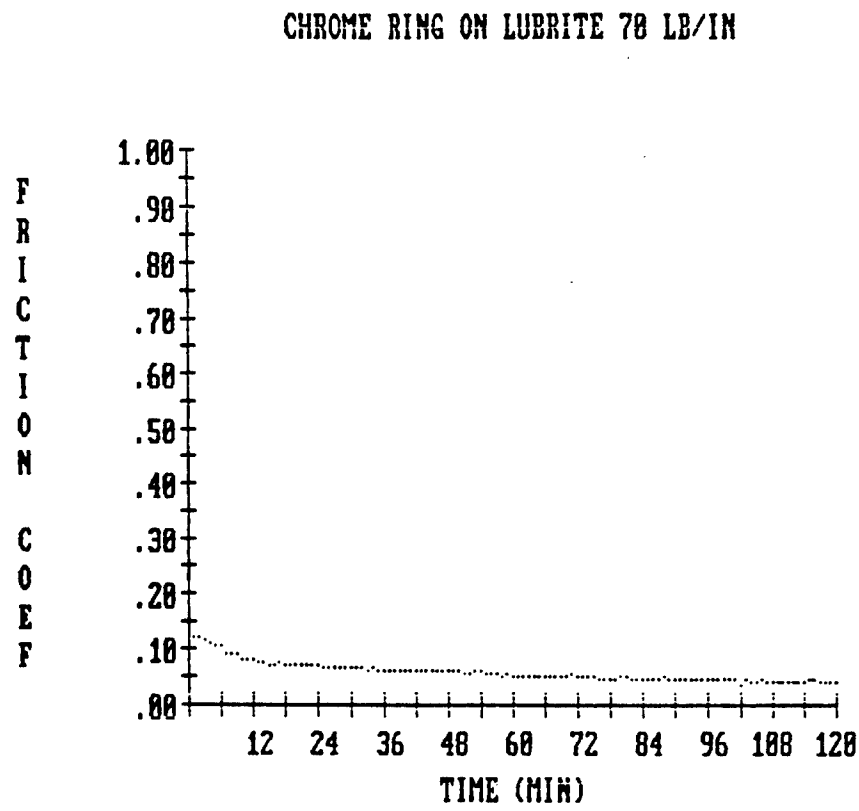

Figure 5-69. Average Friction Coefficient During Test, Baseline Engine Materials, Lubricated

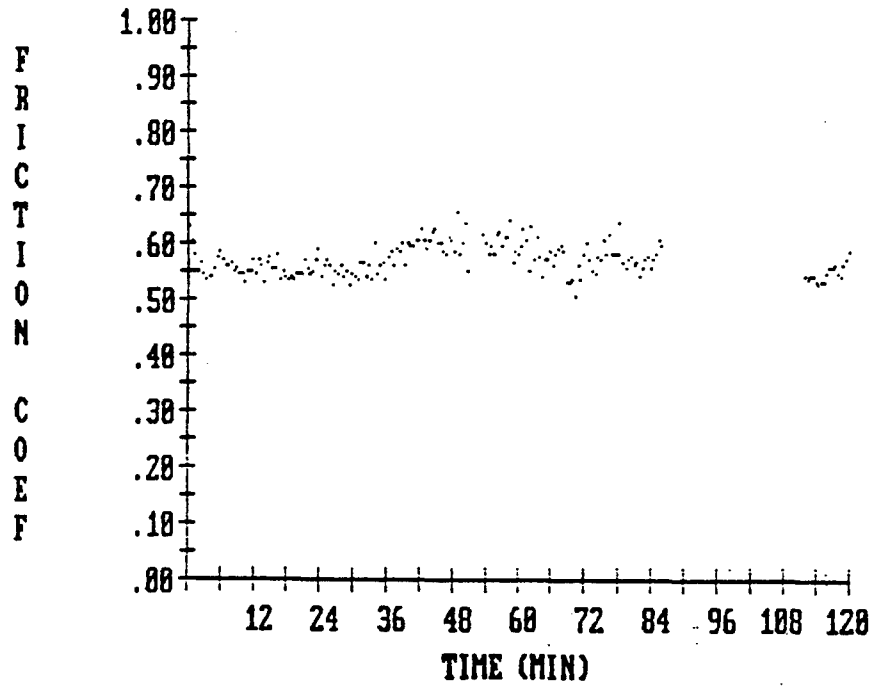

Figure 5-70. Average Friction Coefficient Over Test, Titanium Carbide Ring on Chromium Carbide Liner, No Lubrication

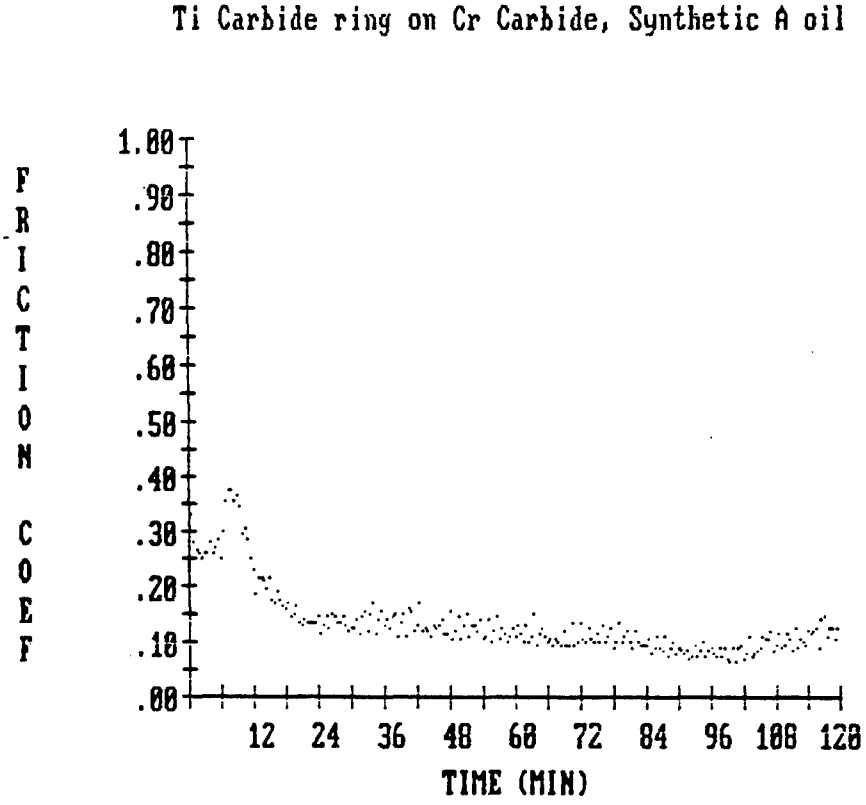

Figure 5-71. Average Friction Coefficient Over Test, Titanium Carbide Ring on Chromium Carbide Liner, Synthetic Lubricant

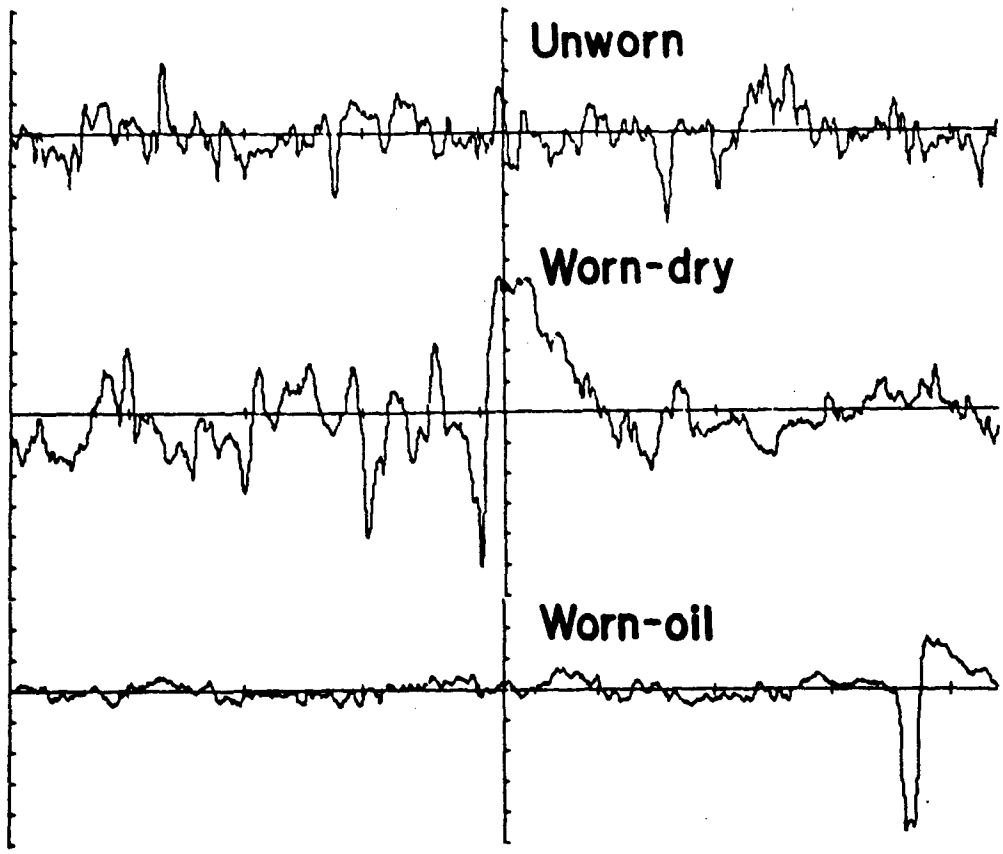

Figure 5-72. Proficorder Roughness Traces of Plasma Sprayed Chromium Carbide Liners, Before and After Two-Hour Test Against Titanium Carbide Plasma Sprayed Ring, Scale: vert = 0.25 um/div, Horiz = 0.1 mm/div, Sample Interval of 1.0 um

The data in Figure 5-72 showed the AC components of the surface roughness. Figure 5-73 shows the DC components. The extent of material removal is apparent along the 2.54 cm wear scar. Clearly the amount of material removed was less when lubricated.

5.4.3.3. Plasma-Sprayed Chromium Oxide Ring and Liner Coatings. Figure 5-74 shows average friction coefficient results from the simulator for plasma-sprayed chromium oxide ring and plasma-sprayed chromium oxide liner coating, without lubrication at 427 C. Note that the friction coefficient increased somewhat during the course of the test. This is combination 2 of Table 5-6. After two-hours of testing, the friction coefficient reached 0.55.

The use of synthetic oil reduced the friction coefficient significantly, Figure 5-75. This is combination 4 of Table 5-6. After two hours, the friction coefficient averaged about 0.15. Wear rates were too low to be measurable, but significant smoothing occurred.

Figures 5-76 and 5-77 shown Proficorder measurements for the chromium oxide samples, similar to those shown in Figures 5-72 and 5-73 for the chromium carbide specimens. In viewing Figure 5-76, it is apparent that significant smoothing occurred when the synthetic lubricant was used, and some roughening occurred when run dry. Figure 5-77 shows that very little material was removed in either case.

In comparison with the titanium carbide, chromium carbide results of Figure 5-70, this combination shows relatively little surface wear or roughness increase throughout the entire stroke. We may conclude that the simulator ranks this material to be relatively durable under these severe operating conditions. The one apparent negative is the very high friction coefficient of the chromium oxide rubbing surfaces when run dry, although it is not significantly different from that of the chromium carbide, titanium carbide pair.

5.4.3.4. Comparison With Cameron Plint. A comparison of these results with Cameron Plint (TE 77) data measured at Cummins by Dr. Malcolm Naylor, Reference 14 will now be made. Figure 5-78 shows the Cameron Plint results for a variety of material pairs in terms of wear coefficient as a function of temperature. The wear coefficient is defined as the volume of liner removed (cubic millimeters) per millimeter of liner length per Newton of force imposed. Note that the conventional chrome-plated gray iron combination on the lower left-hand corner of the graph gave values of about 3 - 6x10exp(-12) in the temperature range

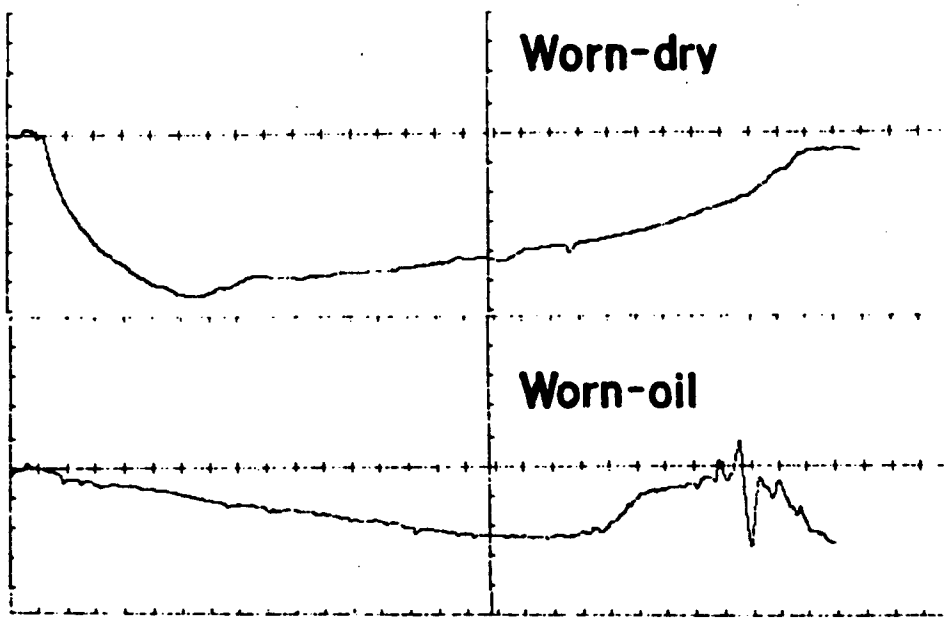

Figure 5-73. Proficorder Traces Showing Wear Scar Geometry on Worn Chromium Carbide Liner Samples, Two-Hour Test, Scale: vert = 5.0 um/div, horiz = 1.0 mm/div, Sample Interval of 7.0 um

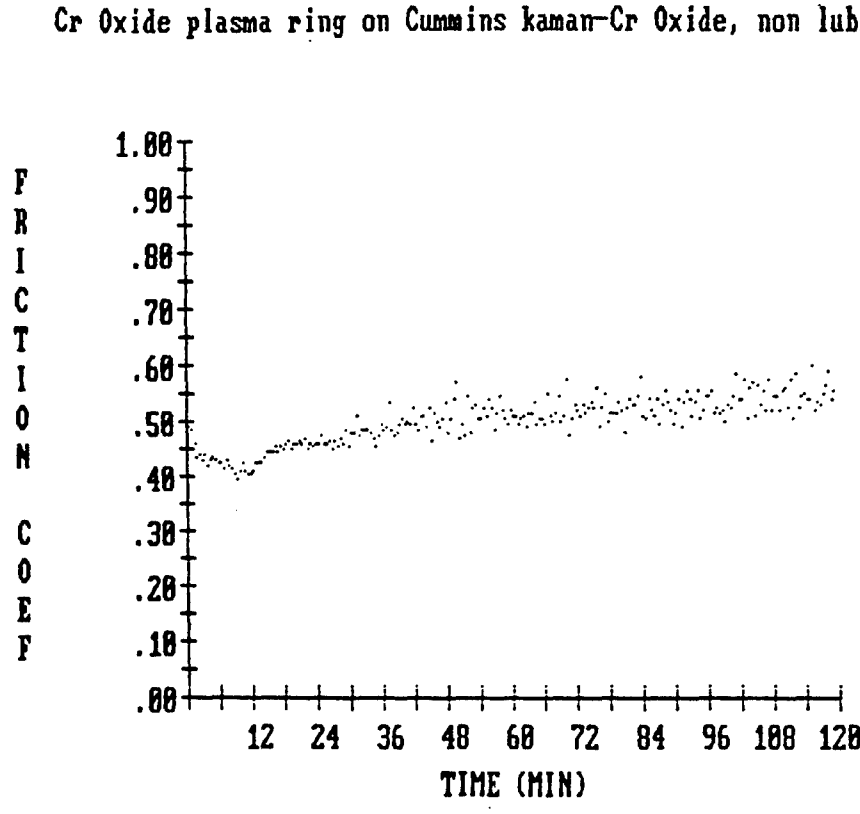

Figure 5-74. Average Friction Coefficient Over Test, Chromium Oxide Ring on Chromium Oxide Liner, No Lubricant

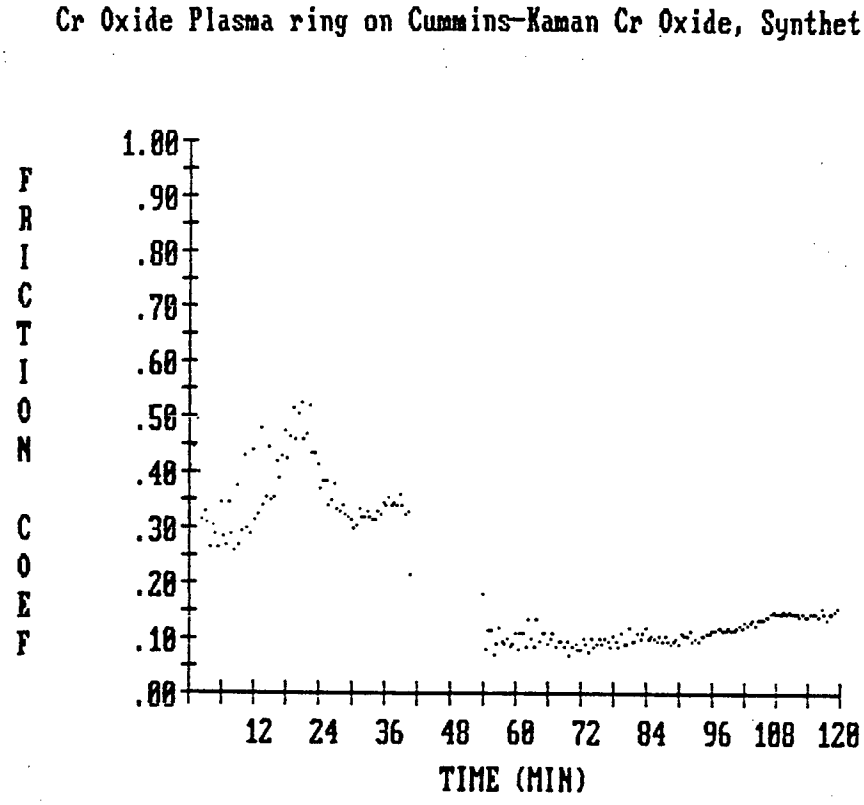

Figure 5-75. Average Friction Coefficient Over Test, Chromium Oxide Ring on Chromium Oxide Liner, Synthetic Lubricant

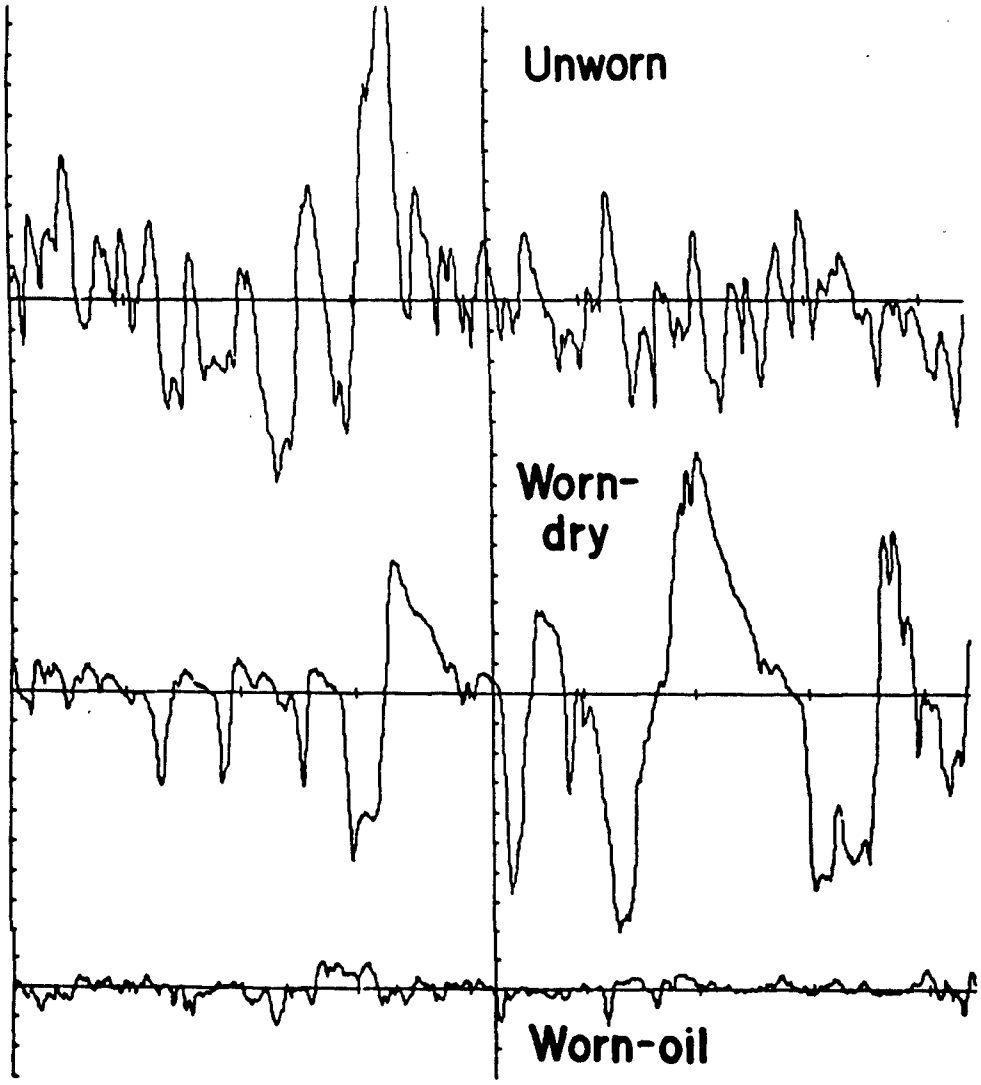

Figure 5-76. Proficorder Roughness Traces of Plasma-Sprayed Chromium Oxide Liners, Before and After Two-Hour Test Against Chromium Oxide Plasma Sprayed Ring, Scale: vert = 0.25 um/div, Horiz = 0.1 mm/div, Sample Interval of 1.0 um

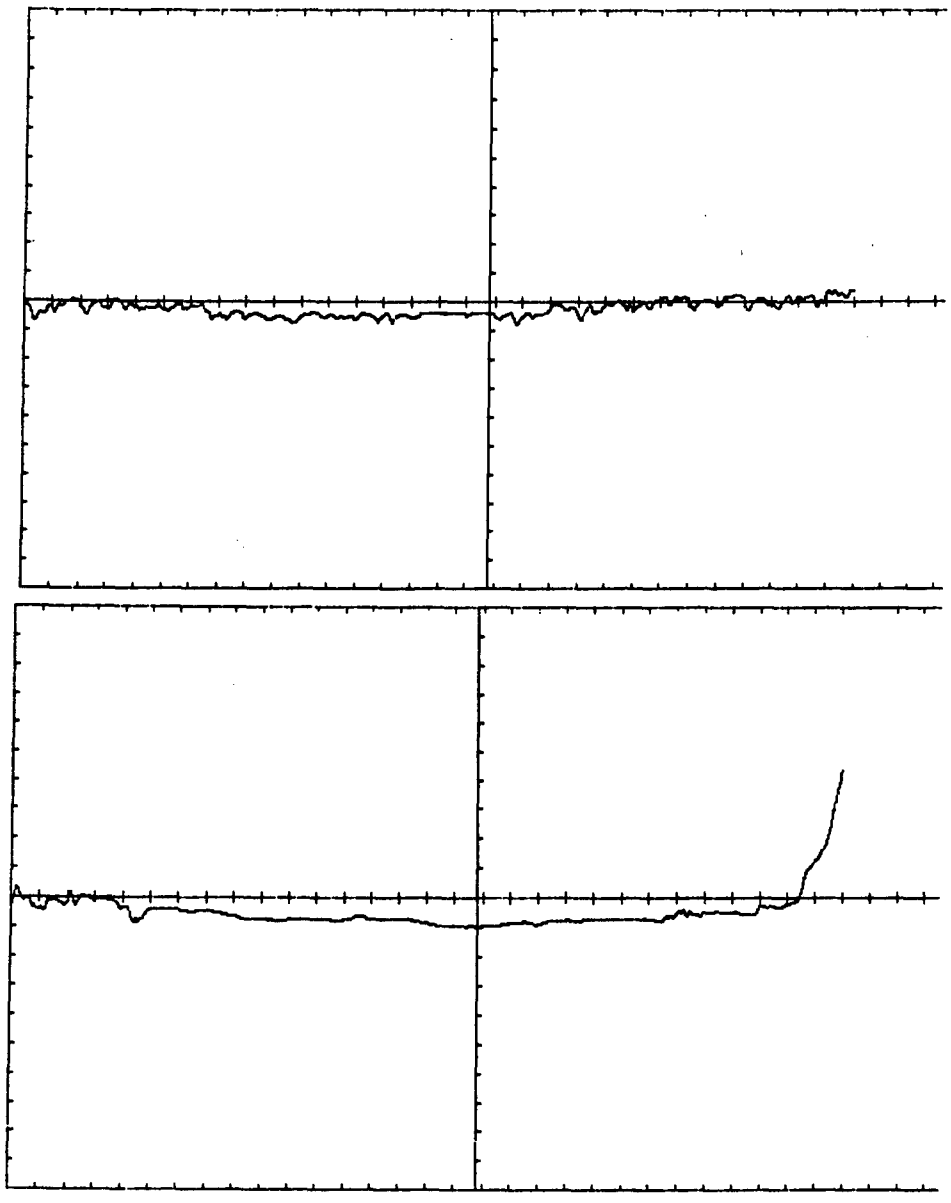

Figure 5-77. Proficorder Traces Showing Wear Scar Geometry on Worn Chromium Oxide Liner Samples, Two-Hour Test, Scale: vert = 5.0 um/div, horiz = 1.0 mm/div, Sample Interval of 7.0 um

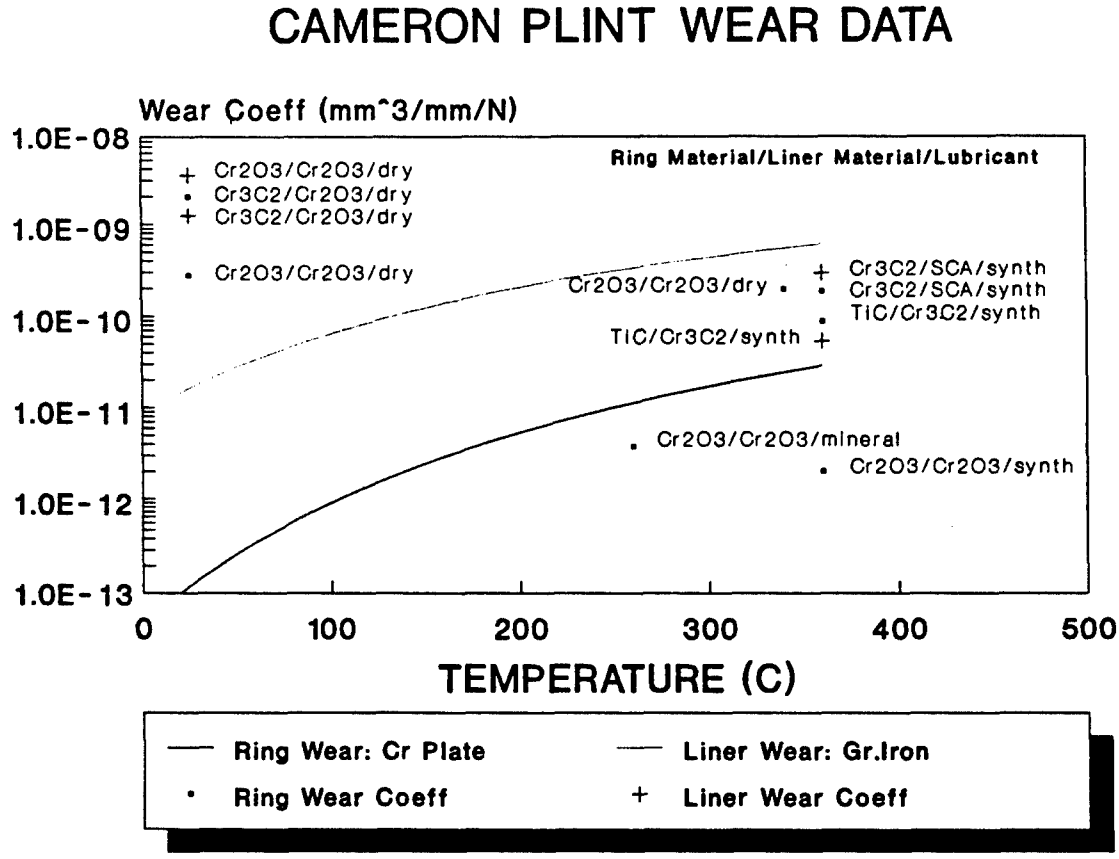

Figure 5-78. Ring and Liner Wear Coefficients from Cameron Plint Tests: Solid and Dashed Lines Show Variations of Ring and Liner Wear with Temperature for Conventional Materials (Cr Plated Ring, Gray Iron Liner) with a Commercial CE/SF 15W40 \Mineral Oil Based Lubricant; Points are for Various Ceramic Coatings; Captions Refer to Ring Material, Liner Material, and Lubricant Combination; Cr2O3, and Cr3C2 are Plasma Sprayed; TiC is Plasma Sprayed with CaF2, Ni, and Cr; SCA is Silica-Chromia-/Alumina Slury Coating

150 - 200 C. Such temperatures would be considered normal for highly turbocharged engines. As temperature increased, the conventional chrome-plated, gray iron combination deteriorated significantly, giving a wear coefficient of about 3x10exp(-11) at 350 C. The results given in Table 5-6 show good correlation between the bench simulator and Cameron Plint.

5.4.3.5. Comparison with Engine Results. The wear in the simulator of the unlubricated ring and liner correlated well with results from uncooled NTC-250 high-temperature engine tests. This 6-cylinder, heavy-duty diesel engine, with a displacement of 855 cubic inches, was operated for 300 hours without cooling water. Top-ring reversal temperature approximated 427 C. Because of the increased stress placed on the lubricant at the higher operating temperatures, coatings (Table 5-7) were used on the ring and liner surfaces to control wear. Of several combinations tested, the plasma-sprayed chromium oxide coating and the TiC/Cr3C2 ring/liner combinations were found to have the lowest and highest wear rates respectively, based on profilometer traces (Figures 5-79 and 5-80) of the components from the above tests.

As discussed previously, unlubricated wear simulator evaluations were performed on the same wear couple combinations using samples of rings and liners used for the 300 hr engine test. Profilometer traces from these tests (Figures 5-72 and 5-76) show the performance of the chromium oxide and TiC/Cr3C2 couples to agree with the engine wear results on a relative basis.

5.4.3.6. Interface Oil Quantity and Quality Considerations. One of the significant differences between the present simulator and earlier versions is the means by which the friction force is obtained. Currently, the simulator employs strain-gauged pivots (see Figure 5-8 for location), which permits measurement of right and left friction forces simultaneously. Viewing these results, it was apparent that side-to-side differences initially existed. Unlike an engine, the oil supply at the wear interface of the simulator can be systematically varied in both quantity and quality. Differences in results side-to-side are virtually eliminated when oil quantity and quality are also equal side to side.

Figures 5-81 and 5-82 show how average friction coefficient history varied when oil supply quality was more equalized side-to-side. Test results are for production gray iron liner, chrome-plated top-ring, and CE/SF 15W40 oil. Between tests, oil supply tube targeting was improved, and spray

Table 5-7. Uncooled NTC-250 Ring and Liner Coatings

Piston Ring Coatings	Liner Coatings
A. Best Combinations	
Cr_2O_3	Cr_2O_3
Cr_2O_3	Kaman SCA (Cr_2O_3 Based)
Cr_2C_3	Cr_2O_3
Tribaloy	Tribaloy
B. Other Combinations	
Tribaloy	Cr_2O_3
TiC	Cr_2C_3
Cr_2C_3	Kaman SCA (Cr_2O_3 Based)
Cr_2O_3	Al_2O_3
Al_2O_3/TiO_2	SiC
VC	Tribaloy
TiN	NiCr/Al_2O_3

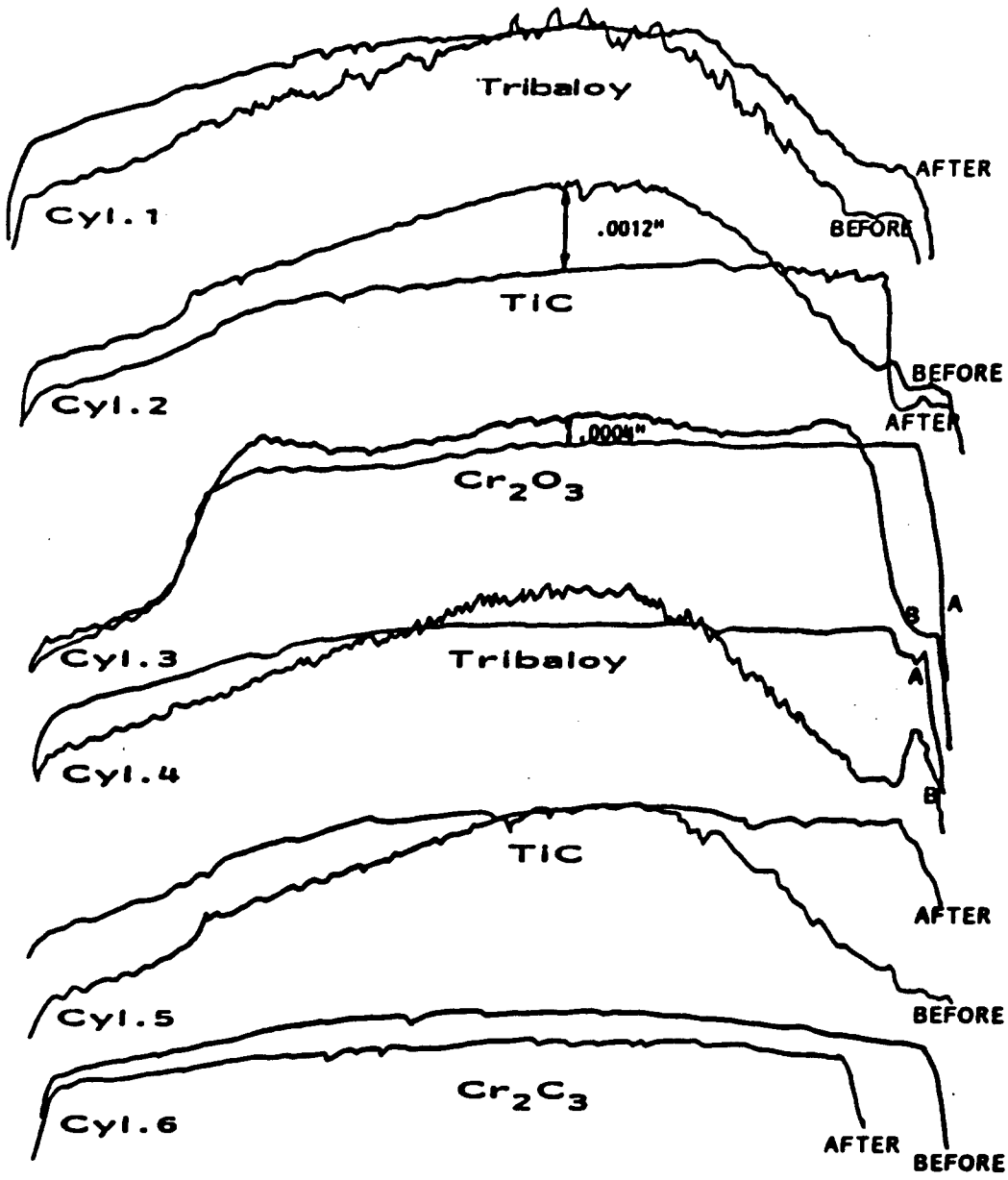

Figure 5-79. Profilometer Traces From Engine-Tested Piston Rings

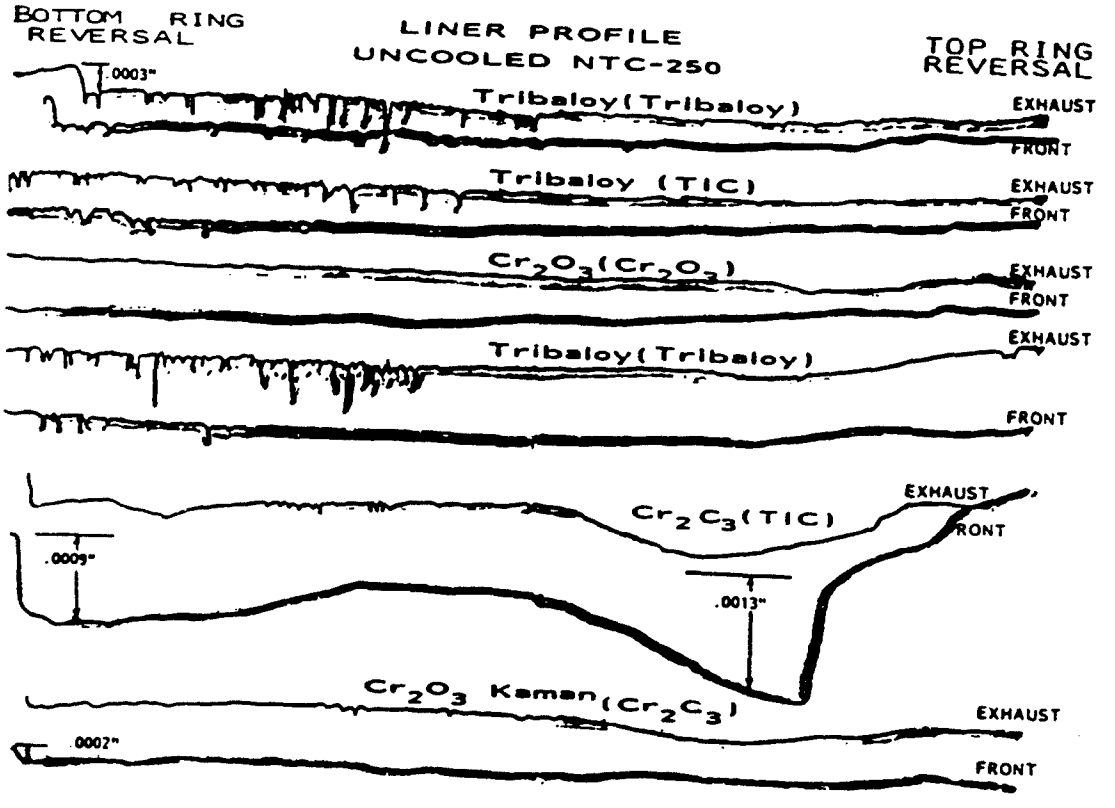

Figure 5-80. Profilometer Traces From Engine-Tested Liners

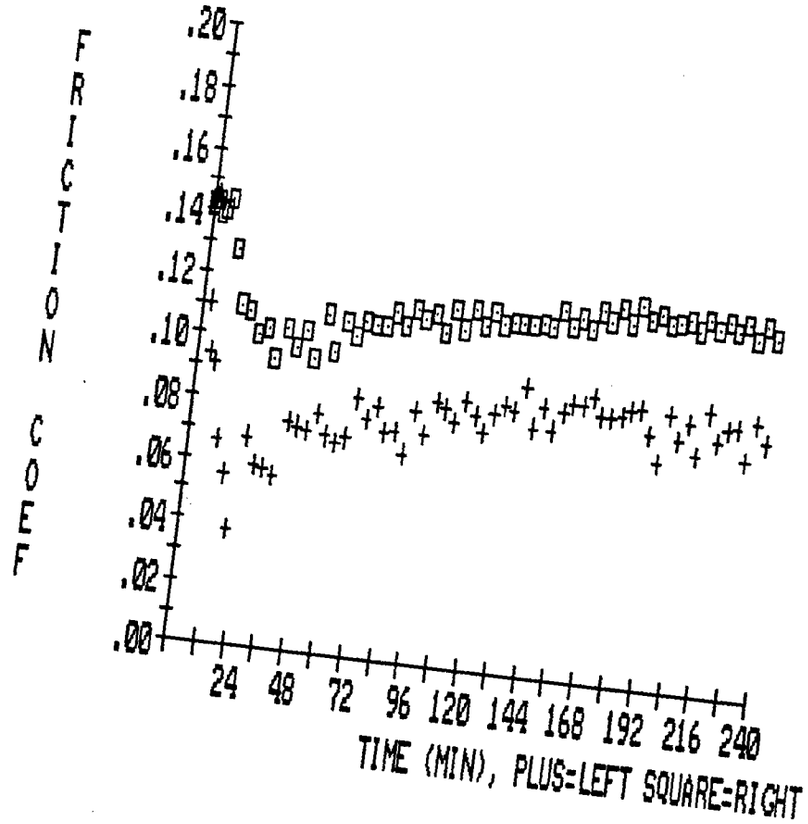

Figure 5-81. Right and Left (+) Side-Friction Coefficient Over Test Before Side-to-Side Lubrication Balance. CE/SF 15W40 Mineral Oil, Chrome-Plated Ring, Gray Iron Liner, 149 C, 180 N Load, 500 RPM

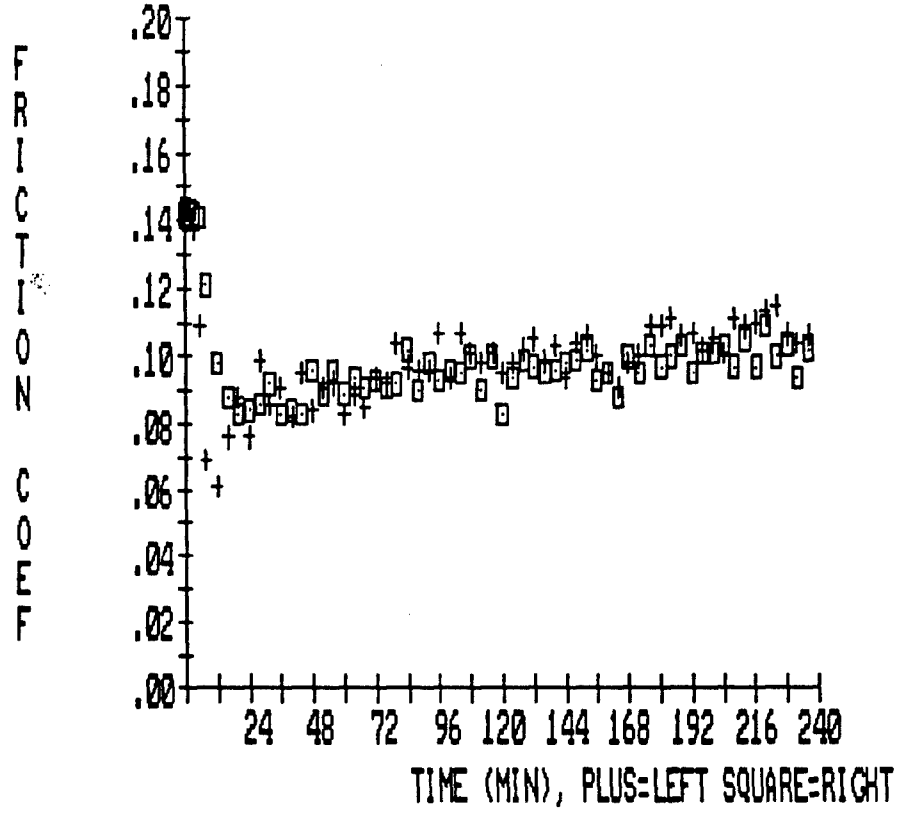

Figure 5-82. Same as Figure 5-81, Except After Partial Lubrication Balance

pattern was made more uniform by use of pressurized air added to the oil injection tubes. With even better oil delivery, side-to-side differences were virtually eliminated, Figure 5-83.

Interesting data which demonstrate side-to-side similarity, as well as lubricant effects, are shown by comparing Figures 5-83 and 5-84. The use of synthetic SDL-1 oil (Figure 5-84) not only eliminated the break-in period but also lowered friction coefficient from a stabilized value of 0.14 to about 0.12, when compared to the CE/SF 15W40 commercial oil.

5.4.3.7. Simulator Repeatability. Table 5-8 gives data showing simulator repeatability at a fixed operating condition with the two different oils discussed above. Both liner weight loss and average friction coefficient, for the last half hour of the four hour test, are shown. While minor variations are evident from sample to sample, it is quite clear that the SDL-1 gave consistently lower wear and friction coefficients under the test conditions employed.

5.4.3.8. Photomicrograph Results from Engine Tests. Several coated liners were run in engines at Cummins. Specimens were cut from these at two positions, near top-ring reversal (TRR) and bottom-ring reversal (BRR). The surfaces were observed under both a polarized light microscope and scanning electron microscope (SEM). Liner coating materials were Cr2O3 and Cr2C3. Ring coatings were Cr3O4 and TiC + CaF2.

Observations were made on the morphology of the worn surface, damage of surface features, and cross-section microhardness. Material hardness was measured, as well as qualitative visual evidence of strength, brittleness and toughness, porosity, and adherence of the ceramic-coating to the cast iron. An attempt was made to identify temperature problems, lubricant problems, and contact problems. However, there was little evidence available for reaching firm conclusions on these points. One interesting observation was the formation of films on the sliding surfaces, which made the surfaces smooth. The role of these films in changing sliding coefficient of friction and wear rate is not known.

Photographic Cross-Section Analysis of Coated Liners - Engine Samples. The atomic structure of ceramics differs from that of metals. This strongly affects the adherence of the ceramic-coating to a metallic liner. Cross-section examination of unworn areas, just below the BRR, showed that the Cr2O3 coating was separated from the metal in several small regions (Figure 5-85), but with Cr2C3, separation was

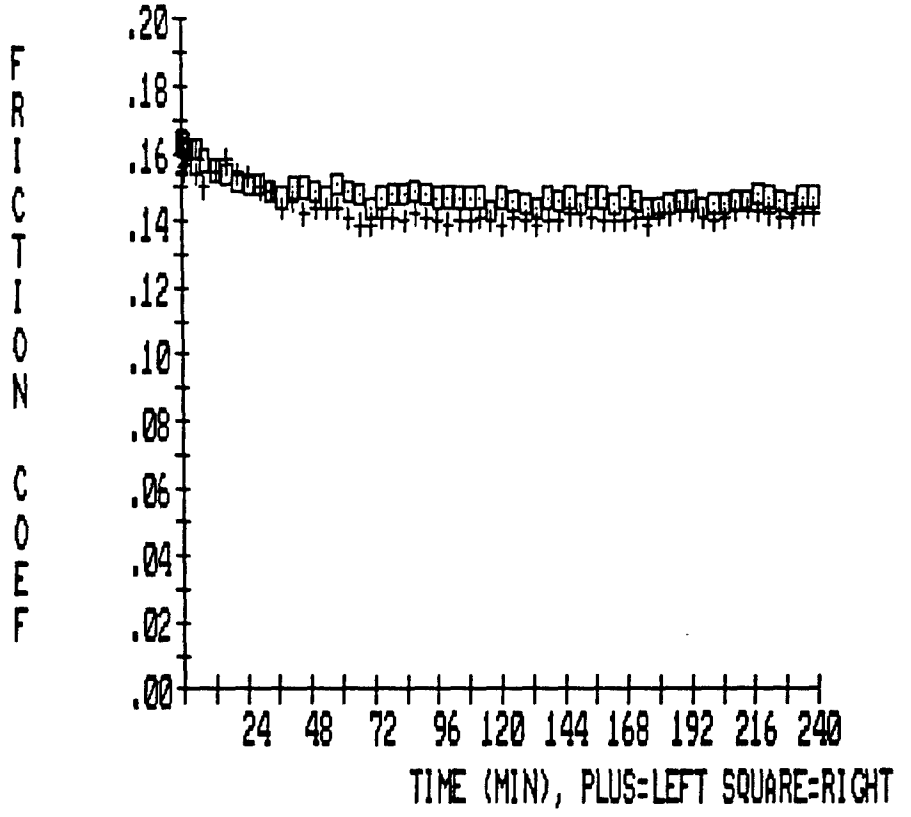

Figure 5-83. Same as Figure 5-81, Except After Full Lubrication Balance

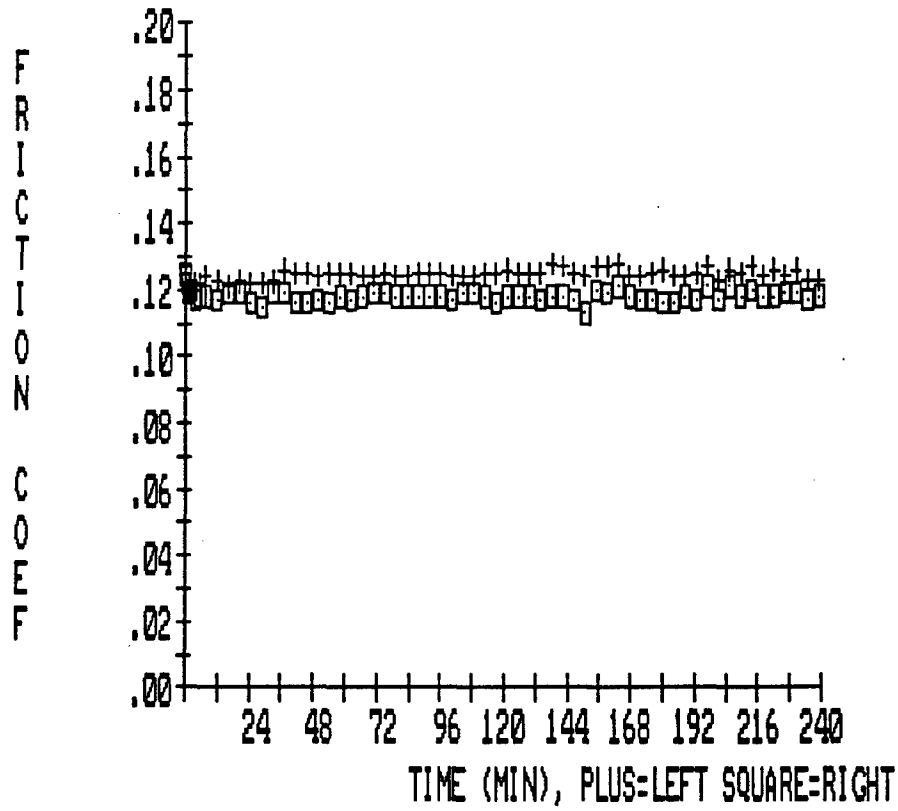

Figure 5-84. Same as Figure 5-83, Except SDL-1 Synthetic Lubricant

Table 5-8. Side-to-Side and Repeatability Comparison

A. Test Conditions: Cummins V-903 Engine Components

Speed:	500 rpm
Oil rate:	2 ml/hr each side
Ring:	Chrome-plated, 140 mm dia, 3.8 mm width
Liner:	Two cast-iron samples, 6.9 mm width
Stroke:	25.4 mm
Temp:	149oC
Load:	180 N normal force (simulates 6.9 MPa pressure behind ring)
Time:	4 hour tests

B. Results

CE/SF: Commercial 15W40 mineral oil

Liner Side	Liner Weight Loss, grams	Average Friction Coef (last 1/2 hr)
L	0.0034	0.14
R	0.0025	0.14
L	0.0027	0.14
R	0.0022	0.14
L	0.0027	0.15
R	0.0013	0.14
L	0.0033	0.14
R	0.0019	0.13

Synthetic Oil: Commercial Polyol Ester, SDL-1

L	0.0010	0.12
R	0.0010	0.12
L	0.0005	0.13
R	0.0004	0.11
L	0.0003	0.13
R	0.0004	0.12

Figure 5-85. Cr2O3 Coated Cross-Section, Unworn Position, Surface Layer Separation from Substrate, #19, Build 4, Cylinder 3, B.R.R., S.E.M., Magnification X 500

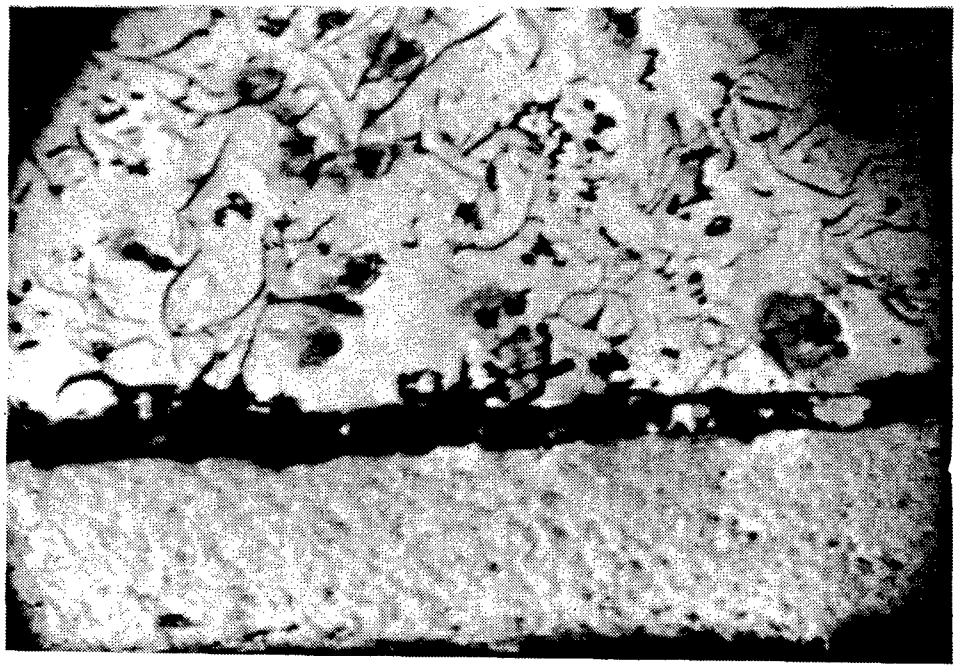

Figure 5-86. Cr2C3 Coated, Unworn Position, Severe Separation at Interface Shown in Cross-Section, #14, Build 3, Cylinder 5, B.R.R., Objective Lens: 16/0.22 Photo Lens X 10, Magnification X 155

severe (Figure 5-86).

The separation tendency of the coatings was determined by indenting, in cross-section, the interface between the coating/substrate with a Knoop microhardness indentor, using 2 kg for Cr2O3 and 1 kg for Cr2C3. Results are shown in Figure 5-87 and 5-88 for indentations in worn areas of the samples. A second indentation was made in the sample of Photo 3 at the middle of the coating layer. Cracks were observed only at the corners of the indentation mark. The cracks were more extensive when a 2 kg load was applied to this sample (Figure 5-89).

Figure 5-90 shows results of a 2 kg load applied on a Cr2C3 coated surface layer. The cracks were not at the corners of the indentation but were scattered about the sample. This result indicates that the Cr2O3 had greater strength than the Cr2C3. The surface layer microhardness was:

	HKnoop	Surface layer Thickness
Cr2O3	900-950	0.07 to 0.12 mm
Cr2C3	634-710	0.07 to 0.12 mm

The Cr2O3 coated surface was harder than the Cr2C3.

Photographic Analysis of Worn-Cylinder Walls - Engine Samples. In the portion that follows, observations on several worn engine-liner samples. Figures 5-91 and 5-92 show the surface of the Cr2O3 liner at about 14 to 46 mm from the top of the liner. This is near the TRR point. A polarized light microscope was used. The pictures suggest that this region endured severe temperatures and pressures. There are many axial and radial cracks on the Cr2O3 coated surface, but none on the Cr2C3 surface (not shown). As a point of interest, thermal expansion coefficients are:

Cast Iron	8.1 to 19.3 * 10exp(-6)/K
Cr2O3	7.5 * 10exp(-6)
Cr2C3	9.8 * 10exp(-6)

Visual observations suggest that the Cr2O3 was harder, more brittle, and had a finer porosity. This might be the reason that the Cr2O3-coated surface had the crack structure observed.

Figure 5-92 shows a Cr2O3-coated liner in the same relative wear position, but with higher magnification using the S.E.M. Peaks still exist, but relatively few scratch lines. Porosity is very fine.

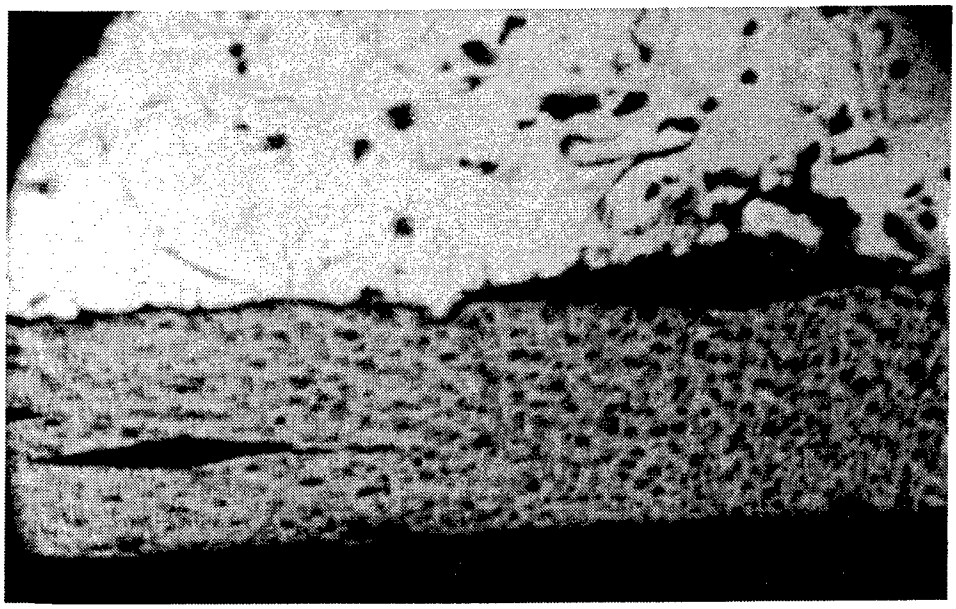

Figure 5-87. Cr2O3 Coated, 2 Kg Load Knoop Indenter Trace Applied on Interface Shows Good Adhesion, 1 Kg Load Applied at Middle of Surface Layer Shows Cracks Along Corner, #19, Build 4, Cylinder 3, T.R.R., Objective Lens: 16/0.22, Photo Lens: X 10, Magnification: X 155

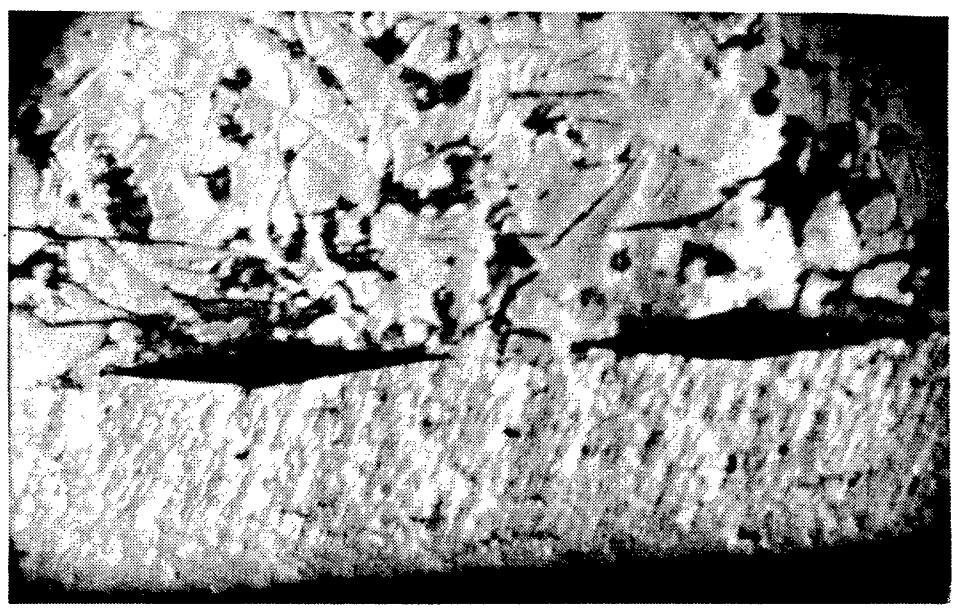

Figure 5-88. Cr2C3 Coated,Worn Position, 1 Kg Load Knoop Indenter Trace Applied on Interface Shows Good Adhesion, #14, Build 3, Cylinder 5, B.R.R., Objective Lens: 16/0.22, Photo Lens: X 10, Magnification: X 155

Figure 5-89. Cr2O3 Coated, 2 Kg Load Knoop Indenter Applied on Middle of Surface Layer, Cracks Along Corner Evident, #19, Build 4, Cylinder 3, T.R.R., Objective Lens: 16/0.22, Photo Lens: X 10, Magnification: X 155

Figure 5-90. Cr2C3 Coated, 2 Kg Load Applied on Middle of Surface Layer, Cracks Scattered, #14, Build 3, Cylinder 5, B.R.R. Unworn Position, Objective Lens: 16/0.22, Photo Lens: X 10, Magnification: X 155

Figure 5-91. Cr2O3 Coated, Many Axial and Radial Cracks Exist Within 14-46 mm From Top Side of the Cylinder, #19, Build 4, Cylinder 3, T.R.R., Objective Lens: 16/0.22, Photo Lens: X 10, Magnification: X 155

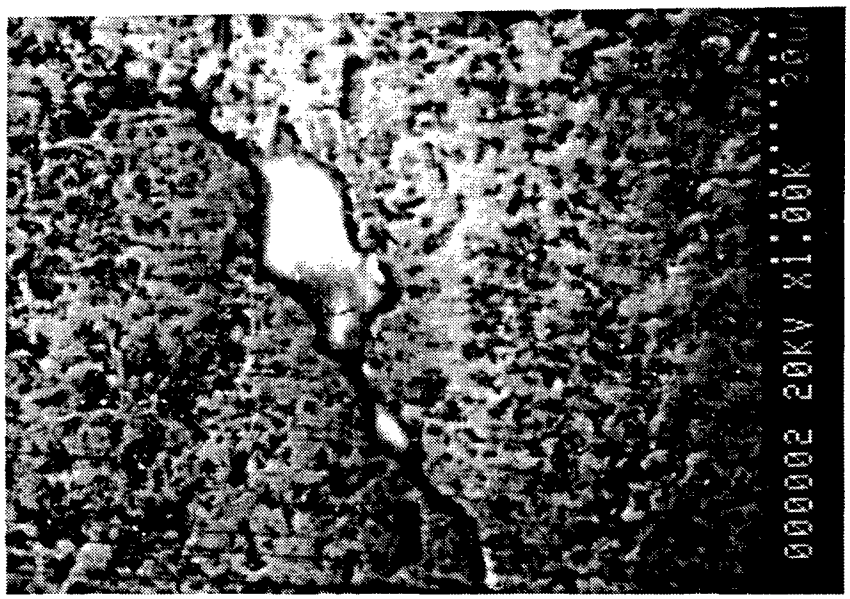

Figure 5-92. Cr2O3 Coated, Many Axial and Radial Cracks Exist Within 14-46 mm From Top Side of the Cylinder, A Few Sratch Lines, #19, Build 3, Cylinder 5, T.R.R., Magnification: X 1000

Figures 5-93 and 5-94 show the Cr2C3 morphologies at different magnifications. The yellow color indicates areas of worn peaks. Figures 5-95 and 5-96 are Cr2O3-coated liner morphologies at different magnifications. Many peaks remain. Figures 5-93 to 5-96 show comparative morphologies near the BRR point of the samples. The Cr2O3 appears better from a wear standpoint.

Summary of Observations - Engine Samples.

1. With both coatings, the adhesion was generally good. However, on the unworn region, below BRR, there was some coating separation. The separation with the Cr2C3 was severe enough that it was visible with the optical microscope, where that of the Cr2O3 was visible only with the S.E.M.

2. Based on the morphologies of the microhardness traces and wear features, the Cr2O3 coating was harder, stronger, and exhibited better wear resistance.

3. The Cr2O3 surface exhibited finer porosity.

4. Based on the morphologies of worn samples near the BRR, many peaks existed on the Cr2O3-coated surface, and a few scratch lines were evident. The peaks of the Cr2C3 coating were well worn.

5. The major problem of the Cr2O3 coating was that there were many cracks between 14 and 46 mm from the top of the liner, the TRR region. This region was near the combustion process, and the material underwent severe environmental stresses there.

Specimen Photomicrograph Results from Simulator. The simulator was run using both fresh and aged samples.

Fresh Samples. Examinations of the specimens from the simulator were examined in a manner similar to the specimens described above, which were from a running engine. Figure 5-97 shows the laboratory simulator and data acquisition system set-up in the laboratory. Test conditions were:

Sliding Speed	266 rpm
Applied Load	70 lbf/in
Normal Force	19 lbf
Test Temperature	427 C
Test Time	2 hours
Oil	Synthetic A

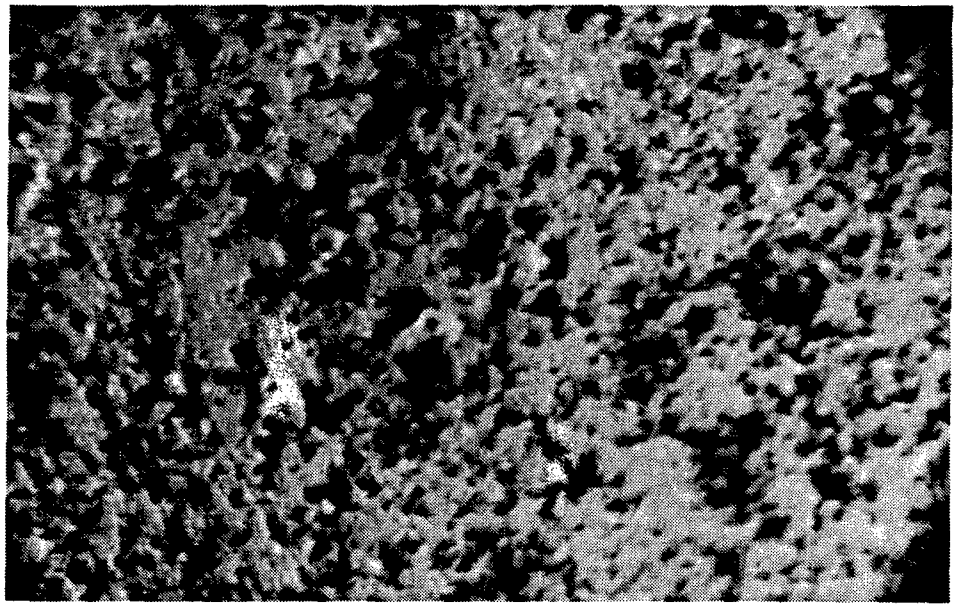

Figure 5-93. Cr2C3 Coated, Light Areas are Worn Surface, Large Porosity, #14 Build 3, Cylinder 5, B.R.R., Objective Lens: 16/0.22, Photo Lens: X 10, Magnification: X 155

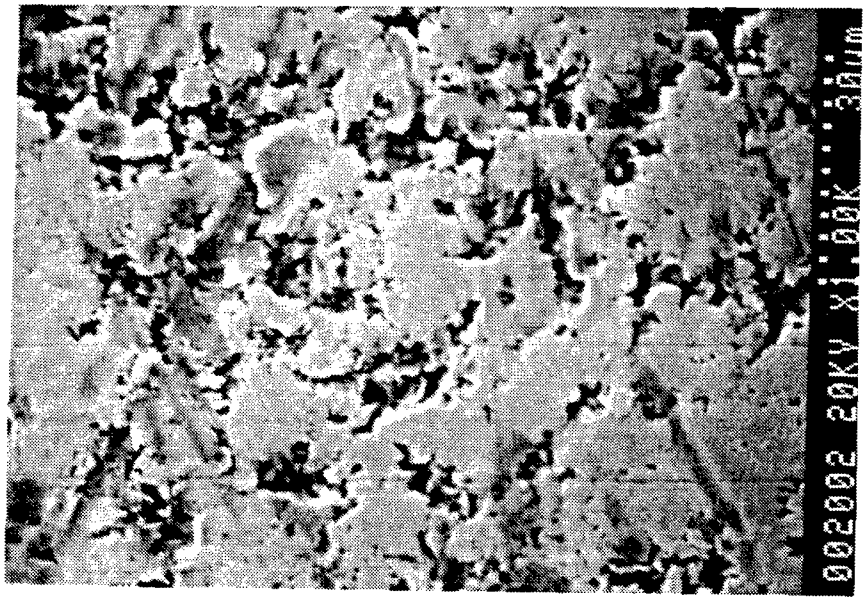

Figure 5-94. Cr2C3 Coated, Top of Peaks Show Scratches and Flats, Worn Position, #14 Build 3, Cylinder 5, B.R.R., S.E.M., Magnification: X 1000

Figure 5-95. Cr2O3 Coated, Worn, More Bumps Still Exist, Fine Porosity, #19, Build 4, Cylinder 3, B.R.R., Objective Lens: 16/0.22, Photo Lens: X 10, Magnification: X 155

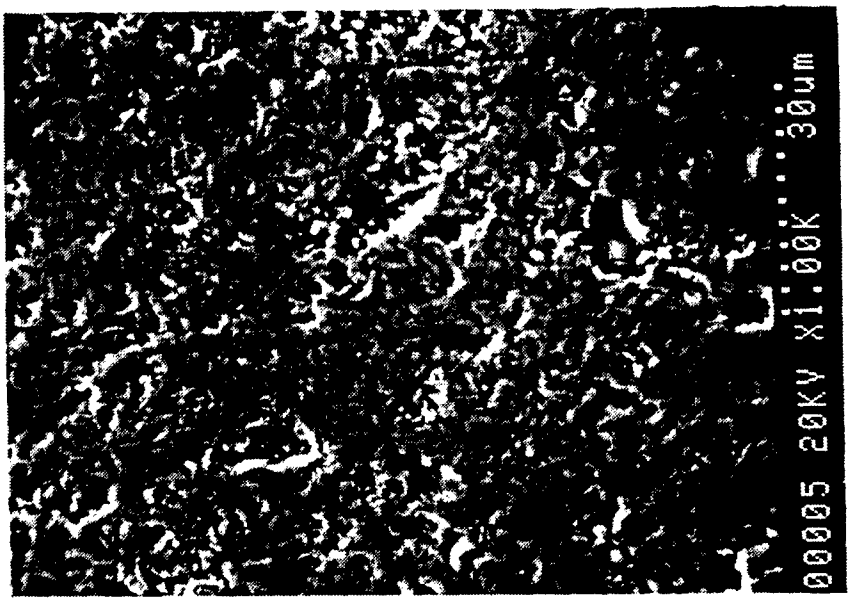

Figure 5-96. Cr2O3 Coated, Slightly Worn (Less Than T.R.R.), Almost No Scratch Lines on Bumps, #19 Build 4, Cylinder 3, B.R.R., S.E.M., Magnification: X 1000

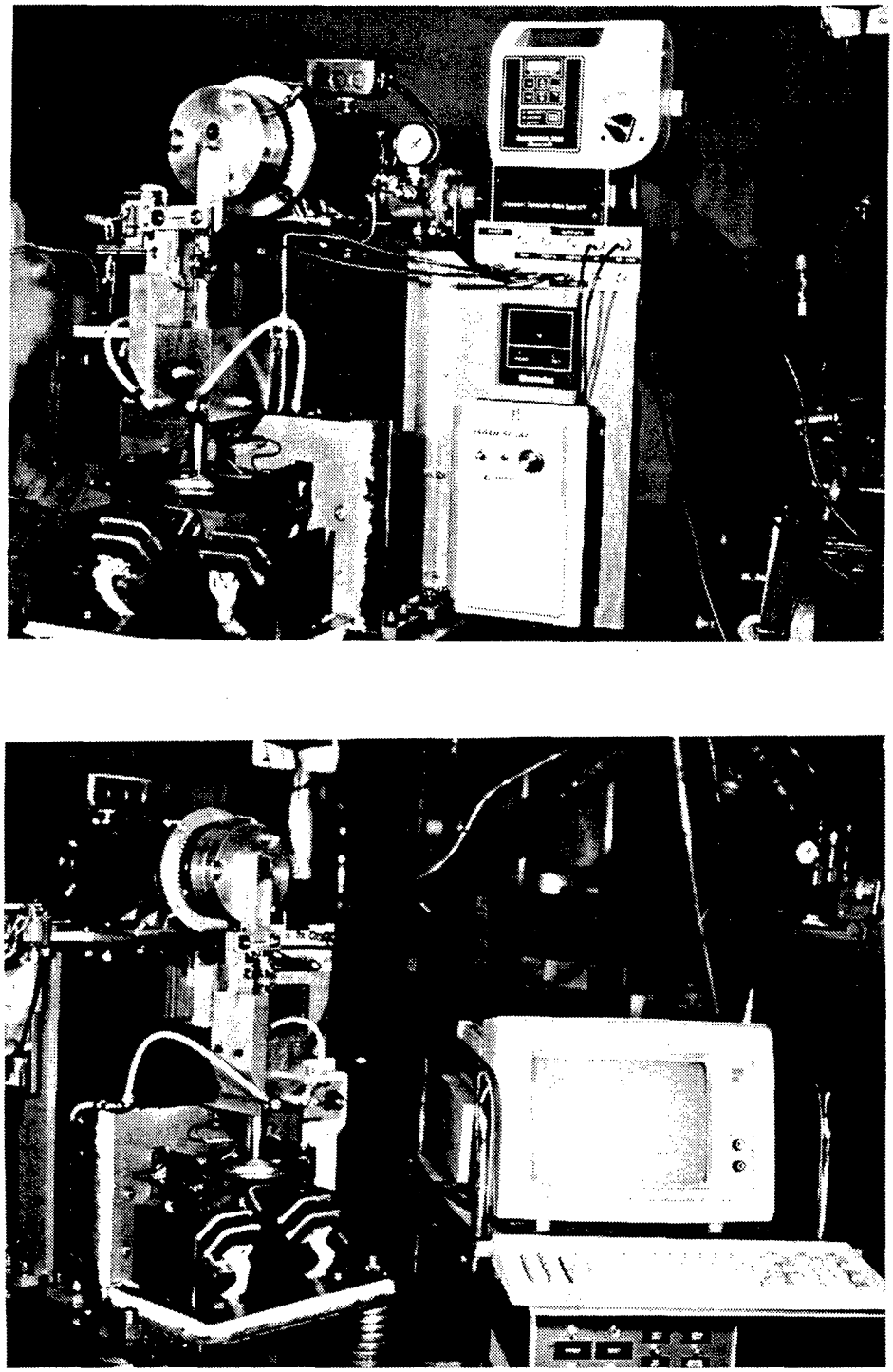

Figure 5-97. Photographs of Wear and Friction Bench Simulator

Prior to running, the Modified Kaman Science Process Cr2O3 coating was 0.035 mm and the plasma spray Cr2C3 coating was 0.18 mm thick. Microhardness was found by indentation using the Vickers tester. Figure 5-98 shows results for the Cr2O3 (MKS) coating with a 0.1 kg load. A small crack was observed in one corner, which does not show in the picture. The Knoop indentation with 0.1 kg produced clear cracks at the corners, which show clearly in Figure 5-99.

The Cr2C3-coated specimen had different morphology. Figure 5-100 shows scattered cracks at the end of the Vickers indentation with 0.1 and 1 kg loads applied. A Knoop indentation with 1kg load shows (Figure 5-101) no cracks at the corners. A 2 kg load with the Vickers tester produced scattered crush lines surrounding the indentation (Figure 5-102).

The Cr2O3-coated surface layer was thinner, harder, and more brittle than the Cr2C3. The Cr2C3 layer had a lower tensile strength. These property differences are expected to provide significantly difference performance in the test environment.

Worn Samples. Figure 5-103 shows results of the Kaman Cr2O3-coated liner run with a piston ring with a Cr3O4-coating. Testing was without oil. Test length was two hours. This is combination 2 of Table 5-6. Many peaks were worn away, but many valleys remained. Figure 5-104 shows similar results for the Cr2C3 liner and TiC +CaF2 ring combination. The ring surface wore completely through. There were many deep scratches in the surface. This is combination 3 of Table 5-6. Clearly the Cr2O3 was better. Hardness and strength might be principle reasons for this result.

Figure 5-105 shows the Cr2O3 liner morphology when tested with oil under the same test conditions. The worn surface was much smoother than when run dry. Perhaps wear debris filled the valleys. The morphology of the Cr2O3 run dry and the microhardness test showed that it was harder, stronger, and less likely to crumble than the Cr2C3-coating.

After two hours in simulator, the Cr2O3-coating near the TRR exhibited significant film formation when running with oil. This was observed under optical microscopic examination. The film looked similar to glass (Figure 5-106) and was not removed by acetone in an ultrasonic cleaner. Figure 5-105 is a view of the center of the same specimen. The region is characterized as being mainly flat with a few worn bumps. It appears as if some new substance is filling the valleys.

Figure 5-98. Cr2O3-Dipped Coating, Unworn, Surface Layer Thickness 0.035 mm, 0.1 Kg Load Vickers Test, Small Cracks at Left Corner, Objective Lens: 50/0.85, Photo Lens: X 10, Magnification: X 430

Figure 5-99. Cr2O3-Dipped Coating, Unworn, 0.1 Kg Load Knoop Test Corner Cracked, Surface Layer Thickness 0.035 mm, Objective Lens: 50/0.85, Photo Lens: X 10, Magnification: X 430

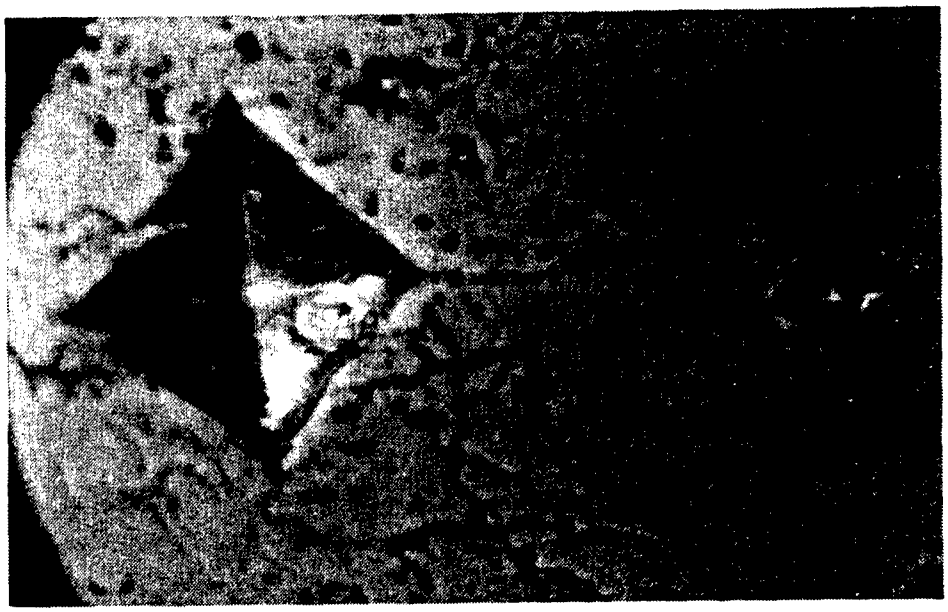

Figure 5-100. Cr2C3 Coating, Unworn, Surface Layer Thickness 0.18 mm, 0.1 and 1.0 Kg Load Vickers Test, Scattered Cracks, Objective Lens: 50/0.85, Photo Lens: X 10, Magnification: X 430

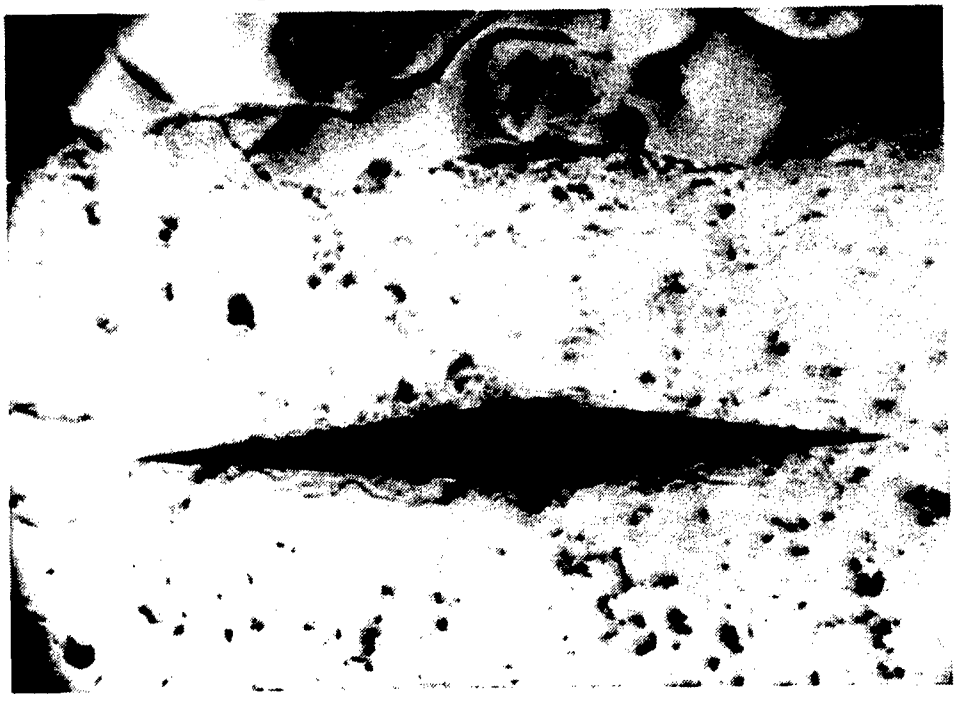

Figure 5-101. Cr2C3 Plasma-Sprayed Coating, Unworn, 1 Kg Knoop Test, Scattered Cracks, Objective Lens: 25/0.50, Photo Lens: X 10, Magnification: X 300

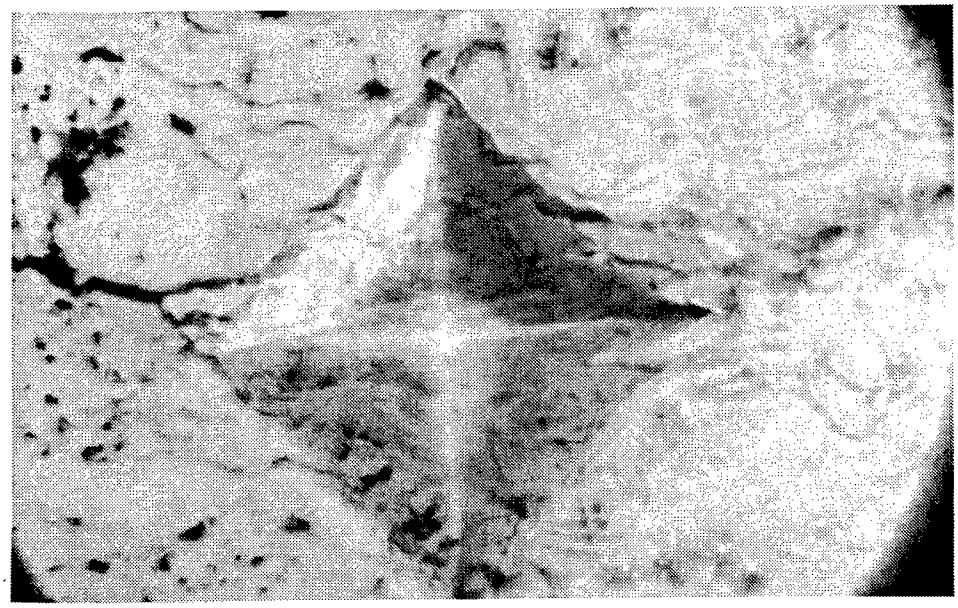

Figure 5-102. Cr2C3 Plasma-Sprayed Coating, Unworn, 2 Kg Vickers Test, Many Scattered Cracks, Objective Lens: 50/0.85, Photo Lens: X 10, Magnification: X 430

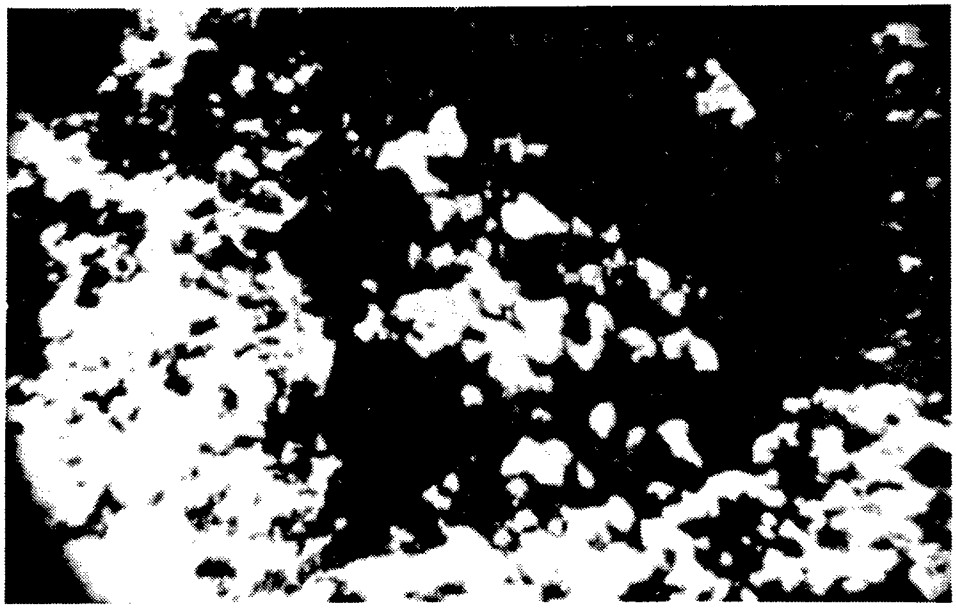

Figure 5-103. Cr2O3-Dipped Coating, Run Dry, 266 RPM, 70 Lbf/In Load, 427 C, Normal Force 19 lbf, 2-Hour Test, Some Peaks Worn-Out, Some Kept Unworn Morphology, Objective Lens: 16/0.22, Photo Lens: X 10, Magnification: X 155

Figure 5-104. Cr2C3 Plasma-Sprayed Coating, Run Dry, 266 RPM, 70 Lbf/In Load, 427 C, Normal Force 19 lbf, 2-Hour Test, Many Scratch Lines, No Bumps, Objective Lens: 16/0.22, Photo Lens: X 10, Magnification: X 155

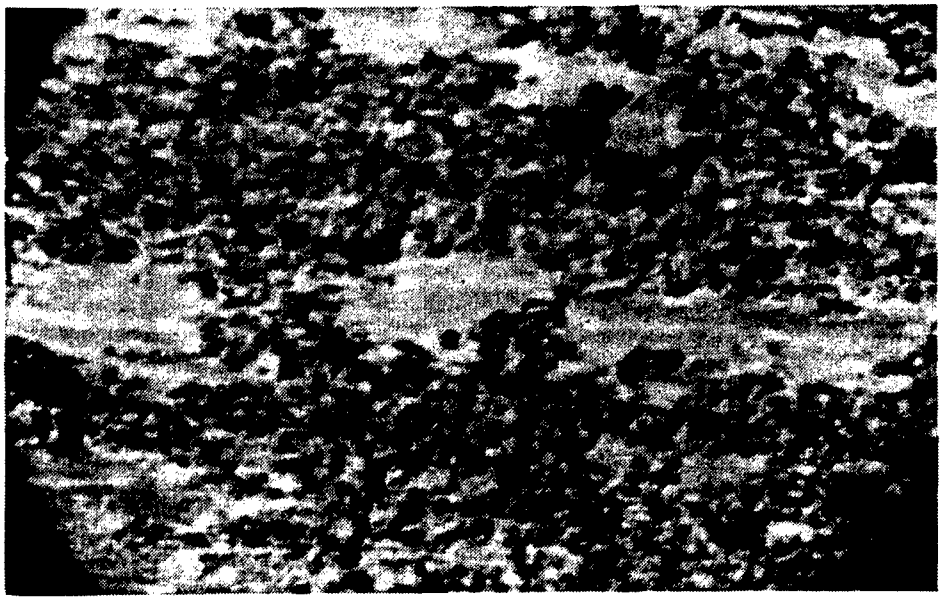

Figure 5-105. Cr2O3-Dipped Coating, Synthetic Oil, 266 RPM, 70 Lbf/In Load, 427 C, Normal Force 19 lbf, 2-Hour Test, Some Peaks Remain, Objective Lens: 16/0.22, Photo Lens: X 10, Magnification: X 155

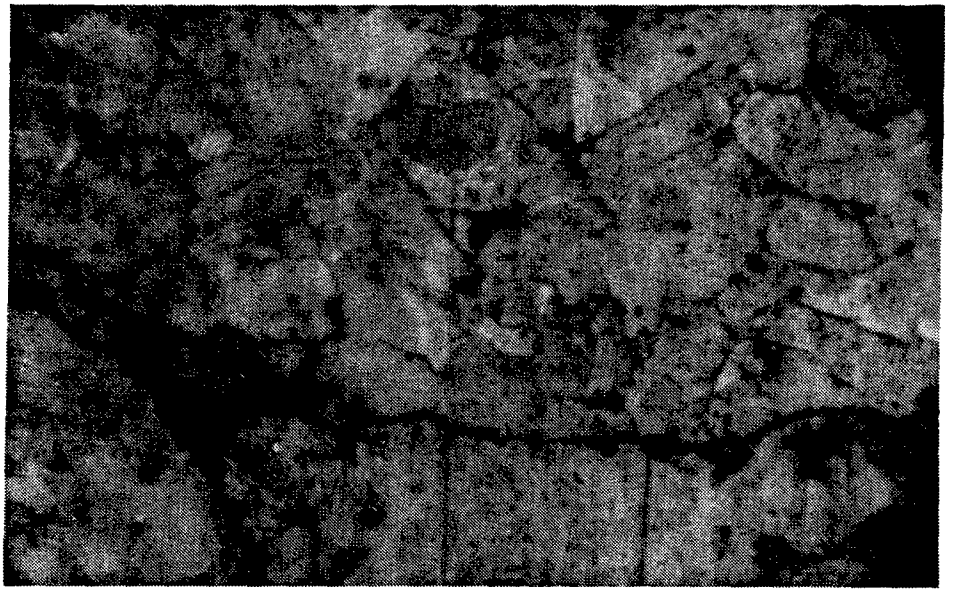

Figure 5-106. Cr2O3 Plasma-Sprayed Coating, Synthetic Oil, Photo Near T.R.R., 266 RPM, 70 Lbf/In Load, 427 C, Normal Force 19 lbf, 2-Hour Test, Extensive Glass Like Film was Produced, Objective Lens: 25/0.50, Photo Lens: X 10, Magnification: X 430

The Cr2C3-coating run with oil also exhibited a film at the TRR, and this was thicker than with the Cr2O3 (see Figure 5-107). The film thickness is indicated below on the sketch. Several measurements are reported. It is seen that the film thickness varied from thicker near the end of travel, to thinner near the center.

Figure 5-107. Cr2C3 Plasma-Sprayed Coating, Synthetic Oil, Worn Near T.R.R., 266 RPM, 70 Lbf/In Load, 427 C, Normal Force 19 lbf, 2-Hour Test, More Film than Cr2O3 for Same Condition, Objective Lens: 25/0.50, Photo Lens: X 10, Magnification: X 430

LIST OF REFERENCES

1 Uras, H. M. and Patterson, D. J., "Measurement of Piston and Ring Assembly Friction by the Instantaneous IMEP Method," SAE Paper 830416 (1983)

2 Uras, H. M., "A Study of Piston-Ring Assembly Friction," Ph.D. Thesis, The University of Michigan (1984)

3 Uras, H. M. and Patterson, D. J., "Effect of Some Lubricant and Engine Variables on Instantaneous Piston and Ring Assembly Friction," SAE Paper 840178 (1984)

4 Uras, H. M. and D. J. Patterson, "Oil and Ring Effects on Piston-Ring Assembly Friction by the Instantaneous IMEP Method," SAE Paper 850440 (1985)

5 Uras, H. M. and Patterson, D. J., "Effect of Some Piston Variables on Piston and Ring Assembly Friction," SAE Paper 870088 (1987)

6 Uras, H. M. and Patterson, D. J., "Measurement of Piston and Ring Assembly Friction in Reciprocating Machines," ASME Paper 87-ICE (Feb. 1987)

7 Ku, Young-Gon, "A Study of Piston and Ring Friction in an Internal Combustion Engine," Ph.D. Thesis, U. of Mi. (1987)

8 Ku, Young-Gon and Patterson, D. J., "Piston and Ring Friction by the Fixed-Sleeve Method," SAE Paper 880571 (1988)

9 Morrison, K. M. and Patterson, D. J., "Friction of Piston and Ring Assembly in a Diesel Engine," Proc. of the 1987 Coatings for Advanced Heat Engines Workshop, US Dept. of Energy Conference 870762, Castine Maine (July 27-30, 1987)

10 Patterson, D. J. et. al., "Piston and Ring Friction Studies in Cummins 903 Engine," Progress Rept. No. 1 to US Army (June 1985)

11 Patterson, D. J. et. al., "Piston and Ring Assembly Friction Studies in Cummins 903 Engine," Progress Rept. No. 2 to US Army (October 1986)

12 Patterson, D. J. et. al., "Piston and Ring Friction Studies in Cummins 903 Engine," Progress Rept. No. to US Army (January 1988)

13 Slone, R. J. et.al., "Upper Cylinder Wear Simulation in Heavy Duty Diesel Engines," Proc. of the 1987 Coatings for Advanced Heat Engines Workshop, US Dept. of Energy Conference 870762, Castine Maine (July 27-30 1987)

14 Naylor, M. G. S., "Development of Advanced Diesel Wear Coatings," Proc. of the 1987 Coatings for Advanced Heat Engines Workshop, US Dept. of Energy Conference 870762, Castine Maine (July 27-30, 1987)

15 Slone, R. J. et. al., "Wear of Piston Rings and Liners by Laboratory Simulation," SAE Paper 891046 (1989)

DISTRIBUTION LIST

	Copies
Commander Defense Technical Information Center Bldg. 5, Cameron Station ATTN: DDAC Alexandria, VA 22304-9990	12
Manager Defense Logistics Studies Information Exchange ATTN: AMXMC-D Fort Lee, VA 23801-6044	2
Commander U.S. Army Tank-Automotive Command Attn: ASQNC-TAC-DIT (Technical Library) Warren, MI 48397-5000	2
Commander U.S. Army Tank-Automotive Command Attn: AMSTA-CF (Dr. Oscar) Warren, MI 48397-5000	2
Dr. Walter Bryzik U.S. Army Tank-Automotive Command Van Dyke and 11 Mile Rd. Warren, MI 48090	1
Mr. Ernest Schwarz U.S. Army Tank-Automotive Command Van Dyke and 11 Mile Rd. Warren, MI 48090	1
Director U.S. Army Material Systems Analysis Activity Attn: AMXSY-MP (Mr. Cohen) Aberdeen Proving Ground, MD 21005-5071	1